Contribution to modeling of treatment and reuse of industrial wastewater

vorgelegt von
M.Sc.-Ingenieur
Kang Hu
geb. in JiangXi, P.R.China

von der Fakultät III - Prozesswissenschaften
der Technischen Universität Berlin
zur Erlangung des akademischen Grades

Doktor der Ingenieurwissenschaften
-Dr.-Ing.-

genehmigte Dissertation

Promotionsausschuss:
Vorsitzender: Prof. Dr. rer. nat. Ulrich Szewzyk (TU Berlin)
Gutachter: Prof. Dr.-Ing. Michael Sievers (CUTEC)
Gutachter: Prof. Dr.-Ing. Sven-Uwe Geissen (TU Berlin)

Tag der wissenschaftlichen Aussprache: 29. September 2016

Berlin 2017

Abstract

Membrane bioreactor (MBR) and reverse osmosis (RO) are membrane systems often applied for wastewater treatment and reuse. An integrated water and energy management model (IWEMM) was developed to simulate the water and the related energy fluxes of the production and wastewater reuse processes consisting of a MBR and RO. The results of a pilot-scale MBR and RO process that was conducted by the Complutense University of Madrid in a polyvinyl chloride (PVC) production site were used for calibration and validation. IWEMM is intended to predict the economical and calculate the ecological effects (e.g. impact on water bodies) of water reuse and the related technologies in combination with life cycle assessment (LCA), to optimize water treatment technologies, processes and sites, to demonstrate the potential for freshwater savings as well as the recovery of heat and valuables.

A simulation model based on activated sludge model No.1 (ASM1) was developed and calibrated for the MBR to evaluate performance in terms of effluent quality, energy consumption and operation strategy reliability. Furthermore, a modified aeration model with consideration of the effect of mixed liquor suspended solids (MLSS) on oxygen transfer was proposed. The results indicate that the calibrated ASM1 was sufficiently able to simulate effluent ammonia and nitrate concentrations and MLSS in the aerobic tank in both steady and dynamic states, and that the pilot-scale MBR consumed 0.73 kWh per m^3 permeate production. After the calibration and validation of the MBR process model, a procedure of scenario analysis (SCA) was conducted to analyze the effect of sludge retention time (SRT), recirculation ratio (RO) and dissolved oxygen (DO) on aeration energy demand and effluent quality. Moreover, Latin Hypercube Sampling (LHS) was performed to study the uncertainty of model parameters to judge the reliability of operation strategy to meet certain criteria. It showed that the current operation strategy was able to reach the target with the effluent NH_4-N concentration lower than 2 mg L^{-1} for about 97 % chance.

The solution-diffusion-film model (SDFM) based on solution-diffusion model (SDM) and film theory was proposed to describe rejections of electrolyte mixtures in the MBR effluent which consists of dominant ions (Na^+ and Cl^-) and several trace ions (Ca^{2+}, Mg^{2+}, K^+ and SO_4^{2-}). The universal global optimization method was used to estimate

the ion permeability coefficients (B) and mass transfer coefficients (K) in SDFM. Then, the membrane performance was evaluated based on the estimated parameters, which demonstrated that the theoretical simulations were in line with the experimental results for the dominant ions. Moreover, an energy analysis model with consideration of limitation imposed by the thermodynamic restriction was proposed to analyze the specific energy consumption of the pilot-scale RO system at various scenarios. The results demonstrated that the specific energy consumption of stages 1 and 2 in phase 1 is 0.204 and 0.180 kWh m^{-3} at the recovery of 70 %.

Zusammenfassung

Membran-Bioreaktor (MBR) und Umkehrosmose (RO) sind Membransysteme, welche häufig für die Abwasserbehandlung und -wiederverwertung genutzt werden. Es wurde ein Integriertes Wasser- und Energiemanagement Modell (IWEMM, engl. integrated water and energy management model) entwickelt um die Wasser- und die daran gekoppelten Energieflüsse in der Produktion und in den Abwasserwiederverwendungsprozessen beschreiben zu können. Das Modell wurde mit Ergebnissen der Complutense Universität Madrid, die eine MBR-RO Pilotanlage zur Wiederverwendung von Abwasser in einer Polyvinylchlorid-Anlage betrieben haben, kalibriert und validiert. Das IWEMM wurde entwickelt um wirtschaftliche und ökologische Auswirkungen der Wasserwiederverwendung in Kombination mit Ökobilanz (LCA) für die verwendeten Technologien, Prozesse, Standorte sowie das Potenzial der Wasserwiederverwendung und der Nutzung von Wärme und Wertstoffen vorhersagen und optimieren zu können.

Für die Bewertung von MBRs wurde ein Simulationsmodell, das auf dem Activated Sludge Model No.1 (ASM1) basiert entwickelt, welches die Leistung hinsichtlich der Qualität des gereinigten Abwassers, den Betriebskosten und die Betriebsstrategie zuverlässig vorhersagt. Außerdem wurde ein modifiziertes Belüftungsmodell unter Berücksichtigung der Wirkung des Trockensubstanzgehalts im Belebungsbecken (MLSS) auf den Sauerstofftransfer vorgeschlagen. Die Ergebnisse zeigen, dass das kalibrierte ASM1-Modell in der Lage ist die Ammonium- und Nitratkonzentrationen sowie den Trockensubstanzgehalt im Belebungsbecken mit hinreichender Genauigkeit, sowohl stationär als auch dynamisch, vorherzusagen. Der spezifische Energiebedarf des Pilotanalgen-MBRs betrug nur 0,73 kWh pro m^3 Permeat. Nach der Kalibrierung und Validierung des MBR-Prozessmodells wurde eine Szenariosanalyse durchgeführt, um den Einfluss des Schlammrückhalts (SRT) der Rezirkulationsverhältnisse und des gelösten Sauerstoffs (DO) auf die Ablaufqualität und den Energiebedarf der Belüftung zu analysieren. Außerdem wurde die Latin Hypercube Sampling Methode (LHS) durchgeführt, um die Unsicherheit der Parameter zu bestimmen und damit die Zuverlässigkeit der Betriebsstrategie zu beurteilen und gewisse Ranbedingungen einzuhalten. Die Ergebnisse zeigen, dass die abfließenden NH_4-N Konzentration niedriger als 2 $mg \cdot L^{-1}$ mit etwa 97 % Chance erreichen könnte.

Das Lösungs-Diffusions-Film Modell (SDFM) wurde basierend auf dem Lösung-Diffusion Modell (SDM) und der Filmtheorie für den MBR entwickelt. Damit konnte der Rückhalt der Elektrolytmischungen, die aus dominanten Ionen (Na^+ und Cl^-) und mehrere Spurenionen (Ca^{2+}, K^+, Mg^{2+} und SO_4^{2-}) bestanden, durch das MBR-System beschrieben werden. Die Ionen-Permeabilitätskoeffizienten (B) und die Stoffübertragungskoeffizienten (K) im SDFM wurden mit der „universal global optimization method“ bestimmt. Dann wurde die Membranleistung anhand der geschätzten Parameter ausgewertet. Es zeigte sich dass für die dominanten Ionen die Simulationsergebnisse mit den experimentellen Ergebnissen korrelierten. Außerdem wurde ein Energieanalysemodell unter Berücksichtigung der thermodynamischen Beschränkung vorgeschlagen um den spezifischen Energieverbrauch des Pilot-RO-System in verschiedenen Szenarien vorherzusagen. Die Ergebnisse zeigten, dass der spezifische Energieverbrauch der Stufen 1 und 2 in Phase 1 jeweilige 0,204 und 0,180 $kWh \cdot m^{-3}$ bei einer Wiedergewinnung von 70 % beträgt.

.

Acknowledgement

This research project was partly supported by European Union's Seventh Framework Programme (FP7/2007-2013) under the Grant Agreement No. 280756 and a fellowship from China Scholarship Council (CSC No. 201206150055).

I want to express my honest thanks to my supervisor Prof. Dr.-Ing. Sven-Uwe Geissen for giving me the chance to do my PhD study in Germany and to participate in the E4Water project. I learned a lot from him during my PhD at TU Berlin. He is a great professor and an outstanding engineer who has a never-ending source of knowledge. I also want to thank Prof. Dr.-Ing. Michael Sievers from CUTEC for taking the duty and the responsibility to be my second evaluator. I would say my thanks to my colleague and E4Water project partner Thorsten Fiedler who helped me a lot in the project and in my daily life in Germany.

I also thank my colleagues Anja Bewersdorff, Christina Senge, Gerhard Schulte, Gesine Götz, Kerstin Tang, Liane Kapitzki, Marina Sabelfeld, Max Zeidler, Milton Arimi, Qiqi Zhang, Tobias Sören Hinz, Xiwen Hua and Yongjun Zhang who are my second family in Berlin. My life could be hard, far from China and family, without them and their loves. I am very happy we dined together before Christmas every year, played bowling, paintball and slacklining together. These will be my precious memories forever. They certainly played a big role for me completing my PhD study. I would like to thank Thomas Track and Christina Jungfer from Dechema, David Prieto from Inovyn, Nathalie Swinnen from Solvay, Carlos Negro, Angeles Blanco and Laura Blanco from UCM, Uwe Fortkamp and Christian Junestedt from IVL, Jens Alex from ifak, Simon Zander and Jan-Philip Samson from TUB who are very nice in the cooperation of E4Water project.

I would like to thank my parents Qingnian Hu and Yongxiang Peng who I couldn't be where I am without them. They supported me in every stage of my life. Finally, I really appreciate my wife Fang Zhou. She quitted her job in China and went to Germany with me. She brought a precious gift, our daughter Xiyue Hu, for our family on 28th June 2016.

CONTENTS

List of abbreviations

ASM	Activated sludge model
BOD_5	5-day biochemical oxygen demand
BSM	Benchmark simulation model
CAS	Conventional activated sludge
CDF	Cumulative distribution function
CIP	Clean-in-place
COD	Chemical oxygen demand
DO	Dissolved oxygen
F/M	Food to microorganism ratio
HRT	Hydraulic retention time
IE	Ions exchanger
IWEMM	Integrated water and energy management model
LCA	Life cycle assessment
LHM	$L\ m^{-2}\ h^{-1}$
LHS	Latin hypercube sampling
MBR	Membrane bioreactor
MED	Multi-effect distillation
MF	Microfiltration
MLSS	Mixed liquor suspended solids
MSF	Multi-stage flash desalination
NF	Nanofilteration
OLR	Organic loading rate
PAO	Polyphosphate-accumulating organisms
PAC	Poly-aluminium chloride
PCT	Physicochemical treatment process
PLC	Programmable logic controller
PVA	Polyvinyl alcohol
PVC	Polyvinyl chloride
RO	Reverse osmosis
SAD_m	Specific membrane aeration demand per unit of membrane area
SCA	Scenario analysis
SDFM	Solution-diffusion-film model

SDM	Solution-diffusion model
SRT	Sludge retention time
SS	Suspend solid
SWRO	Seawater reverse osmosis
TDS	Total dissolved solids
TMP	Thermomechanical pulp
TOC	Total organic carbon
TR	Thermodynamic restriction
TSS	Total suspended solids
UASB	Upflow anaerobic sludge blanket reactor
UF	Ultrafiltration
VCM	Vinyl chloride monomer

List of symbols

Symbol	Description	Unit
MBR models:		
AE	Aeration energy	kWh d^{-1}
AOTR	Actual transfer rate of oxygen in wastewater	g O_2 d^{-1}
b_e	Blower efficiency	---
C_{SI}	Unit conversion factor	---
DO	Dissolved oxygen concentration	g m^{-3}
F	Fouling correction factor for the air diffusers (1 for clean diffusers)	---
g	Gravitational acceleration	m s^{-1}
h	Immersion depth of the pressurized aeration	m
k_La	Oxygen transfer coefficient	d^{-1}
MLSS	Mixed liquid suspended solids concentration	g L^{-1}
n	Air constant	---
P_{in}	Absolute inlet pressure	Pa
P_{loss}	Pressure loss associated with piping and diffuser	Pa
P_{out}	Absolute outlet pressure	Pa

R_g	Universal gas constant	J mol^{-1} K^{-1}
R_{air}	Specific oxygen input at wastewater temperature of 20 °C	g m^{-3} m^{-1}
SDO	Dissolved oxygen saturation concentration	g m^{-3}
SOTR	Standard oxygen transfer rate	g O_2 d^{-1}
T	Temperature of wastewater	°C
t_{ev}	Simulation period	d
T_{in}	Absolute inlet temperature	K
V	Tank volume	m^3
V_{air}	Volume airflow rate	Nm^3 d^{-1}
α	Process to clean water correction factor	---
ω	Exponent coefficient for α	---
φ	Correction factor of temperature for oxygen transfer	---
ρ_{air}	Air density at standard condition	kg m^{-3}
ρ_{WW}	Wastewater density	kg m^{-3}

RO models:

A	Water permeability coefficient	m^3 $m^{-2}h^{-1}$ kPa^{-1}
a	The membrane area	m^2
B	Solute permeability coefficient	m^3 $m^{-2}h^{-1}kPa^{-1}$
C_f	Salt concentration in feed stream	mg L^{-1}
C_m	Solute concentrations at retentate side of membrane	mol L^{-1}
C_p	Solute concentrations in the permeate	mol L^{-1}
C_r	Salt concentration in retentate stream	mg L^{-1}
E	Net energy required for cross flow RO	J
E_p	Energy required for permeate production	J
E_r	Energy remaining in retentate stream	J
f_{os}	Osmotic pressure coefficient	Pa L mg^{-1}
i	Number of dissolved solute i.e. ions and non-electrolyte solute	---
J_w	Water volumetric flux	m^3 $m^{-2}h^{-1}$
$M_{f,i}$	Molar concentration in the feed stream	mol L^{-1}
$M_{p,i}$	Molar concentration in the permeate	mol L^{-1}
$\Delta M_{s,i}$	Dissolved solute molar concentration difference	mol L^{-1}

P	Operation Pressure	Pa
Δp	Transmembrane pressure	kPa
Q_p	Product water (permeate) flow rate	$m^3 h^{-1}$
R_g	The gas constant	$kPa \cdot L \cdot K^{-1} \cdot mol^{-1}$
R_o	Observed rejection	%
R_r	Real rejection	%
SEC	Special energy requirement	$kWh\ m^{-3}$
T	Temperature	K
V_f	Feed water volume	m^3
Y	RO recovery	%
$\Delta\pi$	The osmotic pressure gradient	kPa
π_f	The osmotic pressure of feed stream	Pa

Cooling tower model:

$C_{p,W}$	Specific heat capacity of water	$kJ\ kg^{-1}\ °C^{-1}$
H_v	Latent heat of vaporization of water	$kJ\ kg^{-1}$
M_{CW}	Circulating water	$m^3\ h^{-1}$
M_{DW}	Blow-down water	$m^3\ h^{-1}$
M_{EW}	Evaporated water	$m^3\ h^{-1}$
$M_{Make-up}$	Make-up water	$m^3\ h^{-1}$
M_{WW}	Windage loss water	$m^3\ h^{-1}$
T_i	Inlet temperature of water to the tower	°C
$\Delta T_{i,o}$	Water temperature change	°C
T_o	Outlet temperature of water from the tower	°C
T_{wb}	Wet bulb temperature of air	°C
μ_{CT}	Cooling tower efficiency	%
η_{WW}	Windage loss ratio	%

Heat exchanger model:

A	Area	m^2
c	Cold (index)	---
c_w	Specific heat capacity of water	$J\ kg^{-1}\ K^{-1}$
E	Efficiency	---

ex	Heat exchanger (index)	---
h	Hot (index)	---
in	Input (index)	---
k	Thermal conductivity	$W\ m^{-1}\ K^{-1}$
m	Mass flow	$kg\ s^{-1}$
out	Output (index)	---
Q	Heat flow	W
T	Temperature	K
ΔT_{log}	Log-mean temperature difference	K

1. Introduction

1.1 The status of water use and wastewater treatment in industry

Water is either provided by a public supplier or self-supplied in industry; it is generally used for production, cooling purposes, cleaning/washing and employees' use. It is supposed that global industrial water requirements would increase to 1,500 billion m^3 by 2030 under the average economic growth scenario, which would account for 22 % of global water demand (2030 water resources group, 2009). In Europe, industry accounts for almost 40% of total water abstractions. Moreover, the industrial sector is a main water polluter. As reported by statistics based on data from eight European countries, only up to 60 % of industrial wastewater gets treatment before being discharged into the natural water body (Förster 2014).

Nowadays, industries are confronting the critical issues to achieve the stringent wastewater emission requirements. The industrial wastewater derives from varieties of streams such as from production line, boiler or cooling tower. It generally contains various substances, e.g. inorganic materials, virus, bacteria and toxic compounds et al., which may lead to restrict the performance of the conventional biological treatment. Membrane bioreactor (MBR) is a wastewater treatment system combining biological treatment process and membrane separation technology. It can provide high performance in treating wastewater besides having small footprints compared to conventional activated sludge process (Braak et al. 2011), resisting high organic loading and generating less sludge (Meng et al. 2009, Le-Clech et al. 2006). Therefore, MBR became one of the most promising technologies for industrial wastewater treatment and reuse (Bayat et al. 2015).

Reverse osmosis (RO) membrane processes are deemed to be one of the most significant, extensively commercialized and versatile water treatment technologies in the twenty first century. Due to the high rejection of impurities with low associated costs and high permeate quality, RO systems were generally applied to remove soluble ions, dissolved solids and organic substances to polish high-quality tertiary effluent for reuse (Pandey et al. 2012). The early applications of RO systems were specific to

groundwater recharge and water reclamation/reuse. Nowadays, it is also a practical technology for industrial wastewater treatment and seawater desalination (Pandey et al. 2014). The RO process was the first kind of membrane system to be employed in advanced wastewater treatment; it has received great attention as one of the best wastewater reuse processes (Gupta et al. 2012).

The straight combination of MBR and RO (MBR-RO) has emerged as a promising technology for municipal wastewater reclamation and reuse (Dialynas and Diamadopoulos 2009, Ogawa et al. 2010). More recently, the MBR-RO technology has been employed to reclaim several typical industrial wastewaters, including textile dyeing wastewater (De Jager et al. 2014, Lai et al. 2008), coking wastewater (Jiao 2014, Pimple et al. 2016) and oilfield wastewater (Fakhru'l-Razi et al. 2010), etc.

1.2 Membrane bioreactor (MBR) applications in industry

The first MBR system in "side-stream" configuration was developed in the late 1960s, but market penetration became important only after the commercialization of submerged configurations in 1990s. With an average growth rate of 11.6 - 12.7 % per annum, it has been growing markedly faster than the other membrane technologies and advanced wastewater treatment processes (Santos et al. 2011). In the industrial sector, the performance of full-scale commercial applications of MBR technology has been widely studied since 1991, when the first full-scale external MBR was installed in the United States by General Motors in Mansfield, Ohio (Yang et al. 2006). Moreover, the first full-scale internal MBR system to treat industrial wastewater was installed at a food ingredients plant in the Northeast U.S. in 1998 (Mutamim et al. 2013).

1.2.1 MBR in food industry

The agro-food industry is a significant European production activity which represents 16 % of total industrial turnover at approximately 956,000 million Euros. It is essential to use water for the manufacturing activities in food businesses. The water consumption in agro-food industries varies from 8 to 15 % of total consumed industrial water, which accounts for 1 - 1.8 % of total water consumption in Europe (Sanchez Perez et al. 2014).

The constituents of food industry wastewaters are often difficult to predict because of the differences in COD and pH in effluents from food products and the seasonal nature of food processing. Nevertheless, a review of literature demonstrated that wastewater from the food industry is commonly nontoxic, but has a high COD, BOD_5/COD ratio and suspended solid concentration (SS). Since MBRs are capable to treat high concentration organic and SS content wastewaters, attempts were made to evaluate the performance for food industry wastewater. As shown in Table 1-1, the MBR system has been employed to treat the wastewater from crop processing (sugar, wheat, corn and soybean et al.), seafood, milk industry (ice cream and whey), wineries (winery and distillery). The applications covered laboratory, pilot, and full scale studies.

Table 1-1 Summary of MBR systems to treat the food industry wastewater

Type of wastewater	Reactor volume (m^3)	Temperature (°C)	HRT (d)	MLSS (g L^{-1})	Feed COD (g L^{-1})	COD removal (%)	Reference
Soybean processing wastewater	3	30	0.4	2	1.4	78	Kataoka et al. (1992)
Maize processing effluent	2,610	35	5.2	21	15	97	Ross et al. (1992)
Wheat starch and gluten wastewater	24/15	37	0.6/0.4	18/---	19/10	98	Yanagi et al. (1994)
Ice-cream factory wastewater	0.01	25	1.0	---	13.33	95	Scott and Smith (1997)
Palm oil mill effluent	0.05	35	3.2	50-57	68	92	Fakhru'l-Razi and Noor (1999)
Fermentation wastewater	0.03	28-33	2.67	3.1-16.9	24.7	94	Lu et al. (2000)
Dairy industry wastewater	0.06	22-26	1.5	8.1-8.37	2.2-2.6	98	Bae et al. (2003b)
Sauerkraut brine	0.007	30	6.1	45-55	52.7	99	Fuchs et al. (2003)

Type of wastewater	Reactor volume (m^3)	Temperature (°C)	HRT (d)	MLSS (g L^{-1})	Feed COD (g L^{-1})	COD removal (%)	Reference
Cheese whey	0.032	25	0.82-2.8	5.8-14	73-86	94-99	Farizoglu et al. (2004)
Food processing wastewater	0.01 /0.03	24-27	0.21/0.63	----	1.5-2	40-63 /29-46	Wang et al. (2005)
Pet food wastewater	0.027 /0.027	18-20	2.8-6.2 /3.5-6.2	7	8-28.6 /3.1-8.4	93	Acharya et al. (2006)
Cheese whey	0.007 / 0.02	37	1/4	---/3-19.78	8.5	18/79	Saddoud et al. (2007)
Winery wastewater	0.22	---	---	---	0.5-8.6	97	Artiga et al. (2007)
Sugar manufacturing wastewater	5000	20-40	---	---	9.32-15.66	90	Naidoo et al. (2008)
Seafood processing wastewater	0.035	25-30	6.25	1-2.2	1.8	85	Sridang et al. (2008)
Olive mill wastewater	0.015	35	3.75-17.5	0.94-6.0	12.84	58-82	Stamatelatou et al. (2009)
Alcohol distillery wastewater	0.008	21-26	7	3.9-11	29.2-48.2	27-41	Satyawali and Balakrishnan (2009)
Food factory wastewater	0.2	---	0.42	8	0.6-0.8	93.8-95.8	Sun and Zuo (2009)
Winery wastewater	325	30	3.25	10-12	2-16	94	Bolzonella et al. (2010)
Dairy industry wastewater	0.018	22 ± 2	2.8	38	0.92-9	98	Farizoglu and Uzuner (2011)
Dairy industry wastewater	0.0258	---	0.25-0.33	17.25-22.37	1-7	99	Andrade et al. (2013)

1.2.2 MBR in textile industry

Textile industry is an important manufacturing industry which produces lots of extremely toxic and polluted wastewater. It is considered to be a water-intensive sector, since water is used as the main medium for dyes, finishing agents and removing impurities (Brik et al. 2006). The World Bank appraises that the textile industry is responsible for about 17 - 20 % of industrial wastewater. The textile processing industry wastewater is a complex and highly variable mixture of various polluting materials that range from inorganic substances to polymers and organic products (Mutamim et al. 2013). It contains has a poor biodegradability, high toxicity and is persistent coloured that leads to disrupt the total ecological/symbiotic balance of the receiving water environment (Vandevivere et al. 1998). It is recorded that over 100,000 commercial textile dyes are available in the market. Moreover, about 700,000-1,000,000 tons of dyes are produced among which 280,000 tons are emitted to the global environment per year (Ali 2010).

MBRs have been reported to be a preferable alternative to other physicochemical treatments in textile industry, since they can get rid of dyes from huge volumes of wastewater (Pearce et al. 2003). The first MBR system was applied to treat wool-scouring wastewater in 1992 (Hogetsu et al. 1992). It removed 50 % COD at an organic loading rate (OLR) of 15 kg m^{-3} d^{-1}. Table 1-2 summarizes some MBR applications for textile wastewater treatment in literature.

Table 1-2 Summary of MBR systems to treat textile industry wastewaters

Type of wastewater	Reactor volume (m^3)	Temperature (°C)	HRT (d)	MLSS (g L^{-1})	Feed COD (g L^{-1})	COD removal (%)	Reference
Laundry wastewater	3.5-4	---	2.0-2.5	10	1.5-1.7	97	Andersen et al. (2002)
Textile wastewater	0.3-0.5	---	---	5-15	1.28-5.6	96	Badani et al. (2005)
Textile wastewater	3	---	---	10-15	0.2-1.45	90-93	Lubello and Gori (2005)

Type of wastewater	Reactor volume (m^3)	Temperature (°C)	HRT (d)	MLSS (g L^{-1})	Feed COD (g L^{-1})	COD removal (%)	Reference
Dye house wastewater	0.06	---	2.9-5	4	2.31	89-94	Schoeberl et al. (2005)
Synthetic azo dye wastewater	0.003	---	1.5	4.6±0.2	3.5±0.5	94.8	Yun et al. (2006)
Textile wastewater	0.02	32-34	0.7-4	5-15	1.38-6.03	60-95	Brik et al. (2006)
Textile wastewater	0.0125	29	0.625	10-55	---	97	Hai et al. (2006)
Textile wastewater	6	---	---	6-14	1.33	91	Lubello et al. (2007)
Textile wastewater	0.023	---	0.58	13.9-17	0.69-2.28	95	Yigit et al. (2009)
Synthetic azo dye wastewater	0.036/0.018	---	2/1	2.7/2.1	0.31/0.024	92.3/97.5	You and Teng (2009)
Printing wastewater	0.09	---	0.25-0.94	9-11	0.6-1.2	85-92	Huang et al. (2009)
Synthetic dye wastewater	0.018	5-15	0.83	4-5.5	0.78±0.07	90	Qin et al. (2012)
Dyeing wastewater	0.028	---	0.44-0.48	6-9	0.5-0.65	60-94	Bui Xuan et al. (2012)
Synthetic textile wastewater	0.022	---	0.17-2	1-3	2-2.5	88-96	Konsowa et al. (2013)
Synthetic textile dye wastewater	0.057	18±2	1.67-3.33	12	2.45	90-93	Deowan et al. (2013)
Textile wastewater	0.06	24-29	1-3	10	1.46-3.09	93-98	Friha et al. (2015)
Azo-dye wastewater	0.0057	32-34	1-2	1-2	1	94-97	Yurtsever et al. (2015)

1.2.3 MBR in pulp and paper industry

The pulp and paper industry emits big volume of highly polluted wastewater, which may cause colour problems, thermal impacts, slime growth, scum formation and the increased amount of toxic materials in the environment (Kamali and Khodaparast 2015). Depending on the manufacturing process, water is used from the initial stage of debarking, through pulping, washing, bleaching and papermaking with 1 to 16 m^3 per tonne at the different steps (Ugurlu and Karaoglu 2009). Pulp and paper manufacturing requires lots of fresh water, from 10 to 40 m^3 per tonne paper depending on the product type and the mill age. Besides water, chemicals, fillers and sizing agents are also extensively used. Therefore, the generated wastewater normally have a high COD, a low BOD_5/COD ratio and about 200-300 different organic substances and almost 700 inorganic compounds (Karrasch et al. 2006). As a result, the pulp and paper industry has historically been labelled as one of the most polluting industries (Adnan et al. 2010).

Diverse toxic chemicals like resin acids, chlorinated resin acids, diterpene alcohols, unsaturated fatty acids and juvaniones are produced in the pulp and paper manufacturing process (Leiviska et al. 2009). This provides a significant challenge for traditional biological treatment but rendering alternative treatment technologies such as the MBR desirable (Lin et al. 2014, Sheldon et al. 2012). Meanwhile, the pulp and paper industry has been obliged to substantially reduce wastewater discharge, and to manage water use, due to the implementation of stringent regulations (Amat et al. 2005, Merayo et al. 2013). For this purpose, MBR processes are being employed to treat pulp and paper wastewaters to obtain high quality effluent for meeting a stringent emission limit or sustainable treatment and reuse (Dias et al. 2005, Lin et al. 2009). Since three German paper mills invested and operated MBR plants in 2007, the European paper mills are operating more than ten full-scale MBR plants at present (Simstich and Oeller 2010). Some MBR applications in pulp and paper industry are summarized in Table 1-3.

Table 1-3 Summary of MBR systems for treatment of pulp and paper industry wastewaters

Type of wastewater	Reactor volume (m^3)	Temperature (°C)	HRT (d)	MLSS ($g\ L^{-1}$)	Feed COD ($g\ L^{-1}$)	COD removal (%)	Reference
Evaporator condensate	5	53	0.5	7.6	17.8	93	Minami (1994)
Kraft bleach plant effluent	0.015	35	10	7.6-15.7	---	61	Hall et al. (1995)
Chemico-thermo-mechanical pulping effluent	0.09	35	2.0	13	12	82	Dufresne et al. (1998)
Mechanical newsprint mill white water	0.01	55	---	---	5.52	48-58	Ragona and Hall (1998)
Synthetic kraft pulp mill condensate	0.008	55-70	0.12	10	---	99	Berube and Hall (2000)
Kraft pulp mill foul condensates	0.004	33,45,55	0.79	3.0	5.12	87-97	Bae et al. (2003a)
Effluent from UASB treating paper mill wastewater	9	---	0.79	15	0.91	89	Lerner et al. (2007)
Kraft evaporator condensate	0.01	37.55	---	10	10	97-99	Lin et al. (2009)
Black liquor, pulp bleaching effluent and white water	10	25-34	0.75	10	0.6	92.1	Zhang et al. (2009)
TMP white water	0.01	37	2.5	5.7-10	2.6,5.5,10	95	Gao et al. (2010)
Kraft evaporator condensate	0.01	37	0.46-1.08	5-10	2-10	93-99	Xie et al. (2010)

Type of wastewater	Reactor volume (m^3)	Temperature (°C)	HRT (d)	MLSS ($g\ L^{-1}$)	Feed COD ($g\ L^{-1}$)	COD removal (%)	Reference
Paper mill deinking wastewater	0.07	25-50	0.33-1.38	5-18	1.4-2.6	83	Simstich et al. (2012)
Reed pulping medium wastewater	0.015	---	---	4.5-7	1.074	91.3	Na et al. (2013)

1.3 Applications of ASMs to MBR processes

It is acknowledged that activated sludge models (ASMs) were a significant milestone in the modelling of conventional activated sludge (CAS) systems and the application of ASMs has been very well established over the past 30 years. ASMs were initially developed to simulate CAS processes. However, since the late nineties ASMs also have been used to evaluate biomass kinetics for MBRs, provided that some necessary adaptations are made due to the specific behavior (Manser et al. 2006, Sarioglu et al. 2009). There are several versions of ASMs i.e. ASM1, ASM2, ASM2d and ASM3. By means of assimilating the developments in understanding of wastewater treatment systems, these dynamic models have been developed in two decades since the implement of the first version ASM1 (Henze et al. 2000). The Gujer matrix was introduced in ASM1 to present all the biochemical processes in a compact and clear form. However, biological phosphorous removal process was not included in ASM1 though it had already been created. Afterward, ASM2 incorporated the phosphorous related process since it became significant. Then, ASM2d was developed to incorporate the processes of denitrifying polyphosphate-accumulating organisms (PAOs). ASM3 (Gujer et al., 1999) was developed mainly to improve the correctness by incorporating the storage of polymers in heterotrophic activated sludge conversions and introduce a new standard for ASMs.

Most recently, Sperandio and Espinosa commented that both ASM1 and ASM3 could provide satisfactory simulation of submerged MBRs for municipal wastewater

treatment (Spérandio and Espinosa 2008). ASM1 was employed for an aerobic MBR to treat diluted municipal wastewater by Baek et al. The results demonstrated that ASM1 could help to better understand the performance of MBR (Baek et al. 2009). Verrecht et al. applied ASM2d to simulate the domestic water recycling in a MBR. The results showed an accurate dynamic simulation for the nutrient removal and MLSS concentration profiles using default parameter values (Verrecht et al. 2010a). Studies so far have not drawn a conclusion that whether ASM1, ASM2 or ASM3 is more preferable to model MBRs. However, the large number of parameters hampered ASMs' practical application. Therefore, ASM1 is still identified as the state-of-the-art platform for dynamic modelling in wastewater treatment and is more readily applicable in practice (Fenu et al. 2010a). An overview of ASMs is summarized in Table 1-4.

Table 1-4 Overview on ASMs

	ASM1	ASM2	ASM2d	ASM3
Year published	1987	1995	1999	1999
Modelling target	carbon and nitrogen	carbon, nitrogen and phosphorus	carbon, nitrogen and phosphorus	carbon and nitrogen
Content	8 processes 13 components 5 stoichiometric parameters 14 kinetic parameters	19 processes 19 components 22 stoichiometric parameters 42 kinetic parameters	21 processes 19 components 22 stoichiometric parameters 45 kinetic parameters	12 processes 13 components 6 stoichiometric parameters 21 kinetic parameters
Feature	Gujer matrix form was introduced for model presentation	Biological phosphorus removal was added	Role of phosphate accumulation organisms (PAOs) in denitrification was added	Correctness of ASM1 was improved and a new standard for ASMs was presented

1.4 Reverse osmosis (RO) applications in industry

RO industrial applications were just began ten years later after Loeb and Sourirajan developed the asymmetric membranes for reverse osmosis (RO) in seawater desalination field in the 1960s (Wenten and Khoiruddin 2016). RO systems are available at present in very extensive applications: food industry (Miguel Ochando-Pulido and Martinez-Ferez 2015, Ochando Pulido 2016, Prodanovic and Vasic 2013, Satyawali and Balakrishnan 2008), pulp and paper industry (Adnan et al. 2010), and seawater desalination (Elimelech and Phillip 2011, Kim et al. 2009, Ravanchi et al. 2009), etc.

1.4.1 RO in food industry

Distillery wastewaters have very high BOD, COD and BOD_5/COD ratio. Moreover, they contain high amounts of inorganic materials for instance potassium, phosphate, nitrogen, sulphate and calcium (Mohana et al. 2009, Satyawali and Balakrishnan 2008). Different biological and physicochemical treatment processes have been explored to treat distillery wastewaters. Compared to conventional treatment processes, the retentate obtained from the membrane can be used as a fertilizer, feed for biogas production. Besides, distillery wastewaters contain high amount of dead yeast cells, as well as yeast metabolites (amino acids, vitamins and proteins), which have high nutritive values and can be recycled using membranes.

Investigations of Ryan et al. (Ryan et al. 2009) considered viable disposal and options for tertiary treatment of distillery stillage. Among the various processes (chemical flocculation, electrocoagulation, evaporation and membranes, etc.) that can be used for tertiary treatment of stillage, membrane technologies are one of the most suitable for meeting the effluent discharge standards. All four classes of membranes, microfiltration (MF), ultrafiltration (UF), nanofiltration (NF) and reverse osmosis (RO), can be applied for distillery wastewaters treatment, while NF and RO appear to be the most promising methods for stillage purification with ability to produce high-quality water. Many investigations reported the usefulness of RO membrane separation techniques for distillery wastewater treatment. In studies by Madaeni and Mansourpanah (Madaeni

and Mansourpanah 2006), various polymeric RO membranes were employed to purify the biologically treated alcohol wastewater with a COD from 900 to 1,200 mg L^{-1}. The RO membrane showed outstanding results that nearly 100% COD was removed with higher flux (33 kg m^{-2} h^{-1}). Nataray et al. (Nataraj et al. 2006) reported results for total dissolved solids (TDS) removal from distillery wastewater by its purification with NF and RO hybrid processes. The results showed that, at the optimal pressure range of 30-50 bar, TDS in permeate were reduced from 51,500 to 9,050 mg L^{-1}, chloride concentration from 4,900 to 2,650 mg L^{-1} and conductivity from 346 to 15 mS cm^{-1}. Murthy and Chaudhari (Murthy and Chaudhari 2009b) evaluated the purification of distillery wastewater by combination of UF and RO processes. The UF unit permeate was used as a feed for RO. The results demonstrated the rejections of TDS, BOD and colour in RO were 98, 98 and 93 %, respectively.

1.4.2 RO in pulp and paper industry

RO was commercially installed in the pulp and paper industry as early as 1976 to concentrate sulphite pulping liquors. This concentration step enables more water to be removed from the liquors before they are further evaporated and eventually disposed off. Between 1970s and 1990s, RO was applied to the concentration of kraft liquors, paper machine effluents and bleaching effluents. A recent study conducted by Manttari and Nystrom (Manttari and Nystrom 2007) on effluent from three aerobic activated sludge plants of the pulp and paper industry indicated that very clean permeates can be obtained from the RO process. The results showed that average organic carbon concentration in the permeate was below 10 mg L^{-1} when the feed COD_{cr} varied from 460 to 860 mg L^{-1}. This is an encouraging development since the organic contents of these effluents contribute to high values of COD and BOD. An application of RO is in the dissolving pulp industry in treating the pre-hydrolysed liquor resulting from a rayon production process. The liquor is first fermented to convert sugars into yeast and further ultra-filtered to remove these yeasts. The permeate from this process is later filtered using RO and results in almost complete removal of the remaining low molecular weight sugars (Bhattacharya et al. 2005, Rath et al. 2005).

1.4.3 RO in desalination of seawater

Desalination processes have become an effective way to solve potable water shortages; they are extraordinarily significant in many water scarce regions (Kim et al. 2009, Lee et al. 2009). Nowadays, more than 21,000 desalination plants are available in over 120 countries which produce more than 13 million m^3 potable water per day.

Compared to thermal desalination processes such as multi-effect distillation (MED) and multistage flash desalination (MSF), RO membrane desalination is more preferable due to the lower energy consumption for seawater desalination to produce fresh water (Moonkhum et al. 2010). Up to the present, it is the most popular membrane-based process for seawater desalination (Cho et al. 2016, Quevedo et al. 2012). Since the end of the 1970s, energy consumption of RO membrane desalination has been significantly reduced because of process improvement. Nowadays, RO membranes take responsibility for approximately 96 % of the seawater desalination capacity in USA (Tu et al. 2010) and account for 60 % of the total worldwide desalination plants (Peñate and García-Rodríguez 2012, Wenten and Khoiruddin 2016). Table 1-4 shows some SWRO plants in the world.

Table 1-5 Seawater SWRO plants as examples

Country	Location	Capacity (m^3 d^{-1})	Year of begin operation	Membrane manufacturer
Algeria	Oran	500,000	2014	Hyflux
Australia	Dalyston	410,000	2012	---
Israel	Ashdod	384,000	2013	Pentair X-Flow
Israel	Ashkelon	330,000	2006	Dow
Australia	Perth	270,000	2013	---
Australia	Lonsdale	270,000	2013	Hyflux
United Arab Emirates	Fujairah	170,500	---	Hydranautics/Nitto

1.5 Solution-diffusion model for RO

Numerous mechanistic and phenomenological models have been developed to describe the separation of solvent and solute through RO membranes. The classical models include (Murthy and Choudhary 2012, Suchanek 2006): pore-flow models in the 1980s and 1990s in which different permeants are separated by size, frictional resistances and/or charge; the Kedem-Katchalsky and Spiegler-Kedem models which employ irreversible thermodynamic arguments to derive solute and solvent transport equations while treating the membrane as a "black box" and the solution-diffusion model. Among these models, most popular is the solution-diffusion model (Lonsdale et al. 1965). It has become the most widely accepted framework describing mass transport in pervaporation, gas permeation, dialysis and reverse osmosis (Geise et al. 2010, Marchetti and Livingston 2015, Paul 2004).

The solution-diffusion model was proposed to characterize transport in homogeneous and non-porous membranes (Wang et al. 2014). The solvent and solute molecules dissolve in the membrane nonporous layer at the feed-membrane interface, then each diffuses across the membrane due to its own chemical potential gradient, finally dissolve out at the membrane-permeate interface (Kong et al. 2015, Paul 2004). Fig. 1-1 illustrates a schematic of chemical potential, concentration (activity) and pressure in a homogeneous and non-porous membrane. The chemical gradient ($\Delta\mu$) is the result of concentration (activity) and pressure gradients across the membrane and is given by:

$$\Delta\mu_i = R_g T ln\Delta a_i + V_i \Delta P \qquad 1\text{-}1$$

where R_g is the gas constant, T is the temperature, α_i is the concentration of the solute or solvent, V_i is the molar volume and ΔP is the pressure differential across the membrane.

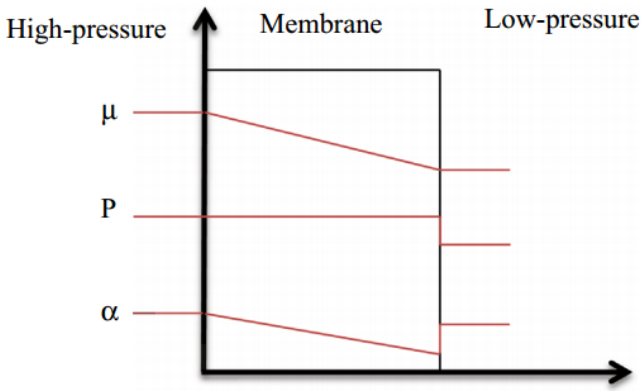

Figure 1-1 Schematic of chemical potential, concentration and pressure (Wang et al. 2014)

The solution-diffusion model was successfully employed for providing a reasonable description for transport of non-ionic and ionic species through RO membranes (Kataoka et al. 1991, Malek et al. 1994, Sekino 1993, Yaroshchuk 1995). Most recently, Hyun-Je Oh et al. (Oh et al. 2009) developed a model integrated multiple fouling mechanisms and the solution-diffusion theory to analyze the performance of RO processes for seawater desalination. It was also used to optimize the RO system to remove boron in low energy requirement. The solution-diffusion pore-flow fluid-resistance model was proposed by Toffoletto et al. (Toffoletto et al. 2010) to analyze the interaction between fluid and membrane permeability in several RO operations by using two different membranes. The results showed estimated and experimental results were in a good agreement, and the model was potential for process design and development applications. Copper rejection of a RO membrane was investigated by Csefalvay et al. (Csefalvay et al. 2009) with copper-sulfate and copper-nitrate solutions as model wastewater. The transport through the membrane was modelled in the function of time with the solution-diffusion model, and the results showed a good agreement between the experimental and the modelled fluxes. A solution-diffusion model was developed by Hung et al. (Hung et al. 2009) to simulate the boron rejection at different operating conditions in a RO process. The results demonstrated the prediction was good agreement with experimental data got from the lab-scale RO system. Srinivasan et al. (Srinivasan et al. 2009) proposed a mathematical model based on solution-diffusion mechanism for the RO module removing dimethyl phenol. The model predicted the permeate and rejection concentration within deviation of 19 and 2 %, respectively. Nir and Lahav (Nir and Lahav 2013) presented a new approach linked solution-diffusion

model and concentration polarization film-layer model to predict boron in the SWRO product water. Compared to the traditional approach, the new approach matched empirical results better.

1.6 Objectives of this thesis

Nowadays, industry has a significant impact on available water sources by consuming several billions m^3 of water a year, and faces the critical issues towards achieving the stringent wastewater discharge requirements. The issue of water shortage and the necessity for rational water management has thus increased the interest in the industrial wastewater treatment and reuse. The chemical industry is a keystone of the European economy, converting raw materials into thousands of different products. It provides the greatest potential for increasing sustainable development in industrial water management. In this view, the European E4Water project (http://www.e4water.eu/) aims at identifying the most suitable new wastewater treatment technologies or combination of technologies leading to the best solutions to produce water with the required quality in six chemical industrial sites.

As a case study of E4Water, a pilot-scale wastewater reuse process which is based on MBR and RO was conducted by the Complutense University of Madrid in a polyvinyl chloride (PVC) production site. An integrated water and energy management model (IWEMM) was proposed to simulate the water and energy behaviours in the production and wastewater reuse processes. IWEMM was intended to estimate and evaluate the economical and ecological effects of water reuse on natural water bodies in collaboration with life cycle assessment (LCA) and to optimize water treatment technologies and processes. It was also applied to analyse the potential for freshwater saving, valuable recovery and heat reuse for the European chemical industry. In the wastewater reuse process, MBR is the major operation unit for removing organics and RO is used for desalination. Therefore, to summarize, the main objectives of this thesis are following:

(1) Calibration and validation ASM1 for MBR performance simulation in terms of effluent ammonia and nitrate concentrations and mixed liquor suspended solids in

bioreactor.

(2) Development a modified aeration model with consideration of the effect of biomass concentration on oxygen mass transfer to analyze MBR energy consumption.
(3) Testing the reliability of MBR operation strategy to meet wastewater reuse requirements based on Latin Hypercube Sampling (LHS) procedure.
(4) Integrating the solution-diffusion model (SDM) and film theory to describe rejections of ions in RO process.
(5) Analyzing specific energy consumption of the RO process with consideration of limitation imposed by the thermodynamic restriction at various scenarios.
(6) Illustrating the behavior of integrated water and heat in the production and wastewater treatment processes of PVC production site in different scenarios.

2. Experimental set-ups and procedures

2.1 Production and wastewater reuse processes in the PVC site

The processes in the PVC site are divided into production and wastewater treatment processes. It includes already complex networks of water flows. As shown in Fig. 2-1, the flows in black are the existing production and wastewater treatment processes; the red part is the proposed wastewater reuse process. In the production process, a groundwater flow is pumped after demineralisation by ion exchanger (IE) and RO into the polymerization reaction tank. In order to stabilize the polymerization reaction, another groundwater flow is pumped into the polymerization tank shell as cooling water to remove excess heat. Afterwards the cooling water is pumped into a cooling tower to drop down the temperature before discharge into natural water bodies. The product of polymerization (i.e. slurry) is pumped into four strippers by means of four pipelines. Simultaneously, steam flows are injected into strippers to separate vinyl chloride monomer (VCM) from slurry, and send VCM back into the polymerization tank for reuse. After that, the slurry is pumped into four decanters to separate PVC and water. The separated PVC is pumped into a dryer to remove water to finally receive the PVC product. The four separated water flows are pumped into the polymerization tank for reuse, in which one flow is reused directly and the others are pre-treated before reuse.

A part of the wastewater (about 100 m^3 h^{-1}) is pumped from the polymerization tank

into the buffer tank to enter the wastewater treatment process. Then the wastewater is distributed to another buffer tank R-216, and a flocculation tank R-206 where it is treated by flocculation using hypochlorite and poly-aluminium chloride. In the next step, it is neutralized with NaOH in the tank R-207. Part of the treated water is pumped back to the buffer tank for adjusting the concentration and the remaining part is discharged after pH- and turbidity-control into a pipeline together with other wastewaters. This pipeline ends offshore in the Mediterranean Sea. It was aimed to increase the closure of the water loop by cascaded treatment units, which are marked in red in Fig. 2-1. The water after treatment will be reused from tank R-214 to the polymerization reaction.

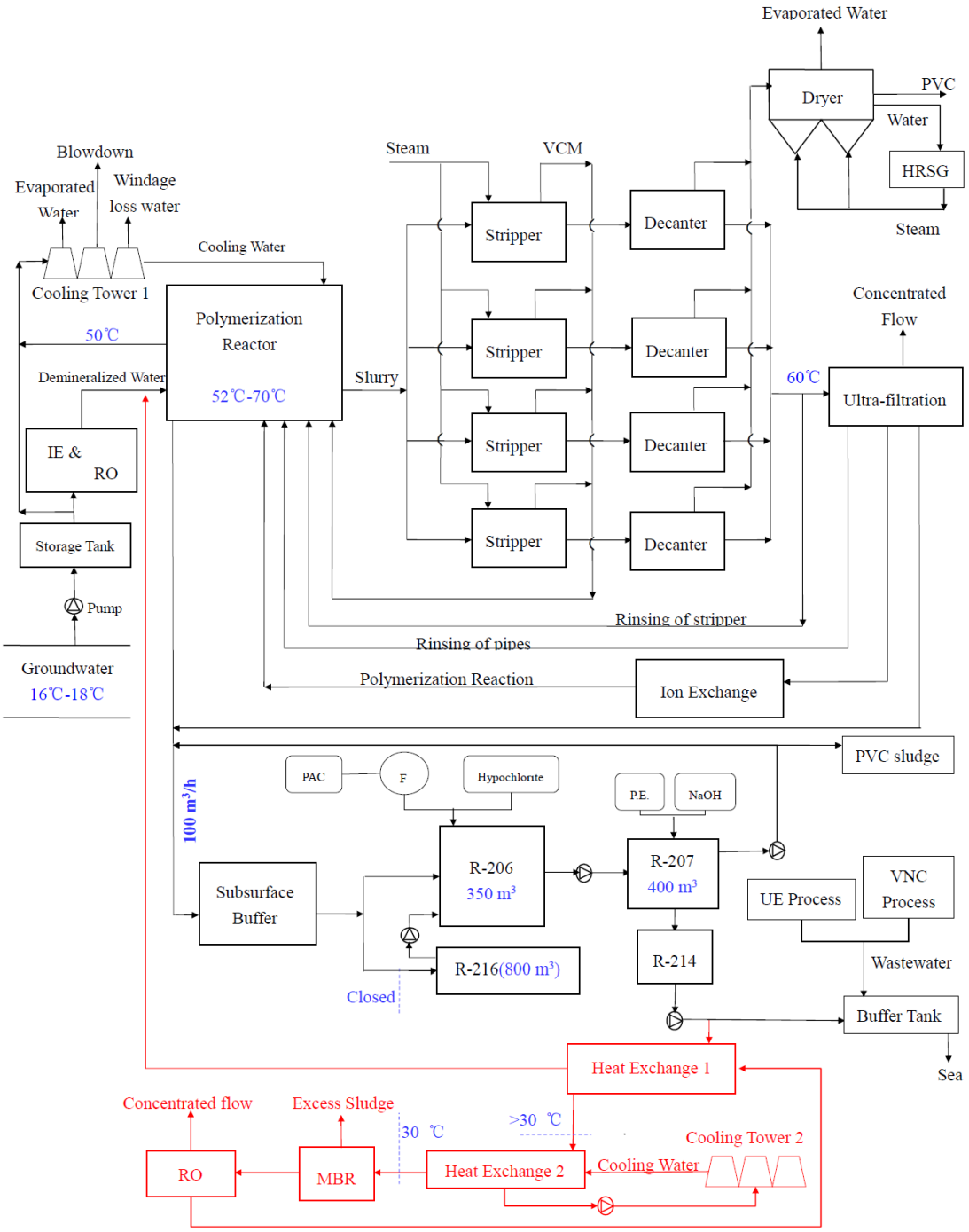

Figure 2-1 Flow scheme of the PVC site

For the determination of design and operational parameters, a pilot-scale MBR and RO process for wastewater treatment and reuse at the PVC production site has been installed, as shown in Fig.2-2. It was operated by the E4Water project partner, Complutense University of Madrid (UCM), from March 2014 to April 2015. Since the temperature of production process wastewater is up to 60 °C and because of the temperature limitation of the membrane material and the bio-sludge stability, it is

necessary to cool down the wastewater before entering the MBR and RO process. The wastewater was cooled down by two heat exchangers. The RO permeate flow is returned back to the first heat exchanger (Heat Exchanger 1) to cool down the wastewater from the PVC production process, and it will be heated up for energy saving to produce PVC resin. Then, the wastewater will be further cooled down by the cooling water coming from a cooling tower in the second heat exchanger (Heat Exchanger 2) to achieve a temperature of 25 to 35 °C. The details of operation units in the pilot plant are introduced in the following sections.

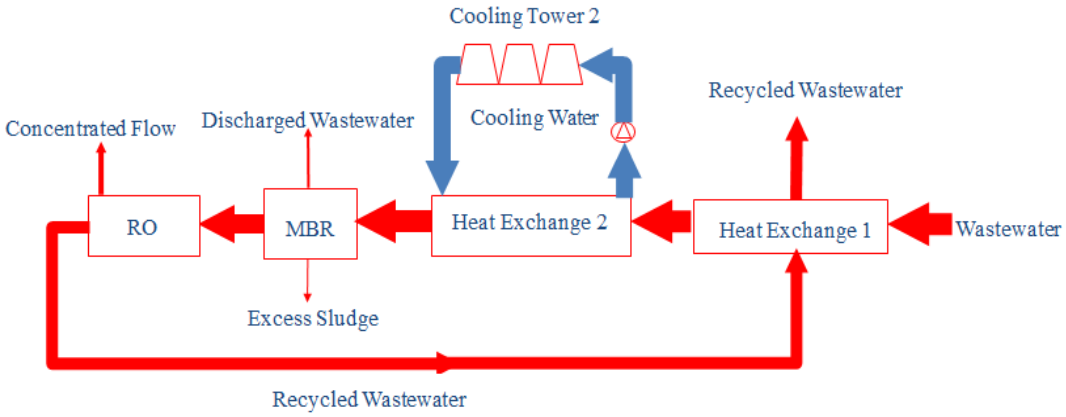

Figure 2-2 Pilot wastewater treatment and reuse process

2.2 MBR system configuration and operation

2.2.1 MBR system description

As shown in Fig.2-3, the pilot-scale MBR process produced an average effluent flow of 60 m^3 d^{-1} for the following reverse osmosis (RO) in demineralization step. An outside/in ultrafiltration hollow fibre membrane train (ZeeWeed-500D) from Zenon (GE, USA) was used for the ultrafiltration step. The polymer wastewater was treated in physicochemical treatment process (PCT) as pre-treatment and buffering, in which poly-aluminium chloride (PAC) and NaClO was added to remove particles. Then, effluent from PCT was cooled from 75 to 30 ºC by heat exchanger and was pumped to the MBR process. In order to avoid high solids content may enter in the biological treatment in case of problems during clarification step, two filters in parallel (500 µm) were installed. Pre-filters were installed prior to heat exchanger in order not to damage it in case of failures during the clarification step. The detail dimensional and operational

parameters is showed in Table 2-1.

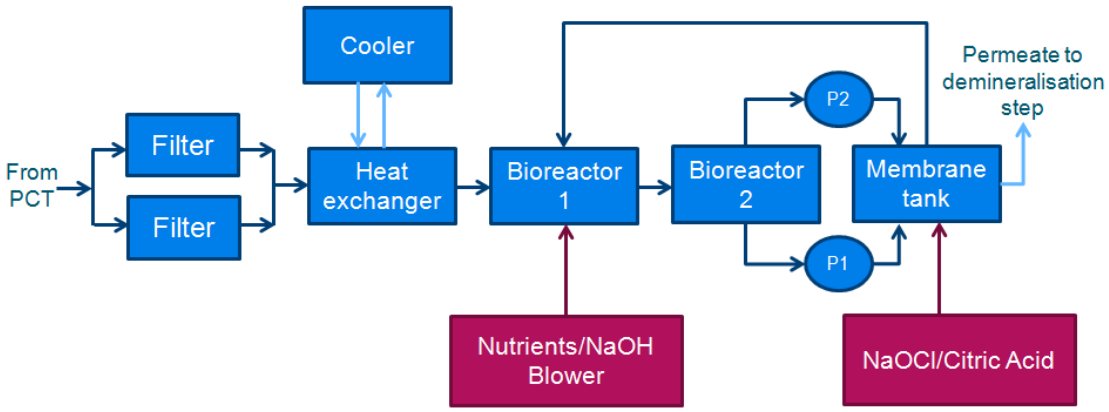

Figure 2-3 The flow diagram of the MBR system (Blanco et al. 2015)

Table 2-1 Pilot MBR dimensions and operational parameters

Parameter	Unit	Value
Bioreactor 1		
Volume	m^3	7
Bioreactor 2		
Volume	m^3	11
Membrane Tank		
Volume	m^3	2
Membrane surface	m^2	3×31.6
Membrane mean pore size	µm	0.04
Membrane flux	$L\ m^{-2}\ h^{-1}$	15-25
Filtration time	s	600
Backwash time	s	40
Backwash flux	$L\ m^{-2}\ h^{-1}$	10-26
Recirculation flow	$m^3\ d^{-1}$	180

As shown in Figs.2-3 and 2-4, Bioreactor 1 equipped with agitator was used to test anoxic conditions. A sensor level was installed for controlling wastewater feeding and hydraulic retention time (HRT). Air diffusers were also installed for testing full aerobic

conditions. Bioreactor 2 stocked with membrane air diffusers was used to apply aerobic conditions. A pipe fixed in the bottom of the tanks connected both bioreactors. Hence, Bioreactor 2 was full of bio-sludge coming from the Bioreactor 1. Three hollow fibre membrane trains (31.6 m^2 each) were submerged in a 2 m^3 membrane tank with intermittent aeration. For feeding the membrane tank, two pumps were used: a submerged pump inside the Bioreactor 2 (P1), which supplied 10 m^3 h^{-1} as the maximum flow and it was controlled by a manual rotameter; and an external screw pump (P2), which was used for increasing bio-sludge recirculation between Bioreactor 2 and membrane tank (in the range of 0-8 m^3 h^{-1}). These pumps were continuously controlled by the programmable logic controller (PLC) and were used for testing the recirculation ratio effect on the MBR performance. Next to membrane tank was installed a smaller tank for collecting MBR permeate, which was used for clean-in-place (CIP) cleanings and back-pulse cycles.

Figure 2-4 A sight of MBR in the PVC site (Blanco et al. 2015)

2.2.2 MBR operation phases

The operation can be divided into four phases:

Phase 1: bio-sludge adaptation, from March 2014 to July 2014. MBR seeding was done using bio-sludge from an existing VCM production wastewater treatment plant. The seedings were continued for achieving a solid content close to 3 g L^{-1} at the beginning of the experiments. In addition, bio-sludge got from a municipal wastewater treatment plant was added two weeks after the start-up with the aim to provide enough nitrifying bacteria for the biological treatment. Lower flux values and higher hydraulic retention time (HRT) were implemented for improving bacteria stabilization and adaptation.

Phase 2: nitrification/denitrification at low recirculation ratio (R=3), from July 2014 to December 2014. After bio-sludge adaptation to polyvinyl alcohol (PVA), which means PVA in the wastewater was completely degraded by the biological activity, different HRT and sludge retention time (SRT) were studied for testing and optimizing the biological treatment in anoxic-aerobic conditions using low recirculation ratio. In this phase, membrane feeding flow was set at 10 m^3 h^{-1} using only pump P1. Both denitrification and nitrification processes were tested under anoxic and aerobic conditions, respectively. Besides a complete PVA removal, another main purpose was to reduce the ammonium in the permeate below 2 mg L^{-1}. In addition, a complete BOD_5 removal is necessary for assuring a suitable performance as further reduction of conductivity is required. PVC effluent was fed to Bioreactor 1 as it is known that anoxic bacteria show better performance when the carbon source is directly supplied. The air flow in Bioreactor 2 was set to provide a DO of at least 2 mg L^{-1}. Once a complete ammonium removal was achieved in the aerobic reactor, the amount of nitrate subjected to be transformed into nitrogen gas in the anoxic tank was dependent on the recirculation ratio between the membrane tank and the anoxic reactor. At low recirculation ratios, nitrogen removal and nitrate concentration have been evaluated.

Phase 3: nitrification/denitrification at high recirculation ratio (R=6), from December 2014 to February 2015. Results from MBR treatment using a higher recirculation ratio (R=6) in anoxic/aerobic conditions were collected and compared with phase 2 to assess the influence of this parameter.

Phase 4: full aerobic conditions, from February 2015 to April 2015. With the aim to test full aerobic conditions, several membrane air diffusers were installed in Bioreactor 1. In this phase, both Bioreactors 1 and 2 worked as aerobic bioreactors. Removal of organics and nitrogen was then evaluated under these conditions.

2.2.3 MBR influent characterization

A typical suspension polymerization technique which is used to produce almost 80 % PVC in the world (Tacidelli et al. 2009), is employed in the PVC production site. Concentrations of the important parameters are listed in Table 2-2; phosphate concentration is relatively low. Compared to the wastewater characterized by Sun et al

(Sun et al. 2013), the concentration of COD, PVA and NH_4-N of wastewater used in this study are 120, 2,330 and 370 % higher, respectively. Similar to described by Sher et al. (Sher et al. 2013), the PCT process removed total suspended solids (TSS) and turbidity up to 91 % and 99 % respectively, and can buffer the influent to benefit MBR process performance.

Table 2-2 Average characteristics of wastewater used to feed the MBR

Variable	Unit	Average	STD.
PVA	mg L^{-1}	35	17
COD	mg L^{-1}	322	223
COD_f	mg L^{-1}	188	35
BOD_5	mg L^{-1}	109	59
TOC	mg L^{-1}	65	10
TN	mg L^{-1}	38	9
NH_4-N	mg L^{-1}	30	8
PO_4-P	mg L^{-1}	0.02	0.01
Conductivity	µS cm^{-1}	1,102	150
pH	-----	7.7	0.4

2.3 RO configuration and operation

2.3.1 RO system description

The RO system in the PVC production site is represented in Fig.2-5. A 750 L buffer tank was installed to collect the MBR effluent for feeding to the RO process. A pipe was fixed at the bottom of the buffer tank. So, water was available for feeding RO system even when back pulse cycles were performed in the MBR. RO was only stopped during the clean-in- place (CIP) system of the MBR which was operated for approximately 7 minutes about 5 times every day. Intensive chemical cleaning was performed once a month. For these occasions, a flushing with RO permeate and biocide was applied for avoiding biofouling in the RO membranes. As shown in Fig.2-5, the RO system comprises two passes and each pass consists of three modules with 2:1 array ratio configuration. Each module has five 8.73 m^2 membrane elements. The high rejection membranes, FILMTEC™ LC HR-4040, used during the piloting were

supplied by Dow Chemical, Netherlands. Permeate from the first pass was collected in a CIP tank installed inside the RO container for feeding the second pass. This permeate was also used for back flushing cycles. Because of the high rejection, the absolute concentration of ions in the permeate from Pass 2 were very low resulting in a relatively low accuracy of concentration analysis. Indeed, for these series of measurements the permeate concentrations were mostly less than 0.05 mg L^{-1}. Therefore, only the ion rejections and energy consumptions in Pass 1 were analyzed in this thesis.

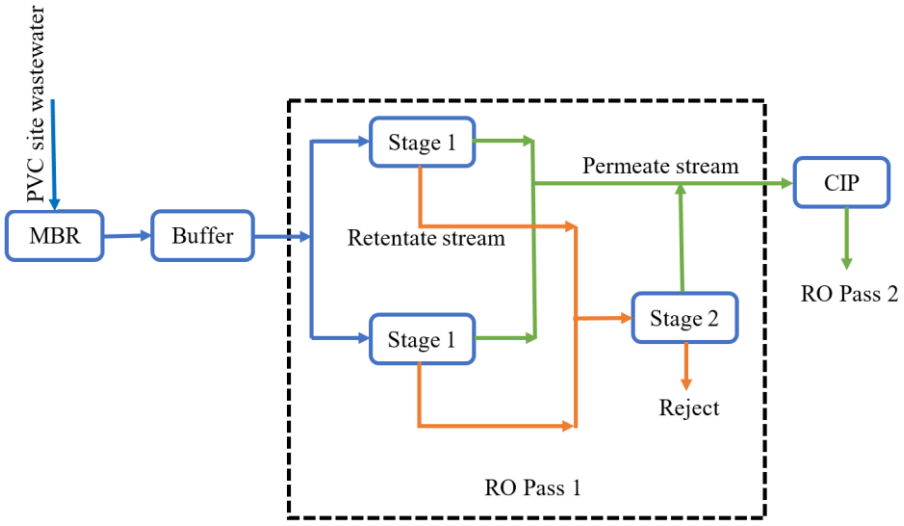

Figure 2-5 Schematic of the pilot-scale RO process

2.3.2 RO operation phases and influent characteristics

For RO pass 1, two phases were tested during the RO piloting in terms of water recovery. The first phase was from 18th July 2014 to 10th February 2015, the recovery was set at 60 %. The recovery was set at 76 % in the second phase from 10th February 2015 to 29th April 2015. Operational conditions are listed in Table 2-3. Table 2-4 shows the average concentrations of the important influent ions in the two phases.

Table 2-3 Average operational values during RO piloting

	Phase 1	Phase 2
T (ºC)	29.2	28.5
Permeate flow of stage 1 (m^3 h^{-1})	0.94	1.2
Permeate flow of stage 2 (m^3 h^{-1})	0.64	0.65

	Phase 1	Phase 2
Total permeate flow ($m^3 h^{-1}$)	1.58	1.85
Reject flow ($m^3 h^{-1}$)	1.05	0.59
Flux (LHM)	12	14
Membrane area (m^2)	131	
Recovery (%)	60	76

Table 2-4 Average characteristics of MBR effluent used for feeding the RO

		Phase 1		Phase 2	
Variable	Unit	Average	STD.	Average	STD.
Cl^-	mg L^{-1}	280.00	51.55	296.22	116.04
SO_4^{2-}	mg L^{-1}	25.90	14.20	40.69	30.23
Ca^{2+}	mg L^{-1}	28.24	12.90	36.29	15.37
Mg^{2+}	mg L^{-1}	6.99	3.60	8.69	4.74
Na^+	mg L^{-1}	210.50	35.78	211.43	39.05
K^+	mg L^{-1}	15.00	4.68	15.87	5.62

3. Integrated water and energy management model for the PVC site

The IWEMM was developed in Simba software (ifak - Institut fuer Automation und Kommunikation e.V., Magdeburg, Germany). As shown in Fig.3-1, IWEMM mainly includes blocks of operating units in production process such as polymerization reactor, cooling tower, stripper, decanter and dryer, and operating units in wastewater treatment process like ultrafiltration, buffer tank, ion exchange unit, physicochemical treatment unit, heat exchanger, cooling tower, RO and MBR. The mathematical models developed for the operating units were included in the blocks. These blocks were divided into three types. The yellow block is scenario definition block. As shown in Fig.3-2 it is used to define different PVC production capacities, groundwater and cooling water temperatures and wastewater reuse ratio scenarios. It also includes some values of physical parameters for calculation. Blue ones are models of the operating units, which are used to simulate the water and heat characteristics in the operating units. Each blue block contains the material and energy balance model. In addition, several special models were developed and included in blocks for cool tower, heat exchanger, MBR

and RO. The details of these models are discussed in the next sections. These blocks are connected by the defined flows and receive values from the scenario definition block via the grey signal lines. The block updates flow variables entering and leaving with the calculated results. The two green blocks are used to transfer the model results as life cycle assessment (LCA). Those results have been applied in Gabi software. IWEMM can be used to simulate the integrated water cycle and heat flows in the PVC production site. Moreover, all the compounds included in the model can be traced. The traced substance is marked by bold lines and the mass flow rate or concentration will be indicated in the flow line. The enlarged diagrams of IWEMM are added in Figs.7-1 and 7-2 in the Appendix.

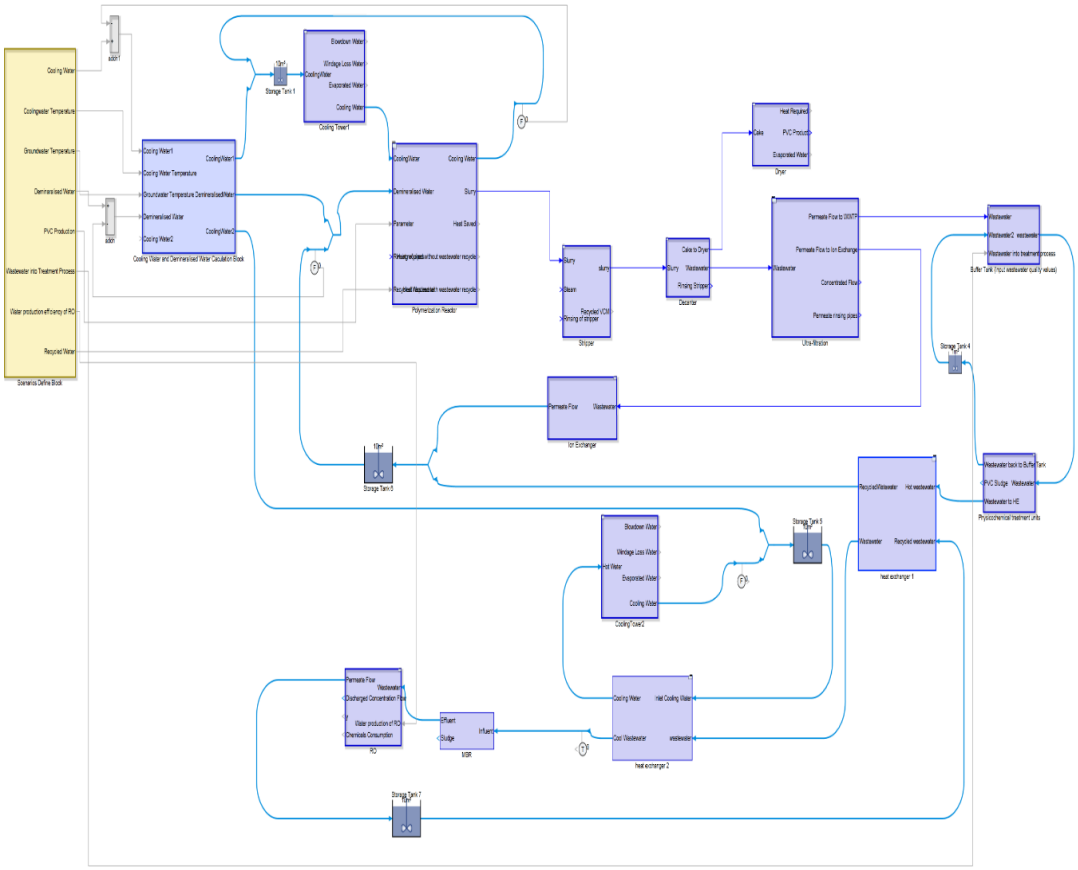

Figure 3-1 Structure of IWEMM

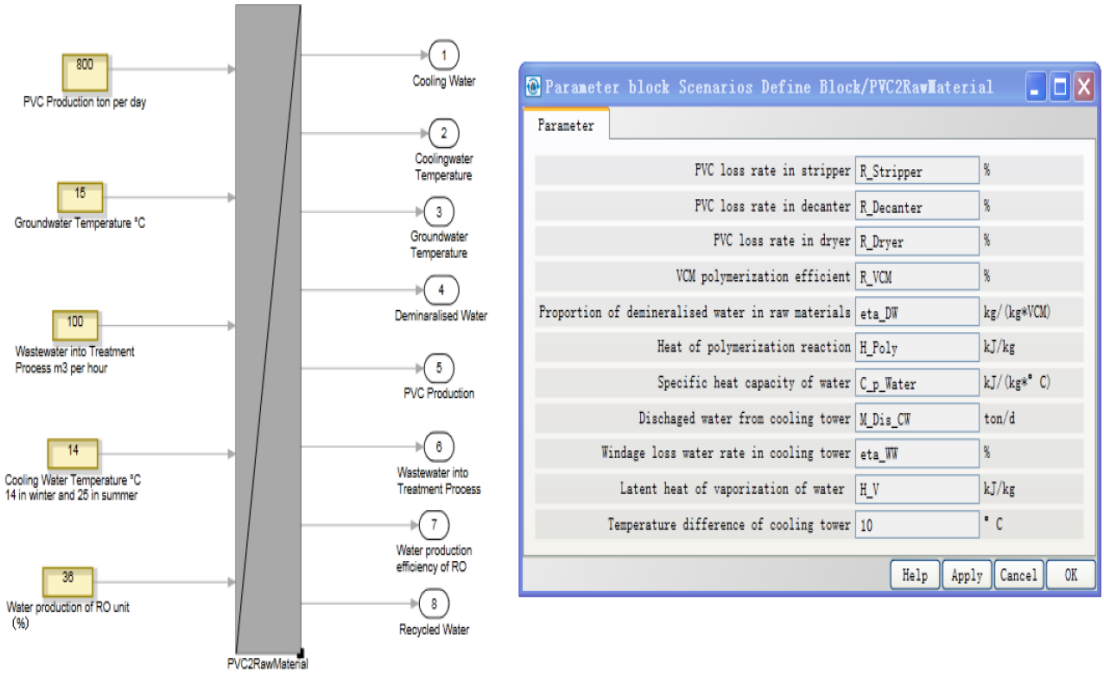

Figure 3-2 Scenario definition block

3.1 Simulation of MBR system

3.1.1 Steady and dynamic state plant modelling

As shown in Fig.3-3, a MBR process model for dynamic simulations based on Fig. 2-3 and Table 2-2 was developed in Simba (ifak GmbH, Magdeburg, Germany). ASM1 (Henze et al. 2000) with the default parameter set from mbr_asm1hsg (Hochschulgruppe Simulation, http://www.hsgsim.org) (Alex et al. 2007) was applied as the bio-chemical model for organic matter and nitrogen. The default values of the parameters in ASM1 and mbr_asm1hsg are showed in Table 4-2. The influent and effluent quality data in total 100 days from September 2014 to December 2015 were collected to calibrate the model. Then, the steady state validation of the process model was conducted using the data showed in Table 2-2. Moreover, another 30 data sets were chosen randomly for the dynamic validation.

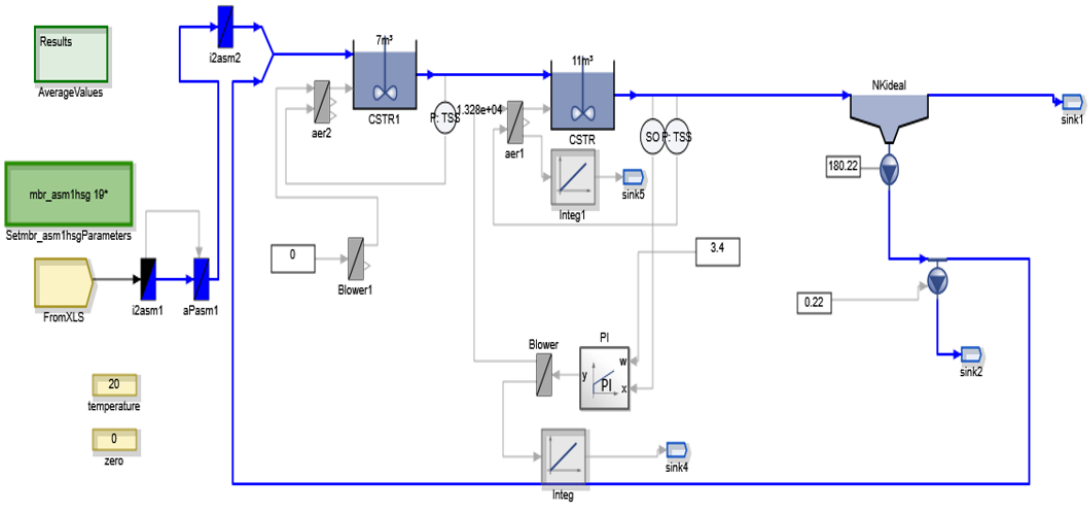

Figure 3-3 MBR system model developed in Simba

3.1.2 Energy consumption modelling

Since the MBR process model prediction results will be employed for energy consumption calculations, it is exceedingly significate to use an adequate aeration model. With consideration of the effect of MLSS on oxygen transfer (Germain et al. 2007, Judd and Claire 2010, Verrecht et al. 2008), a modified and extensive version of the aeration model described by Verrecht et al. (Verrecht et al. 2010a) was adopted in this thesis.

$$AOTR = SOTR \cdot \varphi^{(T-20)} \qquad 3\text{-}1$$

$$SOTR = k_L a \cdot (SDO - DO) \cdot V \qquad 3\text{-}2$$

$$\alpha = e^{-w \cdot MLSS} \qquad 3\text{-}3$$

$$k_L a = \frac{\alpha \cdot R_{air} \cdot h}{SDO \cdot V} \cdot F \cdot V_{air} \qquad 3\text{-}4$$

As shown in Table 3-1, the parameter values in Eqs. 3-1 to 3-4 are mean values or at least in the range of reported values (Maere et al. 2011). In this study, the MBR process

was operated without control strategies for open loop operation, the aeration flow into the aerobic zone varied from 1.8 to 5.5 $Nm^3\ h^{-1}\ m^{-3}$. At a MLSS of about 5 g L^{-1}, 1.8-2.7 $Nm^3\ h^{-1}\ m^{-3}$ was sufficient. However, with higher MLSS and higher temperature, air flow was increased to 4.5- 5.5 $Nm^3\ h^{-1}\ m^{-3}$ to assure DO in the aerobic tank is at around 3.4 mg L^{-1}. In addition, energy consumption of aeration and pumping was adapted in kWh d^{-1}. The aeration energy ($AE_{bioreactor}$) over the simulation period t_{ev} is given by:

$$AE = \frac{24}{t_{ev}} \cdot \int_0^{t_{ev}} \frac{V_{air}(t) \cdot \rho_{air} \cdot R \cdot T_{in}}{24 \cdot 3600 \cdot C_{SI} \cdot n \cdot b_e} \cdot \left[\left(\frac{P_{out}}{P_{in}}\right)^n - 1\right] \cdot dt \qquad 3\text{-}5$$

$$P_{out} = \rho_{WW} \cdot g \cdot h + P_{in} + P_{loss} \qquad 3\text{-}6$$

Pumping energy for sludge (PE_{sludge})in this study was derived from four pumped flows: influent (Q_{inf} - $m^3\ d^{-1}$), membrane tank influent (Q_{MT} - $m^3\ d^{-1}$), excess sludge discharge flow (Q_w - $m^3\ d^{-1}$), return activated sludge flow (Q_r - $m^3\ d^{-1}$). According to the values for the MBR plant in Schide, Belgium, the pumping energy factor for influent was set as 0.034 kWh m^{-3} (Fenu et al. 2010b). 0.0075 kWh m^{-3} was applied as the pumping energy factor for membrane tank influent and return activated sludge flow, referred to values of the MBR plants in Nordkanal and Varsseveld (Fenu et al. 2010b). 0.05 kWh m^{-3} for excess sludge discharge flow was taken from benchmark simulation model for MBR (BSM-MBR) (Maere et al. 2011). Pumping energy ($PE_{effluent}$) relating to effluent (Q_{eff} - $m^3\ d^{-1}$) was calculated also using a pumping energy factor of 0.075 kWh m^{-3} from Schide. Furthermore, a typical mixing energy (ME) factor 8 W m^{-3} was applied for the anoxic, aerobic and membrane tanks (Verrecht et al. 2010b).

Table 3-1 Aeration energy consumption parameter values

Parameter	Unit	Value	Parameter	Unit	Value
φ	---	1.024	T	°C	20
SDO	g m^{-3}	8.637	V	m^3	11
ω	---	0.056	R_{air}	g m^{-3} m^{-1}	18
h	m	2.8	F	---	0.8

Parameter	Unit	Value	Parameter	Unit	Value
ρ_{air}	kg m^{-3}	1.2	R_g	J mol^{-1} K^{-1}	8.314
T_{in}	K	293.15	C_{SI}	---	29.7
n	---	0.283	b_e	---	0.5
P_{in}	Pa	101,325	ρ_{WW}	kg m^{-3}	1,000
g	m s^{-1}	9.81	P_{loss}	Pa	13,789

3.1.3 Scenario analysis

After the calibration and validation of the MBR process model, a procedure of scenario analysis (SCA) was performed to analyze the effect of sludge retention time (SRT), recirculation ratio (R) and dissolved oxygen (DO) on aeration energy demand and effluent quality. A data set of influent quality in 37 days got from the pilot-scale MBR process which ran under normal conditions was applied as input of SCA. Using the values described below, 720 different scenarios can be employed to study the impact on aeration energy demand and nitrogen removal.

- SRT: 9 values between 0.19 and 1.54 m^3 d^{-1} for the excess sludge discharge rate was used which resulted in SRT ranging from 10 to 80 days.
- R: 8 equally spaced values between 60 and 480 m^3 d^{-1} was used resulting in recirculation ratio from 1 to 8.
- DO: 10 equally spaced values between 0.5 and 4 mg L^{-1} was applied.

3.1.4 Uncertainty analysis procedure

Application of ASM1 is generally based on some uncertainties and assumptions of influent composition and model parameter values (Sin et al. 2005). Due to the limited information about the exact parameter value, the uncertainty is characterized by a certain range of values in the model. The uncertainty analysis is able to gain probability distributions of model outputs to infer the mean, variance and quantiles of model predictions (Helton and Davis 2003). In this study, the procedure of uncertainty analysis involved the following four steps (Sin et al. 2011, Sin et al. 2009) :

(1) specifying the uncertainty of stoichiometric, biokinetic and influent parameters for ASM1
(2) sampling the uncertainty
(3) propagating the uncertainty through ASM1 to get the uncertainty of model outputs
(4) representation and interpretation probability distributions

In step 1, an expert review process was conducted, and the result of uncertainty specifying for this study was summarized in Table 4-4 (Henze et al. 1987, Henze et al. 2000, Spérandio and Espinosa 2008). Then, Latin Hypercube Sampling (LHS) was employed to get a sampling matrix in step 2. The row and column corresponds to samples and parameters in matrix, respectively. In step 3, ASM1 simulations were performed based on the sampling matrix. Finally, the results were represented in terms of percentiles and cumulative distribution functions (CDF). It should be pointed out that the correlation of the input parameters was not considered in step 2 since there is no exact information about the correlation.

3.2 Simulation of reverse osmosis

3.2.1 Solution-diffusion model

In RO membranes, differences in solubility and diffusivity of permeates resulted in the separation phenomenon. The RO membrane performance can be judged both by the volume of the water flux (J_w) and the percentage of salt rejection (R) (Yun et al. 2011). J_w derives from Henry's law and Fick's first law of diffusion, which is associated with water permeability (A) as follows (Lopes et al. 2015):

$$J_w = A(\Delta p - \Delta \pi) = \frac{Q_p}{a} \qquad 3\text{-}7$$

where A is the water permeability coefficient, Δp is transmembrane pressure, $\Delta \pi$ is the osmotic pressure difference between feed and permeate solutions. Q_p is the product water flow rate, a is the membrane area. The osmotic pressure gradient ($\Delta \pi$) is calculated based on van't Hoff law using the following equation (Hung et al. 2011):

$$\Delta\pi = R_g T \sum_{i=1}^{N} \Delta M_{s,i} = R_g T \sum_{i=1}^{N} \left(M_{f,i} - M_{p,i}\right) \quad 3\text{-}8$$

In which, R_g is the gas constant, T is the temperature, i is the number of dissolved solute i.e. ions and non-electrolyte solutes, $\Delta M_{s,i}$ is the dissolved solute molar concentration difference between feed and permeate streams, $M_{f,i}$ and $M_{p,i}$ are molar concentrations in the feed and permeate streams, respectively. The solute flux (J_s) derives from Fick's law which is based on the assumption that the driving force is almost entirely because of concentration differences:

$$J_s = J_w C_p = B\left(C_m - C_p\right) \quad 3\text{-}9$$

Where B is solute permeability, C_m and C_p are the solute concentrations at the retentate side of the membrane and permeate stream, respectively. The definition of solute rejection by a membrane is either the observed rejection (R_o) or real rejection (R_r). Observed rejection is calculated from feed concentration (C_f) and the permeate concentration (C_p) according to:

$$R_o = 1 - \frac{C_p}{C_f} \quad 3\text{-}10$$

while the real rejection is calculated from membrane surface and the permeate concentrations as:

$$R_r = 1 - \frac{C_p}{C_m} \quad 3\text{-}11$$

Here, the difference between C_m and C_f is due to rejected solute concentration polarization. Combining Eqs. 3-7, 3-10 and 3-11, the real rejection can be written as:

$$R_r = \frac{J_w}{J_w + B} \quad 3\text{-}12$$

3.2.2 Solution-diffusion-theory model

In the RO membrane separation process, the rejected salt accumulates near the retentate side resulted in the salt concentration increase, which causes the concentration polarization phenomenon. The concentration polarization can reduce the permeate stream production because of the osmotic pressure increase (Anqi et al. 2015). The material balance based on the film theory and relevant boundary conditions is given as (Murthy and Chaudhari 2009a):

$$\left(\frac{C_m - C_p}{C_f - C_p}\right) = exp\left(\frac{J_w}{K}\right) \qquad 3\text{-}13$$

where K is the mass transfer coefficient. When K increases, which can be achieved by increasing the crossflow rate across the membrane surface, C_m will decrease and thereby decrease the effect of concentration polarization. Substitute Eqs. 3-10 and 3-11 into Eq. 3-13, the relation between observed rejection (R_o) and real rejection (R_r) is given as:

$$\frac{R_o}{(1-R_o)} = \left[\frac{R_r}{1-R_r}\right]\left[exp\left(-\frac{J_w}{K}\right)\right] \qquad 3\text{-}14$$

Combining Eq. 3-12, Eq.3-14 is rearranged as the following equation:

$$R_o = \frac{\frac{J_w}{B}\left[exp\left(-\frac{J_w}{K}\right)\right]}{1+\frac{J_w}{B}\left[exp\left(-\frac{J_w}{K}\right)\right]} \qquad 3\text{-}15$$

In this thesis, Eq. 3-15 is the working equation for SDFM. By means of the non-linear parameter estimation technique, unknown membrane characteristic parameters in Eq. 3-15 (i.e. B and K) can be determined by the data of R_o and J_w obtained from experiment.

3.2.3 Energy analysis model

In practice, RO membrane processes are predominantly in the cross-flow configuration.

Moreover, membrane elements are general in series connections in several 6-8 m long pressure vessels. The multi-stage RO process is general deemed to be a longer pressure vessel if there is no inter-stage booster pump (Liu et al. 2011). Due to the pressure drop and the resultant energy consumption in the membrane channel pertaining to friction are assumed to be a constant, more attentions are payed on the major mechanistic points in the following analysis.

When V_f water is pumped into a cross-flow RO process under pressure P, the energy consumption can be simply calculated by (Wilf 1997):

$$E = V_f P \tag{3-16}$$

In the RO process, there are permeate and retentate flows. The energy required for permeate flow production (E_p) and energy remaining in the retentate flow (E_r) can be expressed by:

$$E_p = Y V_f P \tag{3-17}$$

$$E_r = (1 - Y) V_f P \tag{3-18}$$

In which, Y is the recovery defined as $Y=V_p/V_f$. where V_p is the volume of permeate. Generally, the specific energy consumption (SEC) defined as the energy required for per unit permeate production is applied to judge energy consumption performance of RO process. It can be determined by the energy and permeate volume:

$$SEC = \frac{P}{3.6\times10^6} \tag{3-19}$$

The unit of pressure P in Eq. 3-19 is Pa. For convenience, the unit of specific energy consumption calculated by Eq. 3-19 is in kilowatt-hour (kWh) which equals to 3.6×10^6 J. With the osmotic pressure increase due to the high permeate flux, it could be probable to approach the applied transmembrane pressure which is called thermodynamic restriction phenomenon. The specific energy consumption (at a given permeate recovery) for a RO system which operate until the thermodynamic restriction can be

expressed as:

$$SEC = \frac{R_o \pi_f}{Y(1-Y)} = \frac{f_{oc}(C_f - C_p)}{Y(1-Y)} \quad 3\text{-}20$$

Where R_o is the membrane observed rejection, π_f is the feed flow osmotic pressure, Y is the recovery, f_{oc} is the osmotic pressure coefficient (Pa L mg^{-1}), C_f and C_p are feed and permeate concentrations, respectively. The osmotic pressure of the retentate stream can be derived from its salt concentration:

$$\pi_r = f_{os} C_r = f_{os} \frac{C_f}{1-Y} \quad 3\text{-}21$$

Where f_{os} is the osmotic pressure coefficient (Pa L mg^{-1}), C_r and C_f are salt concentrations in retentate and feed streams.

At the limit imposed by thermodynamic restriction, the driving pressure applied in the RO process equals to the osmotic pressure at the end of the membrane channel (Oi et al. 2012, Zhu et al. 2010). In that case, the required driving pressure can be given by (Song et al. 2003):

$$P = \frac{f_{os} C_f}{1-Y} \quad 3\text{-}22$$

Then, the specific energy consumption can be derived from substituting Eq. 3-22 into Eq.3-19:

$$SEC = \frac{f_{os} C_f}{3.6 \times 10^6 (1-Y)} \quad 3\text{-}23$$

Consequently, in this study the specific energy consumption of the pilot-scale RO process was obtained from Eq. 3-20 before thermodynamic restriction (TR), but from Eq. 3-23 after thermodynamic restriction (TR).

3.3 Cooling tower model

The cooling tower can be regarded to be a heat exchanger in which air and water contact with each other directly. It is a heat removal device which is used to transfer waste heat to the atmosphere. The important operating features of cooling towers include the cooling range, approach, cooling load, blow-down and make-up. The cooling range is the temperature difference between the entering-water and cooled-water. The approach is the difference in temperature between cooled-water and entering-air wet bulb temperature. The cooling tower efficiency can be expressed as Eq.3-24. The temperature difference between entering- and cooled-water $\left(\Delta T_{i,o} = T_i - T_o\right)$ normally ranges 10 – 15 °C; and in this case the value for the PVC production site is around 10 °C.

$$\mu_{CT} = 100\times (T_i - T_o)/(T_i - T_{wb}) \qquad 3\text{-}24$$

Where μ_{CT} is the cooling tower efficiency, T_i is entering-water temperature, T_o is cooled-water temperature and T_{wb} is the wet bulb temperature of air.

The schematic process flow diagram for a commonly used wet evaporative cooling tower is showed in Fig. 3-4. The material balance is determined by the operating variables of evaporation and windage losses, make-up flow rate, the concentration cycles and draw-off rate. The water balance model is described in Eq. 3-25. The blow-down is the water which has to be discharged from the cooling tower to prevent the formation of precipitates and scaling inside of the tower. The make-up water is added to the circuit to replace water removed by evaporation, windage loss and blow-down. For the calculation of the make-up water requirement, a few general assumptions were applied in the performance model. As described in Eq. 3-26, the mass of evaporated water is calculated assuming the amount of heat transferred in the tower is 100 % due to evaporation. The windage loss, which represents water droplets that are carried away by the convective flow, is assumed to be between 0.01 % and 0.2 % of the circulating water flow rate (Lucas et al. 2012). The blow-down is typically calculated based on the evaporation losses and the concentration of dissolved minerals. As the cooling tower blow-down in the PVC production site is known and constant at steady state, the

calculation for the determination of blow-down was not incorporated in the model.

$$M_{Make-up} = M_{EW} + M_{WW} + M_{DW} \quad 3\text{-}25$$

$$H_v \times M_{EW} = M_{CW} \times \Delta T_{i,o} \times C_{p,W} \quad 3\text{-}26$$

$$M_{WW} = \eta_{WW} \times M_{CW} \quad 3\text{-}27$$

Where $M_{Make-up}$ is make-up water, M_{EW} is the evaporated water, M_{WW} is windage loss water, M_{DW} is the blow-down water, H_v is latent heat of vaporization of water, M_{CW} is the circulating water, $\Delta T_{i,o}$ is the temperature difference between entering- and cooled- water, $C_{p,W}$ is specific heat capacity of water, η_{WW} is windage loss ratio.

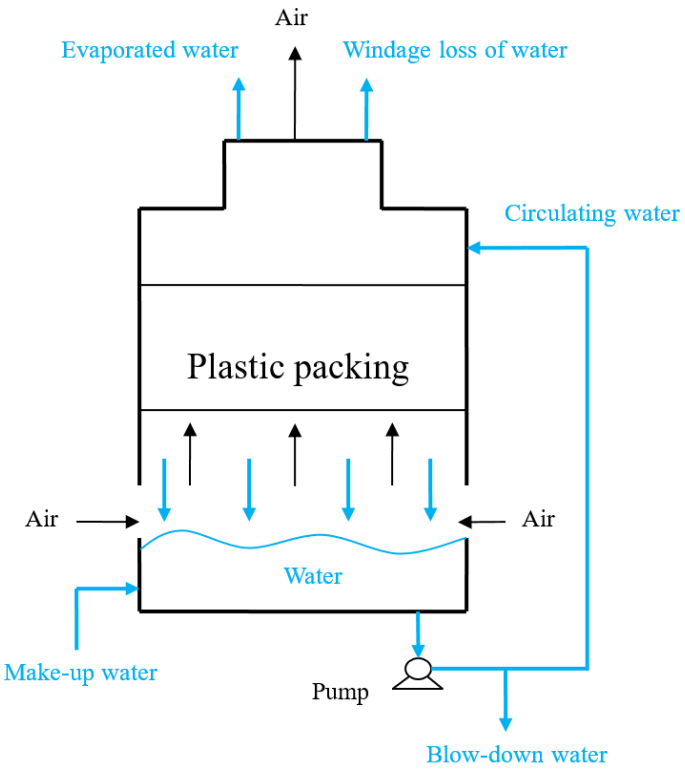

Figure 3-4 Schematic process flow diagram for wet evaporative cooling tower

3.4 Heat exchanger model

Hereinafter a model for a counter current heat exchanger is provided. The required energy can be determined with:

$$Q_h = A_{ex}\, k_{ex}\, \Delta T_{log} \tag{3-28}$$

Where the log-mean temperature difference is defined as:

$$\Delta T_{log} = \frac{(T_{h,in} - T_{c,out}) - (T_{h,out} - T_{c,in})}{ln(T_{h,in} - T_{c,out}) - ln(T_{h,out} - T_{c,in})} \tag{3-29}$$

Furthermore, the energy that is received by the cold water is calculated with:

$$Q_c = m_c\, c_w\, (T_{c,out} - T_{c,in}) \tag{3-30}$$

and the efficiency is defined as follows:

$$E = \frac{Q_c}{Q_h} \tag{3-31}$$

Combining and rearranging Eqs. 3-28 to 3-31 results in the following two equations, with which the output temperatures can be calculated:

$$T_{h,out} = T_{h,in} - \frac{\left(exp\left(\frac{A_{ex}\, k_{ex}}{c_w}\left(\frac{86.4}{V_{h,in}} - \frac{86.4\, E}{V_{c,in}}\right)\right) - 1\right)(T_{h,in} - T_{c,in})}{exp\left(\frac{A_{ex}\, k_{ex}}{c_w}\left(\frac{86.4}{V_{h,in}} - \frac{86.4\, E}{V_{c,in}}\right)\right) - E\,\frac{V_{h,in}}{V_{c,in}}} \tag{3-32}$$

$$T_{c,out} = T_{c,in} + \frac{\left(exp\left(\frac{A_{ex}\,k_{ex}}{c_w}\left(\frac{86.4}{V_{h,in}} - \frac{86.4\,E}{V_{c,in}}\right)\right) - 1\right)(T_{h,in} - T_{c,in})}{\frac{V_{c,in}}{E\,V_{h,in}}\,exp\left(\frac{A_{ex}\,k_{ex}}{c_w}\left(\frac{86.4}{V_{h,in}} - \frac{86.4\,E}{V_{c,in}}\right)\right) - 1} \quad 3\text{-}33$$

The volume flow and the salt concentration remain unchanged, if the temperature dependence of the water density is neglected. Transforming Eq. 3-30 and combining with Eq. 3-31 results in the following expressions:

$$T_{c,out} = T_{c,in} + \frac{E\,Q_h}{m_c\,c_w} \quad 3\text{-}34$$

$$T_{h,out} = T_{h,in} - \frac{Q_h}{m_h\,c_w} \quad 3\text{-}35$$

These equations can be substituted in Eq. 3-29 which in turn can be substituted in Eq. 3-28. This results in the following expression:

$$Q_h = A_{ex}\,k_{ex}\,\frac{Q_h\left(\frac{1}{m_h} - \frac{E}{m_c}\right)}{c_w\,ln\frac{T_{h,in} - T_{c,in} - \frac{Q_h\,E}{m_c\,c_w}}{T_{h,in} - T_{c,in} - \frac{Q_h}{m_h\,c_w}}} \quad 3\text{-}36$$

Eliminating the fraction and the logarithm results in:

$$T_{h,in} - T_{c,in} - \frac{Q_h\,E}{m_c\,c_w} = exp\left[\frac{A_{ex}\,k_{ex}}{c_w}\left(\frac{1}{m_h} - \frac{E}{m_c}\right)\right]\left(T_{h,in} - T_{c,in} - \frac{Q_h}{m_h\,c_w}\right) \quad 3\text{-}37$$

Solving the equation for Q_h results in the following equation:

$$Q_h = \frac{\left(exp\left[\frac{A_{ex}\,k_{ex}}{c_w}\left(\frac{1}{m_h} - \frac{E}{m_c}\right)\right] - 1\right)(T_{h,in} - T_{c,in})}{\frac{exp\left[\frac{A_{ex}\,k_{ex}}{c_w}\left(\frac{1}{m_h} - \frac{E}{m_c}\right)\right]}{m_h\,c_w} - \frac{E}{m_c\,c_w}} \quad 3\text{-}38$$

This expression can be inserted in the Eqs. 3-34 and 3-35, resulting in the following equations:

$$T_{h,out} = T_{h,in} - \frac{\left(exp\left(\frac{A_{ex}\, k_{ex}}{c_w}\left(\frac{1}{m_{h,in}} - \frac{E}{m_{c,in}}\right)\right) - 1\right)\left(T_{h,in} - T_{c,in}\right)}{exp\left(\frac{A_{ex}\, k_{ex}}{c_w}\left(\frac{1}{m_{h,in}} - \frac{E}{m_{c,in}}\right)\right) - E\,\frac{m_{h,in}}{m_{c,in}}} \qquad 3\text{-}39$$

$$T_{c,out} = T_{c,in} + \frac{\left(exp\left(\frac{A_{ex}\, k_{ex}}{c_w}\left(\frac{1}{m_{h,in}} - \frac{E}{m_{c,in}}\right)\right) - 1\right)\left(T_{h,in} - T_{c,in}\right)}{\frac{m_{c,in}}{E\, m_{h,in}}\, exp\left(\frac{A_{ex}\, k_{ex}}{c_w}\left(\frac{1}{m_{h,in}} - \frac{E}{m_{c,in}}\right)\right) - 1} \qquad 3\text{-}40$$

3.5 Simulation of the other operation units

As shown in Fig.3-1, IWEMM includes several blue blocks, which represent models of operational units in the PVC production site. The IWEMM calculates the output flows of operation units based on input flow rates. The blocks update stream variables entering and leaving the envelope with the calculated results. Besides the special models for MBR, RO, cooling tower and heat exchanger mentioned above, the blocks in IWEMM have the function to calculate material balances around an envelope of one or more operation units. They calculate the material balances, but will not perform complex and rigorous kinetic calculations. The material balance equations for the operation units used in IWEMM are as follows:

Overall mass balance:

$$\sum_{i=1}^{NS} S_i M_i = 0 \qquad 3\text{-}41$$

Sub-stream mass balance:

$$\sum_{i=1}^{NS} \sum_{j=1}^{NSS} S_i M_i M_{ij} = 0 \qquad 3\text{-}42$$

Component mass balance:

$$\sum_{i=1}^{NS} \sum_{j=1}^{NSS} \sum_{k=1}^{NC} S_i M_i M_{ij} C_{ijk} = 0 \qquad 3\text{-}43$$

Overall energy balance:

$$\sum_{i=1}^{NS} S_i M_i h_i + \sum_{j=1}^{NH} S_j H_j = 0 \qquad 3\text{-}44$$

Where S_i/S_j: inlet stream is +1, outlet stream is -1, M_i: mass flow of stream i, NS: number of inlet and outlet material streams, M_{ij}: mass fraction of sub-stream j in stream i, NSS: number of sub-streams within material streams, NC: number of components in stream, C_{ijk}: component mass fraction k in sub-stream j of stream i, h_i: mass enthalpy of stream i, H_i: heat flow of heat stream j. There are three types of input parameters for the material balance models:

Parameters of the PVC production site:

- VCM monomer polymerization efficiency
- proportion of each component in raw materials
- nominal PVC loss rate in production process
- steam pressure and temperature
- pressure and temperature in the bottom and the top of the stripper
- heat-transfer area size of polymerization tank
- initial temperature of polymerization tank and raw materials
- temperature of cooling water
- cooling tower efficiency
- water content in slurry entering dryer
- temperature of PVC entering dryer and of PVC after drying
- water productivity of MBR, and of RO.

Physical and chemical properties:

- specific heat capacity of the composition of slurry (i.e. VCM, PVC and water)
- VCM heat of vaporization
- heat of polymerization reaction
- thermal conductivity of polymerization tank.

Parameters controlling water flow and heat:

- yield of PVC

- water content in PVC
- temperature of cooling water entering cooling tower
- amount of wastewater entering treatment process.

Values for all model parameters were developed based the data from the PVC production site and a detailed review of the literature. All of these parameters directly affect the model for management of water flow and heat. A brief description of the various input parameters is given in Appendix 7.2.

4. Results and discussion

4.1 MBR simulation results

4.1.1 Steady state calibration

The treatment of the PVC production wastewater by the pilot MBR resulted in a 95-100 % BOD_5, 85-95 % COD and 85-90 % total organic carbon (TOC) removal. MLSS concentration has seriously impact on the prediction of the aeration energy demand by means of effecting oxygen transfer. Thus, a steady state calibration was conducted to ensure an accurate estimation of the MLSS concentration in this study. As shown in Table 4-1, the results show that using default values of all stoichiometric and biokinetic parameters reported by Henze et al. (Henze et al. 2000) led to an overestimation of MLSS concentration by around 15 % and an underestimation of nitrification and denitrification in terms of effluent NH_4-N and NO_3-N by about 87 % and 49 % respectively. With "mbr_asm1hsg" smaller deviations of 77 %, 46 % and 4 % for NH_4-N, NO_3-N and MLSS concentrations, respectively were achieved. Verrecht et al. calibrated the ASM2d parameters for a MBR treating the domestic wastewater. The results demonstrated an overestimate of NH_4-N, NO_3-N and MLSS concentrations by 383 %, 1.3 % and 0.5 %, respectively (Verrecht et al. 2010a). Sperandio and Espinosa calibrated the parameters μ_A and b_A in ASM1 for a MBR running at a wide range of SRTs. The results illustrated that the default values (0.8 and 0.04 d^{-1}) resulted in the overestimate of ammonia removal for all the SRTs, and recommended μ_A and b_A to be 0.45 and 0.04 d^{-1}, respectively (Spérandio and Espinosa 2008). Moreover, half saturation coefficients (K_{OH}, K_{OA}, K_{NH} and K_{NO}) were reported to be 4-10 times greater than the default values, and to increase considerably along with higher MLSS

concentrations (Sarioglu et al. 2009). At steady state calibration in this study, the correct representations of NH_4-N, NO_3-N and MLSS concentrations can be obtained by making revises to μ_H (1.1 d^{-1} vs. default value of 6 d^{-1}), K_{NO} (1.8 g N m^{-3} vs. default value of 0.5 g N m^{-3}), K_{NH} (1.8 g N m^{-3} vs. default value of 1.0 g N m^{-3}), and K_{OA} (1.25 g COD m^{-3} vs. default value of 0.4 g COD m^{-3}). As shown in Table 4-1, the calibrated values in this thesis can simulate the NH_4-N, NO_3-N and MLSS concentrations in deviations of 42 %, 0.8 % and 3 %, respectively. The calibrated parameter values were showed in Table 4-2.

Table 4-1 Steady state simulation results and measured values

Parameters	Units	Average measured values	---Default ASM1 values (Henze et al. 2000) ---b_A=0.04 d^{-1} (Spérandio and Espinosa 2008)	Default mbr_asm1hsg values	Calibrated ASM1 values
NH_4-N	g m^{-3}	1.1	0.14	0.25	0.64
NO_3-N	g m^{-3}	12.1	6.2	6.5	12.0
MLSS	g m^{-3}	11.2	13.0	11.7	11.6

Table 4-2 Values of the parameters in ASM1, mbr_asm1hsg and calibrated model

	Parameters	Unit	ASM1 default values at 20 °C	mbr_asm1hsg values at 20 °C	Calibrated values at 20 °C
Stoichiometric parameters	Y_A	g COD (g N)$^{-1}$	0.24	0.24	0.24
	Y_H	g COD (g COD)$^{-1}$	0.67	0.4	0.67
	f_P	Dimensionless	0.08	0.07	0.08
	i_{XB}	g N (g COD)$^{-1}$	0.086	0.086	0.086
	i_{XP}	g N (g COD)$^{-1}$	0.06	0.06	0.06
	μ_H	day^{-1}	6.0	6.0	1.1
	K_S	g COD m^{-3}	20.0	5.0	20
	K_{OH}	g O_2 m^{-3}	0.20	0.2	0.6
	K_{NO}	g N m^{-3}	0.50	0.5	1.8

	Parameters	Unit	ASM1 default values at 20 °C	mbr_asm1hsg values at 20 °C	Calibrated values at 20 °C
Kinetic parameters	b_H	day $^{-1}$	0.62	0.1	0.62
	η_g	Dimensionless	0.8	0.8	0.8
	η_h	Dimensionless	0.4	0.4	0.4
	μ_A	day^{-1}	0.80	0.80	0.45
	K_X	g Xs (g X_{BH} COD)$^{-1}$	0.03	0.03	0.03
	k_h	g Xs (g X_{BH} COD day)$^{-1}$	3.0	3.0	3.0
	K_{NH}	g N m^{-3}	1.0	0.7	1.8
	K_{OA}	g COD m^{-3}	0.4	0.4	1.25
	k_a	m^3(g COD d)$^{-1}$	0.08	0.08	0.08
	b_A	day^{-1}	0.04	0.1	0.04

4.1.2 Dynamic calibration

Despite the MBR process upset several times during the simulation period, the calibrated parameters provided satisfactory simulations of the NH_4-N, NO_3-N and MLSS concentrations. Fig. 4-1 compares the simulated NH_4-N, NO_3-N and MLSS with measured concentrations during the intensive 100 days. Measured NH_4-N concentrations are consistently lower than the predicted ones. That is because MBRs can achieve more complete and stable nitrification than CAS systems (Munz et al. 2008). When looking at NO_3-N and MLSS concentrations, the predictions are in good accordance. As shown in Fig.4-1, the average value of discharged excess sludge was used in simulation, but in the experiment the excess sludge discharged varied, which resulted in several peaks of measured MLSS. Therefore, it can generally come to the conclusion that the calibrated ASM 1 is able to provide reasonably prediction for nitrogen and MLSS concentrations.

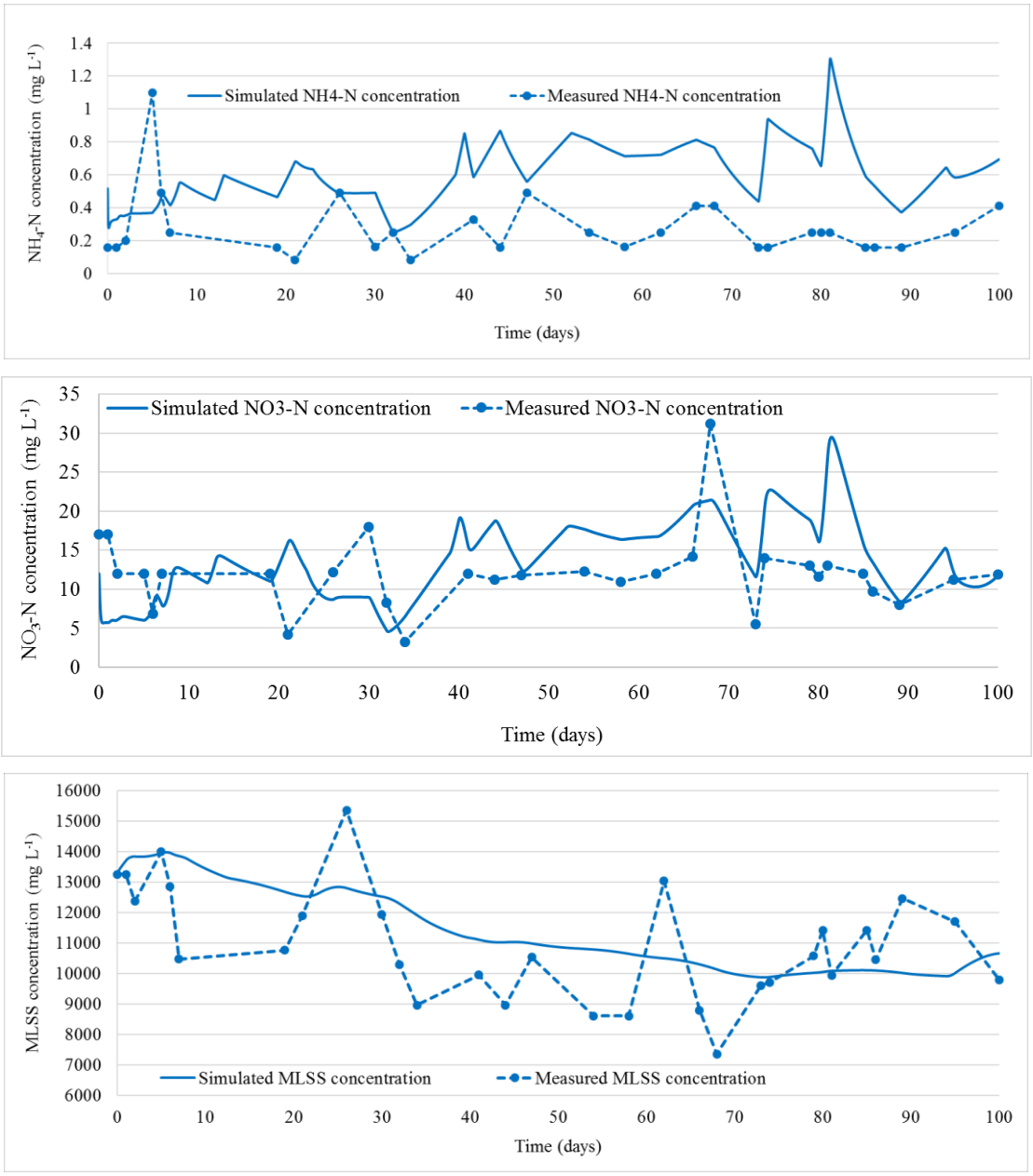

Figure 4-1 Simulated and measured NH_4-N, NO_3-N and MLSS concentrations

4.2 Energy consumption analysis

Due to the high running costs derived from the aeration system, a low specific membrane aeration demand per unit of membrane area (SAD_m) was set at 0.3 $Nm^3\ m^{-2}\ h^{-1}$. It is in the range of typical SAD_m values between 0.2 and 1.28 $Nm^3\ m^{-2}\ h^{-1}$ for sustainable operation (Judd and Claire 2010). Table 4-3 provides an overview of energy consumptions per m^3 permeate for three full-scale MBR plants (Fenu et al. 2010b) and a benchmark simulation model of MBR (BSM-MBR) (Maere et al. 2011), compared

with the results of this study (ASM1-MBR). Despite some energy consumptions are very specific, it seems that the total energy consumption of the MBR process in this study is comparable with the full-scale plants and BSM-MBR. 0.73 kWh m^{-3} is much lower than typical small MBRs which generally range from 1.8 to 6 kWh m^{-3} (Fenu et al. 2010b, Gil et al. 2010). However, it is higher than the large full-scale MBR plants such as Schilde which is as low as 0.52 kWh m^{-3}. Other reported total energy consumption of full-scale MBRs are general in range of 0.6 to 2.0 kWh m^{-3} which depends on design, operation strategy, etc.

Table 4-3 Total and specific energy consumptions

Energy consumption	Unit	Schilde	Varsseveld	Nordkanal	BSM-MBR	ASM1-MBR
ME	kWh m^{-3}	0.05	0.04	0.11	0.03	0.06
PE_{sludge}	kWh m^{-3}	0.10	0.11	0.01	0.05	0.09
$PE_{effluent}$	kWh m^{-3}	0.07	0.12	0.02	0.07	0.08
$AE_{bioreactor}$	kWh m^{-3}	0.07	0.24	0.11	0.21	0.28
$AE_{membrane}$	kWh m^{-3}	0.23	0.34	0.45	0.53	0.22
Total	kWh m^{-3}	0.52	0.85	0.71	0.90	0.73

4.3 Scenario analysis

As shown in Fig.4-2, the evolution of average effluent NO_3-N and NH_4-N concentrations is a function of SRT. It confirms as expected that raising the SRT by decreasing excess sludge discharge rate is beneficial for NH_4-N removal. High SRT creates starvation condition (low F/M ratio) which increases MLSS and autotrophs concentration, good for nitrification (Mutamim et al. 2013). However, Fig. 4-5 shows that raising the SRT will lead to higher demand for aeration. Therefore, there is a trade-off between minimizing the aeration energy consumption and effluent quality. As shown in Fig. 4-2, it leads to almost complete nitrification when operating at SRTs higher than 25 days, similar to observation by Cicek et al. (Cicek et al. 2001) and by Berkir et al. (Bekir Ersu et al. 2008). Fig. 4-3 demonstrates that raising recirculation ratio had a similar but less pronounced impact on nitrification at 30 °C.

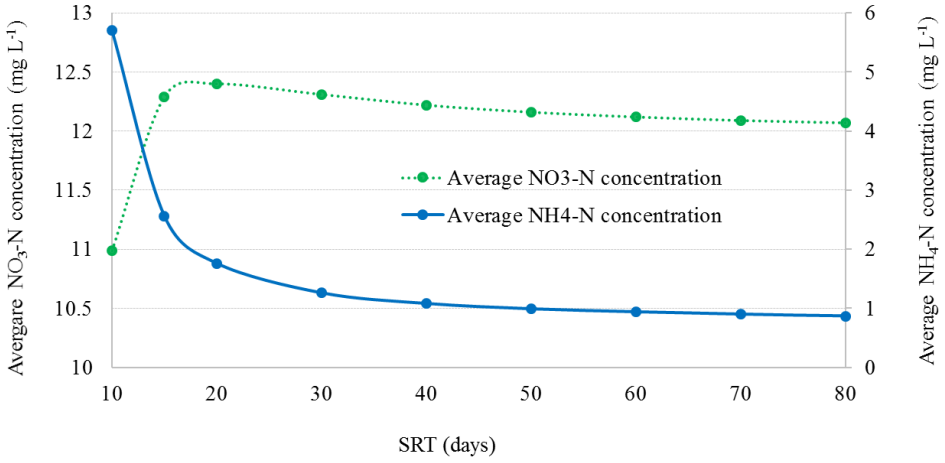

Figure 4-2 Influence of SRT on average effluent NO_3-N and NH_4-N concentrations (DO=2 mg L^{-1}, R=3 and T=30 °C)

As shown in Fig.4-3, during which the DO was controlled at 2 mg L^{-1}, NO_3-N removal efficiency increased when recirculation ratio was increased from 1 to 6. However, a further increase in recirculation ratio from 6 to 8 resulting in a corresponding deterioration in NO_3-N removal. This arises might be because higher recirculation ratios increase the oxygen transfer into the anoxic tank and therefore decrease the nitrate removal efficiency.

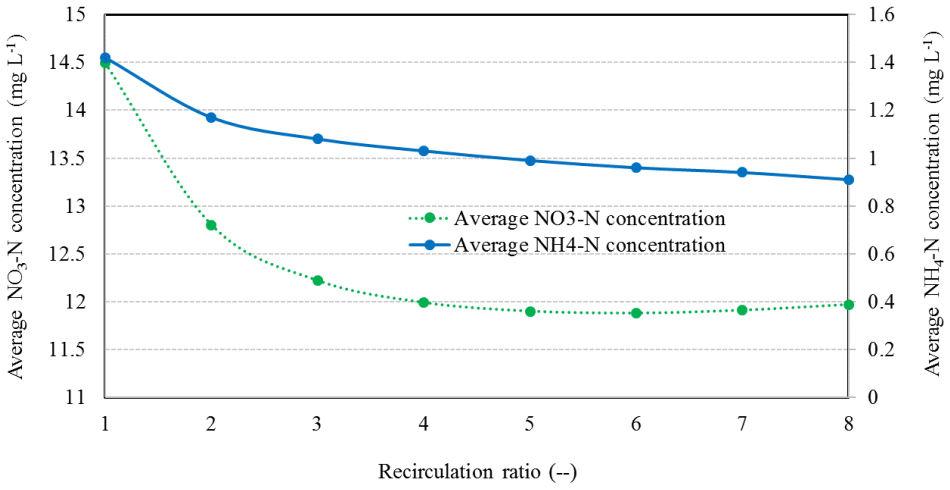

Figure 4-3 Influence of recirculation ratio on average effluent NO_3-N and NH_4-N concentrations (DO=2 mg L^{-1}, SRT=40 d and T=30 °C)

It is generally recommended to control DO higher than 2 mg L^{-1} for nitrification. However, as shown in Fig.4-4, the MBR process can also achieve the good nitrification when DO lower than 2 mg L^{-1}. Tan et al. got a similar conclusion when they investigated the influence of DO on nitrogen removal and membrane fouling in a submerged MBR (Tan and Ng 2008). Furthermore, it can be observed in Fig.4-4 that DO below 1 mg L^{-1} would resulted in nitrification deterioration.

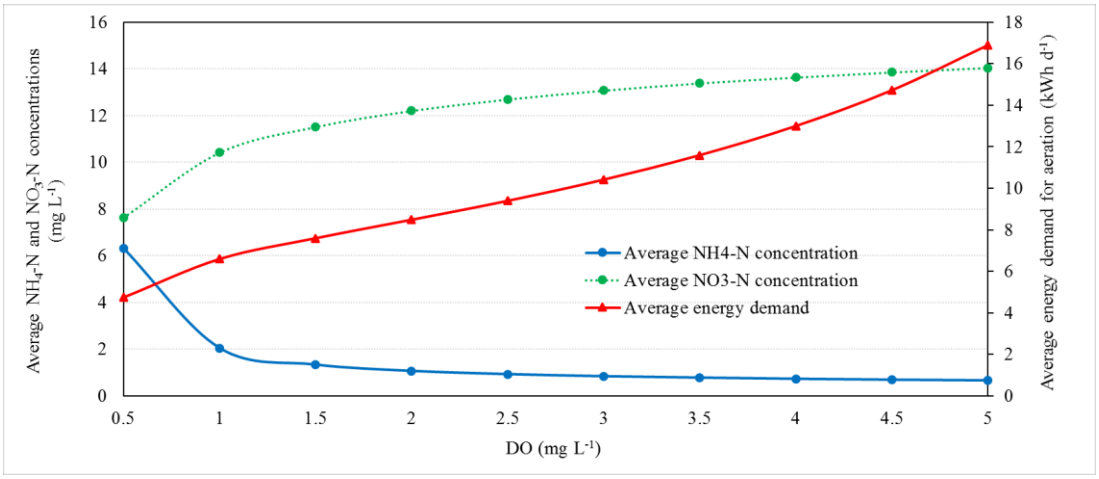

Figure 4-4 Influence of dissolved oxygen on average effluent NO_3-N and NH_4-N concentrations and aeration energy demand (R=3, SRT=40 d and T=30 °C)

As shown in Fig. 4-5, the change of SRT has a greater effect on aeration energy demand than the change of recirculation ratio. More specifically, the aeration energy consumption can change as much as 170 % depending on the excess sludge discharge rate. However, the change is limited to 94 % at varying recirculation ratio. This confirms it is necessary to consider the effect of MLSS on oxygen transfer in the aeration model.

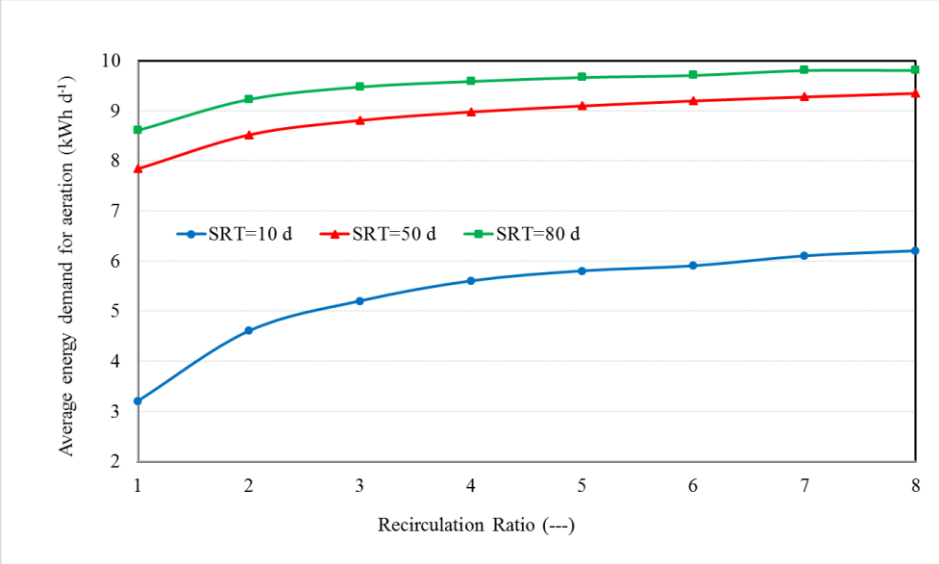

Figure 4-5 Influence of R and SRT on average aeration energy (DO=2 mg L^{-1} and T=30 °C)

4.4 Parameter uncertainty analysis

The uncertainty of ASM1 parameters was characterized by an expert review in this study. It includes interviewing professionals with experience to fix upper and lower bound of parameters in ASM1 (Helton and Davis 2003). In this thesis, model parameters were all assumed to be in a uniform probability distribution. Furthermore, three uncertainty classes were defined as 5, 25 and 50 % of variability around the value (Brun et al. 2002). Therefore, the lower and upper bound of the uniform probability distribution can be derived from (100 %- variability) × value and (100 % + variability) ×value, respectively.

Table 4-4 The uncertainty of calibrated ASM1 parameters and influent characteristics

Parameter	Unit	Value	Min Value	Max value	Uncertainty class
Y_A	g COD (g N)$^{-1}$	0.24	0.23	0.25	1
Y_H	g COD (g COD)$^{-1}$	0.67	0.64	0.70	1
f_P	Dimensionless	0.08	0.06	0.1	2
i_{XB}	g N (g COD)$^{-1}$	0.086	0.043	0.129	3

Parameter	Unit	Value	Min Value	Max value	Uncertainty class
i_{XP}	g N (g COD)$^{-1}$	0.06	0.057	0.063	1
μ_H	day^{-1}	1.1	0.8	1.4	2
K_S	g COD m^{-3}	20.0	10	30	3
K_{OH}	g O_2 m^{-3}	0.60	0.3	0.9	3
K_{NO}	g N m^{-3}	1.80	0.9	2.7	3
b_H	day $^{-1}$	0.62	0.59	0.65	1
η_g	Dimensionless	0.8	0.6	1.0	2
η_h	Dimensionless	0.4	0.3	0.5	2
k_h	g Xs (g X_{BH} COD day)$^{-1}$	3.0	2.25	3.75	2
K_X	g Xs (g X_{BH} COD)$^{-1}$	0.03	0.02	0.04	2
μ_A	day^{-1}	0.45	0.43	0.47	1
K_{NH}	g N m^{-3}	1.8	0.9	2.7	3
K_{OA}	g COD m^{-3}	1.25	0.94	1.56	2
k_a	m^3 (g COD d)$^{-1}$	0.08	0.04	0.12	3
b_A	day^{-1}	0.04	0.03	0.05	2
f_{SI}	g COD (g COD_{total})$^{-1}$	24.5%	18.4%	30.6%	2
f_{SS}	g COD (g COD_{total})$^{-1}$	33.9%	17.0%	50.8%	3
f_{XI}	g COD (g COD_{total})$^{-1}$	14%	7%	21%	3
f_{XS}	g COD (g COD_{total})$^{-1}$	27.6%	13.8%	41.4%	3
f_{SNH}	g N (g TKN)$^{-1}$	78.9%	59.2%	98.6%	2

Latin Hypercube Sampling (LHS) was first introduced by McKay et al. in 1979 (McKay et al. 1979). It is an efficient tool often employed in uncertainty analysis to explore the entire parameter space of a model with a minimum number of computer simulations (Helton and Davis 2002). Unlike random sampling, LHS ensures a full stratification over the range of each sampled variable (Helton et al. 2006). In this thesis, the parameter space was sampled using LHS to create a matrix with the dimension of 500×24. The rows and columns are LHS samples and parameters, respectively. Then, the ASM1 model was simulated 500 times, where each row of the sampling matrix was used as an input parameter set for simulation. Fig.4-6 describes 10th, mean and 90th percentiles of the model output at each simulation. As larger the distance between the 10th and 90th

percentiles and the mean is, as greater the uncertainty of the model output becomes.

Figure 4-6 10th, mean and 90th percentile values of simulation for NO_3-N, NH_4-N and MLSS

The cumulative distribution functions (CDF) for average effluent NH_4-N and NO_3-N and MLSS concentrations are showed in Fig. 4-7 respectively. The y-axis is the cumulative probability, and the x-axis represents the average value of model outputs.

In this study, the uncertainty analysis procedure provided an estimate of uncertainty to judge the reliability of operation strategy to meet effluent discharge limits. Specifically, as shown in Fig. 4-7, there is 50 % chance that the NH_4-N and NO_3-N concentrations will be greater than 0.63 and 13.72 mg L^{-1}, respectively. MLSS concentration and aeration energy demand will be greater than 11,500 mg L^{-1} and 13 kWh d^{-1} respectively by 50 % chance. Considering the need for desalination of the MBR effluent on account of its reuse as production water for polymerization step, NH_4-N concentration target value was set below 2 mg L^{-1} for quality control at MBR effluent. The current operation strategy is able to reach the target with the effluent NH_4-N concentration lower than 2 mg L^{-1} for about 97 % chance.

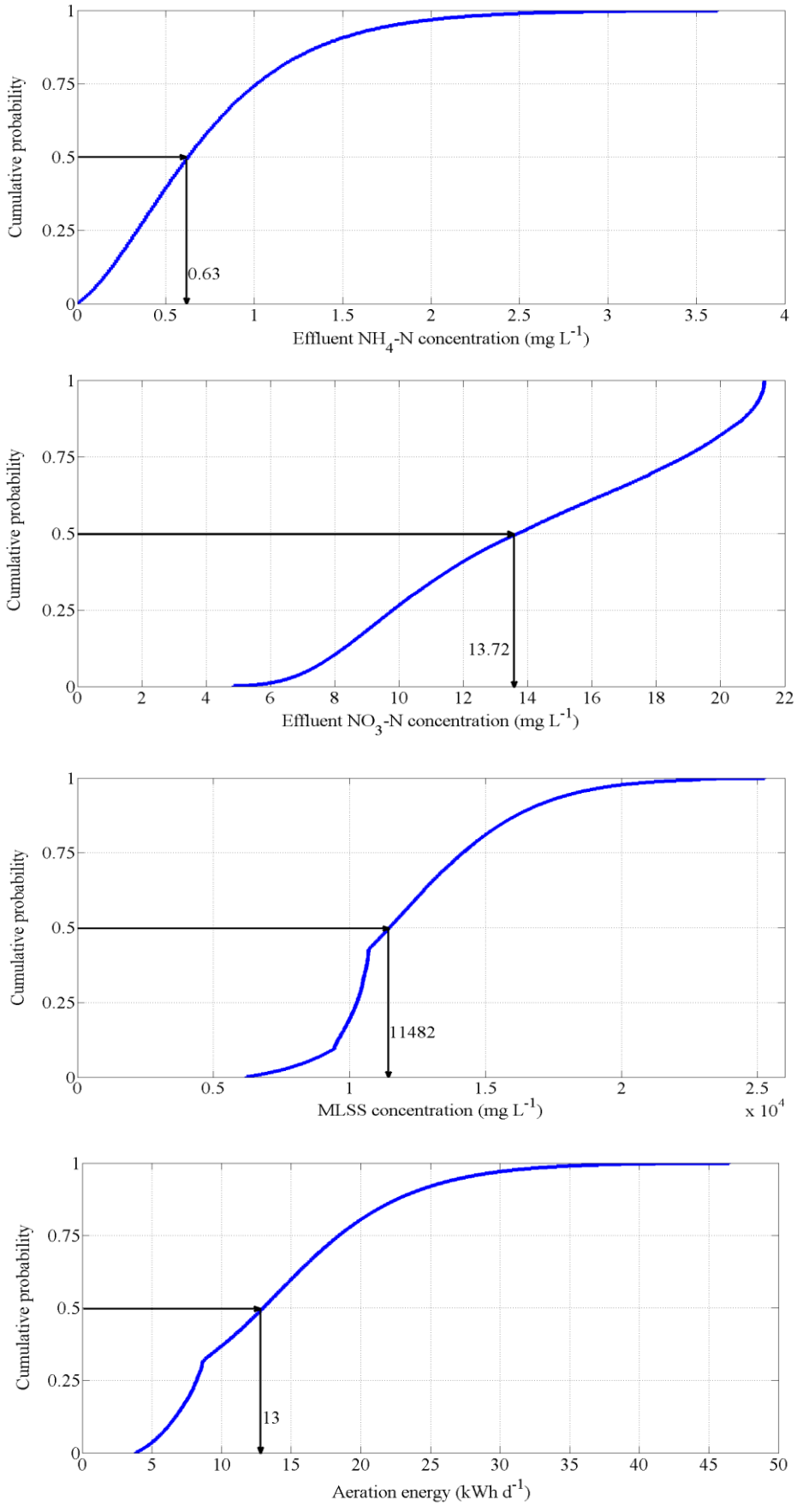

Figure 4-7 The uncertainty of model outputs by cumulative distribution function

4.5 RO simulation results

The RO process was tested in two phases, and the detailed ion concentration analyses were done by UCM. The first phase was from 18th July 2014 to 10th February 2015, and the second phase was from 10th February 2015 to 29th April 2015. The operational conditions are shown in Table 2-3. The average observed rejections of ions are shown in the following Table 4-5.

Table 4-5 Average rejection of ions

Ions	Phase 1 (%)		Phase 2 (%)	
	Stage 1	Stage 2	Stage 1	Stage 2
Cl^-	99.2	99.5	91.6	---
Na^+	98.7	99.1	91.8	---
Ca^{2+}	99.7	99.8	93.4	---
SO_4^{2-}	99.5	99.7	97.1	---
K^+	99.1	99.4	89.0	---
Mg^{2+}	99.2	99.5	93.5	---

In this thesis, the nonlinear parameter estimation program applied to evaluate the membrane characteristic parameters in Eq. 3-15 is based on the universal global optimization method in 1stOpt software (7D-Soft High Technology Inc., China). The data supplied to the software are R_o and J_w obtained at different feed pressures. The feed rate and ion concentrations were kept as constants for each set of data. Table 4-6 shows the fitted values of B and K for ions in stages 1 and 2 in Pass 1. As shown in Table 4-5, membrane permeability coefficients sequence to the ions follows: $B(Na^+)$> $B(Cl^-)$>$B(K^+)$>$B(SO_4^{2-})$>$B(Mg^{2+})$>$B(Ca^{2+})$. These ions performed the similar permeability trend in nano-filtration membranes (Pages et al. 2013, Yaroshchuk et al. 2011). It also showed that the divalent ions have a better rejection than monovalent ions, and the rejection of divalent ions such as sulfate always reaches 99 %. In this study, Na^+ and Cl^- are dominant ions. Although concentrations are almost the same, the membrane permeability of sodium is larger than of chloride ions. Moreover, as the trace ion, the membrane permeability of monovalent ion, potassium, is lower than sodium. Fig. 4-8 and Fig.4-9 show the observed rejections of ions as functions of trans-

membrane flux and their fits by SDFM. The corresponding fitting parameters are listed in Table 4-6.

Table 4-6 B and K estimated values for ions

Ions	Stage 1		Stage 2	
	B ($\mu m\ s^{-1}$)	K ($\mu m\ s^{-1}$)	B ($\mu m\ s^{-1}$)	K ($\mu m\ s^{-1}$)
Cl^-	0.01463	5.6649	0.01035	5.6844
Na^+	0.01940	4.3599	0.01811	7.7927
Ca^{2+}	0.0001438	0.8285	0.0001888	1.2696
SO_4^{2-}	0.00366	2.1563	0.002312	2.4009
K^+	0.006031	2.1513	0.006007	5.1928
Mg^{2+}	0.001382	1.0993	0.001735	1.7239

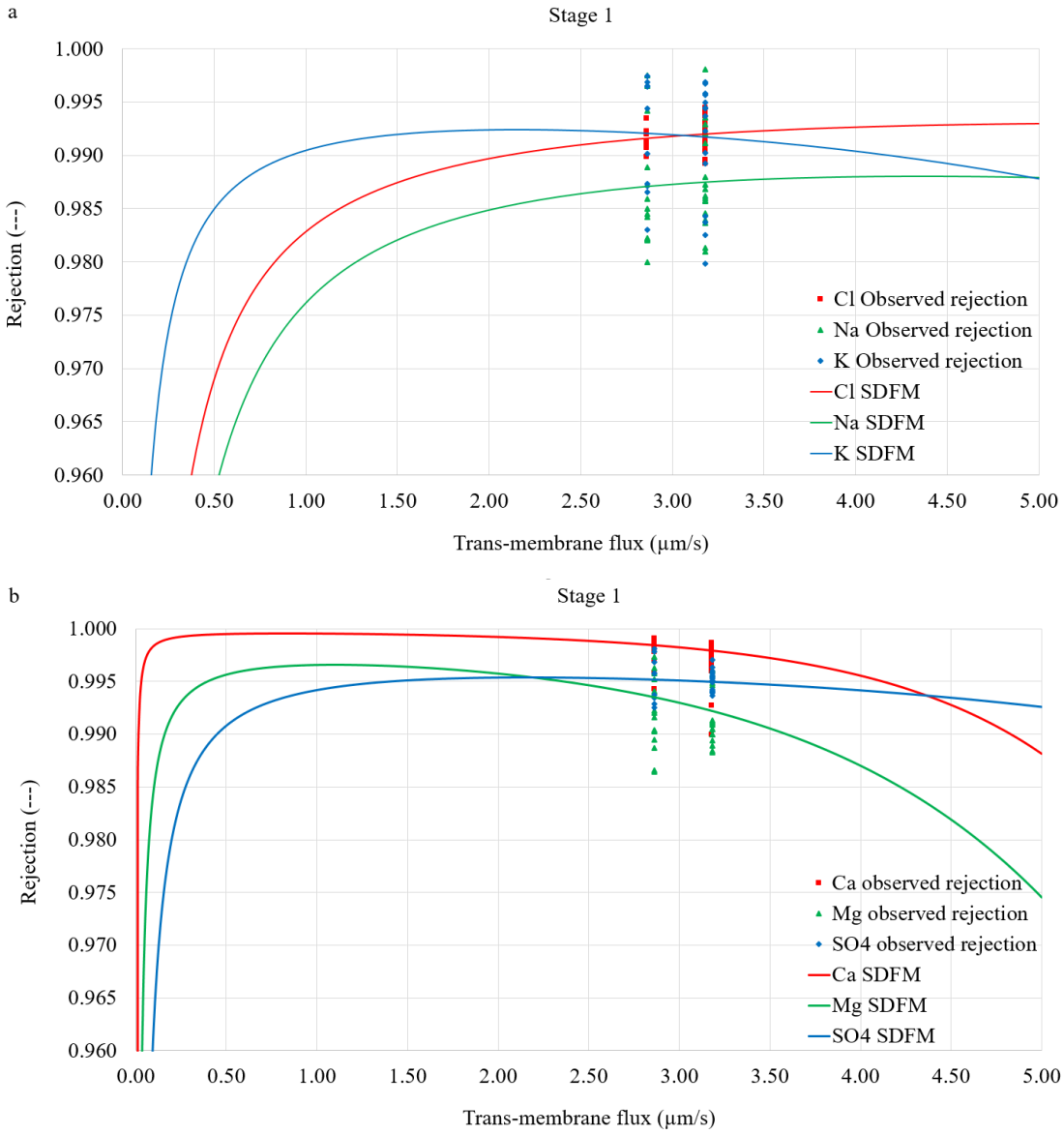

Figure 4-8 Observed and SDFM rejections of ions in stage 1

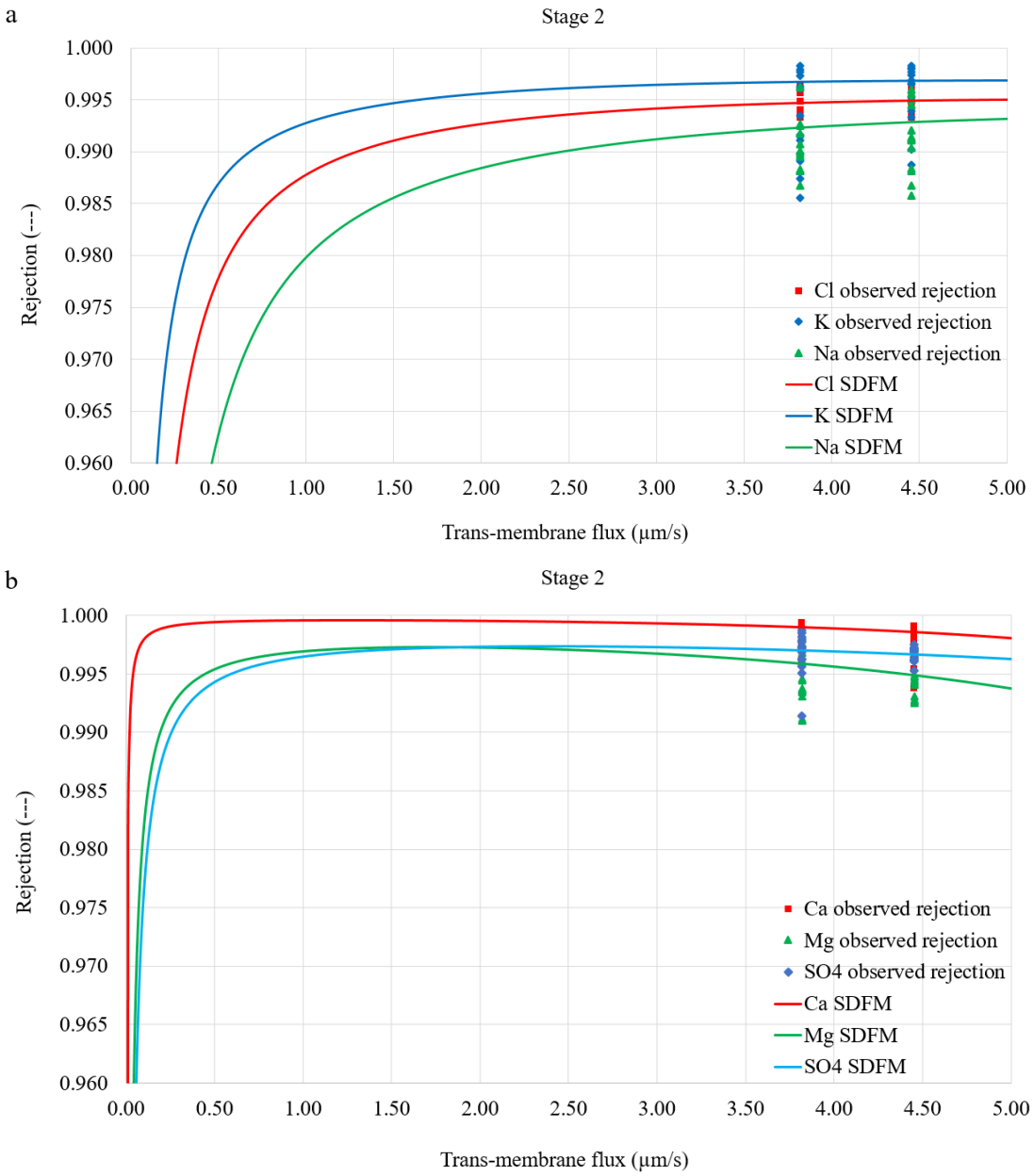

Figure 4-9 Observed and SDFM rejections of ions in stage 2

As shown in Fig.4-10, the total energy consumption in the RO process is divided into three different characteristic fractions. In phase 1, the recoveries of stage 1 and stage 2 are 36 % and 38 %, the driving pressures are 680 kPa and 564 kPa, respectively. Fig.4-11 shows that during phase 2 recoveries of stage 1 and stage 2 are increased to 49 % and 52 % at the driving pressures of 790 kPa and 668 kPa, respectively. In Figs. 4-10 and 4-11, the x-axis is the recovery of RO process and the y-axis represents the driving pressure. According to Eq. 3-16, the area below horizontal pressure line indicates the total energy consumed to pump the wastewater into the RO process. The total consumed

energy consists of two parts which are separated by the vertical recovery line. According to Eqs. 3-17 and 3-18, the area on the left represents the energy consumed for permeate production and the right side indicates the energy remaining in the retentate stream. As shown in Figs. 4-10 and 4-11, the energy consumed for permeate production is divided into two fractions by the broken line which indicates the osmotic pressure curve obtained from Eq. 3-21. The upper area is the additional energy requirement and the part below the broken line is the thermodynamic minimal energy for permeate production. Due to osmotic pressure increased along the membrane channel and economic permeate flux needed in practice, the additional energy beyond the thermodynamic minimal energy is necessary.

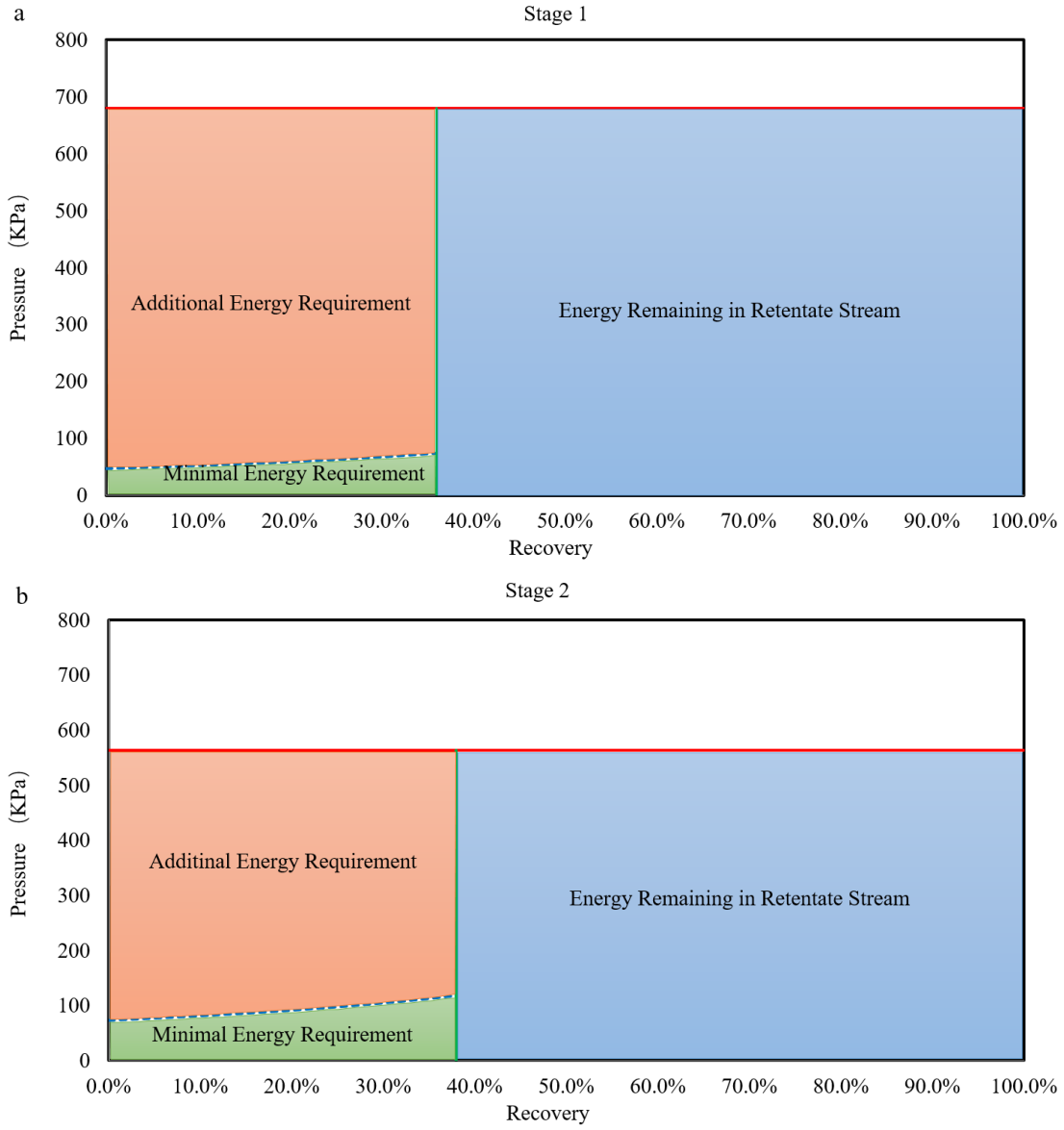

Figure 4-10 Energy analysis diagram for stage 1 and stage 2 in phase1

As shown in Fig.4-10a, 64 % of the total energy consumption is remained in the retentate flow in stage 1. Of the rest 36 % that is consumed for permeate production, only 3 % is the minimal energy and 33 % is the additional energy. As a comparison, Fig. 4-10b with a recovery of 38 % illustrates that the minimal and additional energy requirements become to 6 % and 32 %, respectively. That is because stage 2 operates at a higher recovery and higher ion concentration in the feed flow. This phenomenon is also shown in Fig.4-11a and Fig.4-11b.

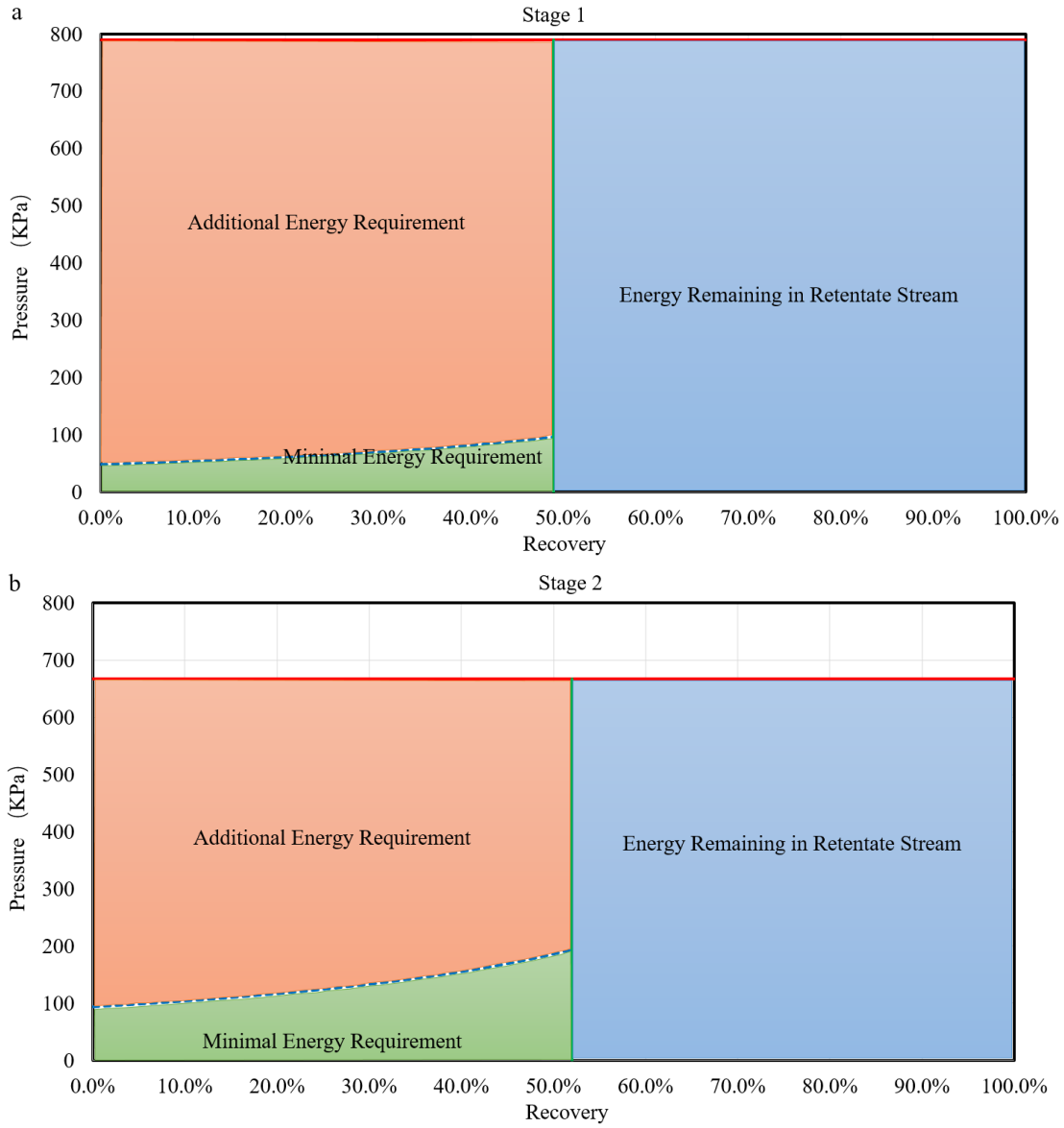

Figure 4-11 Energy analysis diagram for stage 1 and stage 2 in phase 2

The specific energy consumptions calculated by Eq. 3-20 and Eq. 3-23 are listed in Table 4-7. Table 4-7 shows that thermodynamic restriction occurs when recovery is

greater than 90 % in stage 1 and stage 2. Thus, the specific energy consumption was calculated using Eq. 3-20. However, it should be pointed out that the energy consumption calculated and presented here is the net energy consumption. The efficiency of pumps in the RO process has to be included when converted it into the electricity power consumption. The conversion efficiency of the pump is generally about 70 % in the desalination plant. From Table 4-7, the specific energy consumption of stages 1 and 2 in phase 1 at the recovery of 70 % is 0.204 and 0.180 kWh m^{-3}. If the energy remaining in the retentate flow is assumed to be entirely recovered via energy recover devices, the electricity power consumptions for stages 1 and 2 would be 0.291 and 0.257 kWh m^{-3}, respectively.

Table 4-7 Specific energy consumption before and after thermodynamic restriction

Recovery	Phase 1 (kWh m^{-3})				Phase 2 (kWh m^{-3})			
	Stage 1		Stage 2		Stage 1		Stage 2	
	Before TR	After TR	Before TR	After TR	Before TR	After TR	Before TR	After TR
0	0.189	0.013	0.157	0.020	0.219	0.014	0.186	0.026
10	0.190	0.014	0.158	0.023	0.220	0.015	0.187	0.029
20	0.191	0.016	0.159	0.025	0.221	0.017	0.189	0.032
30	0.192	0.019	0.161	0.029	0.222	0.020	0.191	0.037
40	0.193	0.022	0.163	0.034	0.224	0.023	0.194	0.043
50	0.195	0.026	0.167	0.041	0.226	0.027	0.198	0.052
60	0.199	0.033	0.172	0.051	0.230	0.034	0.205	0.065
70	0.204	0.043	0.180	0.068	0.235	0.046	0.216	0.086
80	0.215	0.065	0.197	0.101	0.247	0.068	0.237	0.129
90	0.248	0.130	0.248	0.203	0.281	0.137	0.302	0.259
95	0.313	0.261	0.349	0.405	0.349	0.274	0.431	0.517

4.6 Water and energy analysis in different scenarios

IWEMM can illustrate the behavior of water and heat in the operation units in production and wastewater treatment processes. As shown in Fig.2-2, the process flow

scheme of the wastewater reuse process includes two heat exchangers. The RO permeate flow is returned to Heat Exchanger 1. It will be heated up by the raw wastewater and can be re-used for PVC production. Therefore, as shown in Figure 4-12, the reused wastewater temperature decreases with increased recycling ratio. Compared to the groundwater, reused wastewater has a higher temperature. So, less heat is required to heat up raw material to start the polymerization reaction.

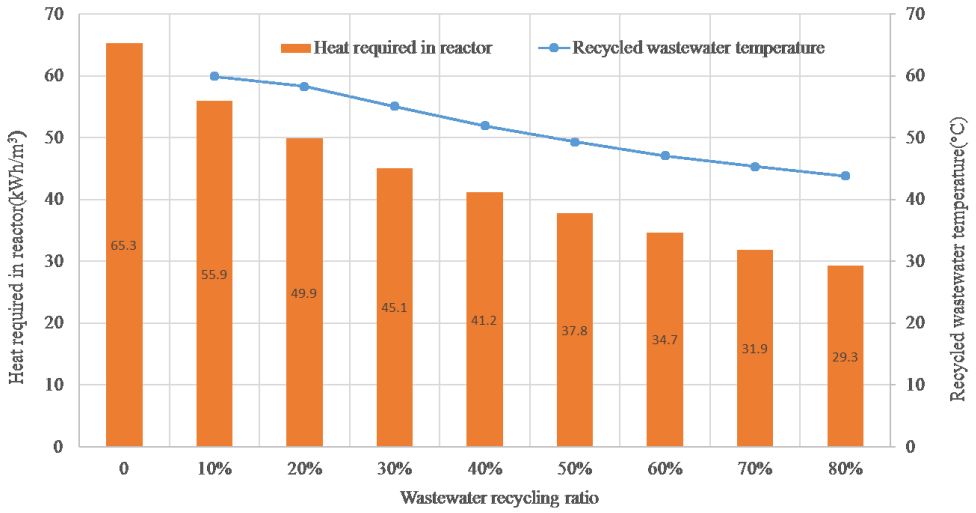

Figure 4-12 Heat required and reused wastewater temperature for different recycling ratios

The present process water treatment system in the PVC production site uses groundwater as source. The system consists of a de-carbonisation unit where precipitation chemicals are added to remove carbon dioxide. The de-carbonised water then flows into RO membrane filtration and IE unit. The process water treatment system consumes chemicals and energy. The costs of treatment for fresh groundwater is 1.75 Euros per m^3. As shown in Figure 4-13, less fresh groundwater and costs are required with an increased recycling ratio.

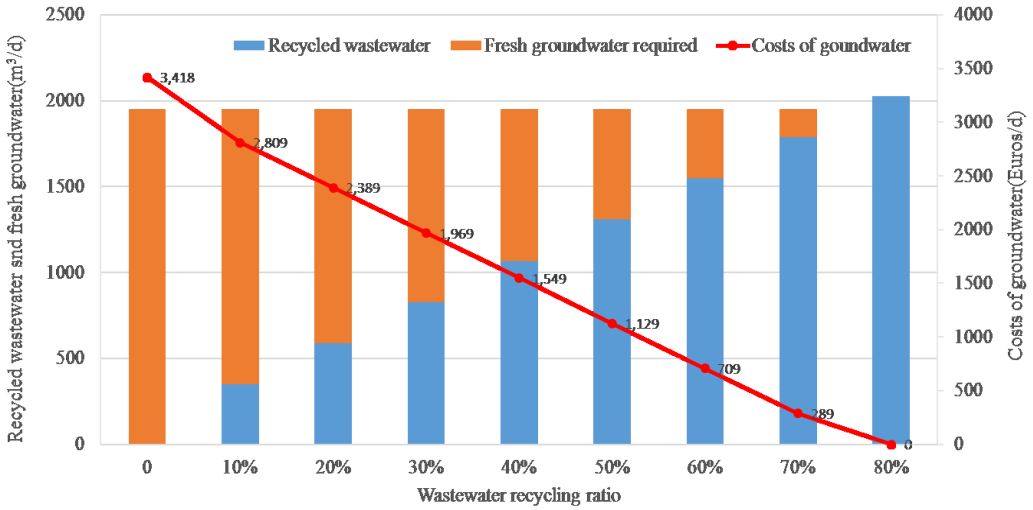

Figure 4-13 Water consumption and costs at different recycling ratios

5. Conclusions and outlook

5.1 Conclusions

The basic objective of this thesis was to carry out an integrated water and energy management model for a PVC production site. The major findings of the work are:

IWEMM is able to simulate the water and energy behaviours in the production and wastewater reuse processes in a PVC production site. It also can supply the information about economical and ecological effects of wastewater reuse for life cycle assessment (LCA), optimize PVC production and wastewater reuse processes, demonstrate the potential for freshwater saving, valuable recovery and heat reuse.

A pilot-scale MBR developed to treat a poly vinyl chloride (PVC) production site wastewater was dynamically modelled by ASM1. The calibrated ASM1 was sufficiently able to simulate effluent ammonia and nitrate, and MLSS in the aerobic tank in both steady and dynamic states. A modified aeration model with consideration of the effect of MLSS on oxygen transfer was proposed. The total energy consumption of the pilot-scale MBR was 0.73 kWh per m^3 permeate production. This value is low when compared to other small-scale MBRs, but it is comparable to existing large scale

MBRs. Moreover, this study performed a procedure of uncertainty analysis for the calibrated ASM 1. It showed that the current operation strategy is able to reach the target with the effluent NH_4-N concentration lower than 2 mg L^{-1} for about 97 % chance.

It has been previously demonstrated that solution-diffusion-film model (SDFM) is useful to analyze ion rejections in RO systems. However, only the single salt was concerned in most cases. In this thesis, SDFM has been extended to a pilot-scale RO process desalinating wastewater from PVC production site which consists of dominant ions (Na^+ and Cl^-) and several trace ions (Ca^{2+}, Mg^{2+}, K^+ and SO_4^{2-}). An energy analysis framework with consideration of limitation imposed by the thermodynamic restriction was implemented to analyze the specific energy consumption of the pilot-scale RO system at various scenarios. The specific energy consumption of stages 1 and 2 in phase 1 is 0.204 and 0.180 kWh m^{-3} at the recovery of 70 %. By using these solution-diffusion-film and energy analysis models, various information could be obtained regarding permeabilities of a commercial RO membrane (FILMTEC^{TM} LC HR-4040) pilot-scale process to several ions (Na^+, Cl^-, K^+, Ca^{2+}, Mg^{2+} and SO_4^{2-}) and the specific energy consumption. This information can be useful to optimize the RO process for wastewater desalination in various applications.

5.2 Outlook to future works

There are some directions in which this research work can be continued. Because of the modular approach, IWEMM can be adapted to different wastewater streams by means of combining different blocks for different processes. Therefore, the next steps could be to evaluate IWEMM for other PVC production sites and then to extend to other industries in which the wastewater is treated by MBR and RO. Moreover, for further improving the performance of existing models, experiments might be necessary to obtain more information about ions removal in RO and membrane fouling in MBR. Furthermore, more operation unit models should be developed to expand the application of IWEMM.

Most findings and conclusions of MBR modeling were based on lab- and pilot-scale experiments. Therefore, more attention should be paid to full-scale model applications to test and verify the applicability of current achievements, and to take full exploitation

of ASMs for plant design and operation. Most recently, some researchers demonstrated the solubilization of inorganic solids entering MBR. Therefore, another future work in the application of ASMs to MBR, in particular long-SRT MBR, is to consider the effect of inorganic compounds in influent on MBR performance and modelling.

For modelling RO membranes, advanced structural characterization information and techniques should be included in transport models to help mechanistically explain solute and solvent transport in RO membrane, and to more accurate predict RO membrane performance. Moreover, one drawback of SDFM is that it does not consider interactions with charged solutes. Therefore, for modelling multicomponent charged mixtures, future work should seek a combined solution-diffusion, convection and electro-migration transport model.

6. References

[1]. 2030 water resources group. (2009) Charting our water future: economic frameworks to inform decision-making. http://www.mckinsey.com/business-functions/sustainability-and-resource-productivity/our-insights/charting-our-water-future.

[2]. Acharya, C., Nakhla, G., Bassi, A. and Kurian, R. (2006) Treatment of high-strength pet food wastewater using two-stage membrane bioreactors. Water Environment Research 78(7), 661-670.

[3]. Adnan, S., Hoang, M., Wang, H., Bolto, B. and Xie, Z. (2010) Recent trends in research, development and application of membrane technology in the pulp and paper industry. Appita Journal 63(3), 235-241.

[4]. Ali, H. (2010) Biodegradation of Synthetic Dyes-A Review. Water Air and Soil Pollution 213(1-4), 251-273.

[5]. Amat, A.M., Arques, A., Miranda, M.A. and López, F. (2005) Use of ozone and/or UV in the treatment of effluents from board paper industry. Chemosphere 60(8), 1111-1117.

[6]. Andersen, M., Kristensen, G.H., Brynjolf, M. and Gruttner, H. (2002) Pilot-scale testing membrane bioreactor for wastewater reclamation in industrial laundry. Water Science and Technology 46(4-5), 67-76.

[7]. Andrade, L.H., Motta, G.E. and Amaral, M.C.S. (2013) Treatment of dairy wastewater with a membrane bioreactor. Brazilian Journal of Chemical Engineering 30(4), 759-770.

[8]. Anqi, A.E., Alkhamis, N. and Oztekin, A. (2015) Numerical simulation of brackish water desalination by a reverse osmosis membrane. Desalination 369, 156-164.

[9]. Artiga, P., Carballa, M., Garrido, J.M. and Mendez, R. (2007) Treatment of winery wastewaters in a membrane submerged bioreactor. Water Science and Technology 56(2), 63-69.

[10]. Badani, Z., Ait-Amar, H., Si-Salah, A., Brik, M. and Fuchs, W. (2005) Treatment of textile waste water by membrane bioreactor and reuse. Desalination 185(1–3), 411-417.

[11]. Bae, T.-H., Han, S.-S. and Tak, T.-M. (2003a) Membrane sequencing batch reactor system for the treatment of dairy industry wastewater. Process Biochemistry 39(2), 221-231.

[12]. Bae, T.H., Han, S.S. and Tak, T.M. (2003b) Membrane sequencing batch reactor system for the treatment of dairy industry wastewater. Process Biochemistry 39(2), 221-231.

[13]. Baek, S.H., Jeon, S.K. and Pagilla, K. (2009) Mathematical modeling of aerobic membrane bioreactor (MBR) using activated sludge model no. 1 (ASM1). Journal of Industrial and Engineering Chemistry 15(6), 835-840.

[14]. Bayat, M., Mehrnia, M.R., Hosseinzadeh, M. and Sheikh-Sofla, R. (2015) Petrochemical wastewater treatment and reuse by MBR: A pilot study for ethylene oxide/ethylene glycol and olefin units. Journal of Industrial and Engineering Chemistry 25, 265-271.

[15]. Bekir Ersu, C., Ong, S.K., Arslankaya, E. and Brown, P. (2008) Comparison of recirculation configurations for biological nutrient removal in a membrane bioreactor. Water Research 42(6-7), 1651-1663.

[16]. Berube, P.R. and Hall, E.R. (2000) Effects of elevated operating temperatures on methanol removal kinetics from synthetic kraft pulp mill condensate using a membrane bioreactor. Water Research 34(18), 4359-4366.

[17]. Bhattacharya, P.K., Jayan, R. and Bhattacharjee, C. (2005) A combined biological and membrane-based treatment of prehydrolysis liquor from pulp mill. Separation and Purification Technology 45(2), 119-130.

[18]. Blanco,L., Blanco,A. and Negrot,C. (2015) Comfirmation of the MBR at technical pilot scale. Economically and Ecologically Efficient Water Management in the European Chemical Industry (E4Water): Deliverable 4.1.

[19]. Bolzonella, D., Fatone, F., Pavan, P. and Cecchi, F. (2010) Application of a membrane bioreactor for winery wastewater treatment. Water Science and Technology 62(12), 2754-2759.

[20]. Braak, E., Alliet, M., Schetrite, S. and Albasi, C. (2011) Aeration and hydrodynamics in submerged membrane bioreactors. Journal of Membrane Science 379(1-2), 1-18.

[21]. Brik, M., Schoeberl, P., Chamam, B., Braun, R. and Fuchs, W. (2006) Advanced treatment of textile wastewater towards reuse using a membrane bioreactor. Process Biochemistry 41(8), 1751-1757.

[22]. Brun, R., Kuhni, M., Siegrist, H., Gujer, W. and Reichert, P. (2002) Practical identifiability of ASM2d parameters - systematic selection and tuning of parameter subsets. Water Research 36(16), 4113-4127.

[23]. Bui Xuan, T., Nguyen Phuoc, D. and Nguyen Thanh, B. (2012) Fouling mitigation in a submerged membrane bioreactor treating dyeing and textile wastewater. Desalination and Water Treatment 47(1-3), 150-156.

[24]. Cho, H.U., Cho, K.H., Kang, S. and Kim, Y.M. (2016) Optimization of operating variables in a pilot-scale reverse osmosis membrane process for reclamation of tunnel construction wastewater. Desalination and Water Treatment 57(26), 12082-12089.

[25]. Cicek, N., Macomber, J., Davel, J., Suidan, M.T., Audic, J. and Genestet, P. (2001) Effect of solids retention time on the performance and biological characteristics of a membrane bioreactor. Water Science and Technology 43(11), 43-50.

[26]. Csefalvay, E., Pauer, V. and Mizsey, P. (2009) Recovery of copper from process waters by nanofiltration and reverse osmosis. Desalination 240(1-3), 132-142.

[27]. De Jager, D., Sheldon, M.S. and Edwards, W. (2014) Colour removal from textile wastewater using a pilot-scale dual-stage MBR and subsequent RO system. Separation and Purification Technology 135, 135-144.

[28]. Deowan, S.A., Galiano, F., Hoinkis, J., Figoli, A. and Drioli, E. (2013) Submerged membrane bioreactor (SMBR) for treatment of textile dye wastewater towards developing novel MBR process. APCBEE Procedia 5, 259-

264.

[29]. Dialynas, E. and Diamadopoulos, E. (2009) Integration of a membrane bioreactor coupled with reverse osmosis for advanced treatment of municipal wastewater. Desalination 238(1-3), 302-311.

[30]. Dias, J.C.T., Rezende, R.P., Silva, C.M. and Linardi, V.R. (2005) Biological treatment of kraft pulp mill foul condensates at high temperatures using a membrane bioreactor. Process Biochemistry 40(3–4), 1125-1129.

[31]. Dufresne, R., Lavallee, H.C., Lebrun, R.E. and Lo, S.N. (1998) Comparison of performance between membrane bioreactor and activated sludge system for the treatment of pulping process wastewaters. Tappi Journal 81(4), 131-135.

[32]. Elimelech, M. and Phillip, W.A. (2011) The Future of Seawater Desalination: Energy, Technology, and the Environment. Science 333(6043), 712-717.

[33]. Fakhru'l-Razi, A. and Noor, M. (1999) Treatment of palm oil mill effluent (POME) with the Membrane Anaerobic System (MAS). Water Science and Technology 39(10-11), 159-163.

[34]. Fakhru'l-Razi, A., Pendashteh, A., Abidin, Z.Z., Abdullah, L.C., Biak, D.R.A. and Madaeni, S.S. (2010) Application of membrane-coupled sequencing batch reactor for oilfield produced water recycle and beneficial re-use. Bioresource Technology 101(18), 6942-6949.

[35]. Farizoglu, B., Keskinler, B., Yildiz, E. and Nuhoglu, A. (2004) Cheese whey treatment performance of an aerobic jet loop membrane bioreactor. Process Biochemistry 39(12), 2283-2291.

[36]. Farizoglu, B. and Uzuner, S. (2011) The investigation of dairy industry wastewater treatment in a biological high performance membrane system. Biochemical Engineering Journal 57, 46-54.

[37]. Fenu, A., Guglielmi, G., Jimenez, J., Spèrandio, M., Saroj, D., Lesjean, B., Brepols, C., Thoeye, C. and Nopens, I. (2010a) Activated sludge model (ASM) based modelling of membrane bioreactor (MBR) processes: A critical review with special regard to MBR specificities. Water Research 44(15), 4272-4294.

[38]. Fenu, A., Roels, J., Wambecq, T., De Gussem, K., Thoeye, C., De Gueldre, G. and Van De Steene, B. (2010b) Energy audit of a full scale MBR system. Desalination 262(1–3), 121-128.

[39]. Friha, I., Bradai, M., Johnson, D., Hilal, N., Loukil, S., Ben Amor, F., Feki, F., Han, J., Isoda, H. and Sayadi, S. (2015) Treatment of textile wastewater by

submerged membrane bioreactor: In vitro bioassays for the assessment of stress response elicited by raw and reclaimed wastewater. Journal of Environmental Management 160, 184-192.

[40]. Fritzmann, C., Lowenberg, J., Wintgens, T. and Melin, T. (2007) State-of-the-art of reverse osmosis desalination. Desalination 216(1-3), 1-76.

[41]. Fuchs, W., Binder, H., Mavrias, G. and Braun, R. (2003) Anaerobic treatment of wastewater with high organic content using a stirred tank reactor coupled with a membrane filtration unit. Water Research 37(4), 902-908.

[42]. Gao, W.J.J., Lin, H.J., Leung, K.T. and Liao, B.Q. (2010) Influence of elevated pH shocks on the performance of a submerged anaerobic membrane bioreactor. Process Biochemistry 45(8), 1279-1287.

[43]. Geise, G.M., Lee, H.S., Miller, D.J., Freeman, B.D., McGrath, J.E. and Paul, D.R. (2010) Water Purification by Membranes: The Role of Polymer Science. Journal of Polymer Science Part B-Polymer Physics 48(15), 1685-1718.

[44]. Germain, E., Nelles, F., Drews, A., Pearce, P., Kraume, M., Reid, E., Judd, S.J. and Stephenson, T. (2007) Biomass effects on oxygen transfer in membrane bioreactors. Water Research 41(5), 1038-1044.

[45]. Gil, J.A., Túa, L., Rueda, A., Montaño, B., Rodríguez, M. and Prats, D. (2010) Monitoring and analysis of the energy cost of an MBR. Desalination 250(3), 997-1001.

[46]. Gupta, V.K., Ali, I., Saleh, T.A., Nayak, A. and Agarwal, S. (2012) Chemical treatment technologies for waste-water recycling-an overview. Rsc Advances 2(16), 6380-6388.

[47]. Hai, F.I., Yamamoto, K. and Fukushi, K. (2006) Development of a submerged membrane fungi reactor for textile wastewater treatment. Desalination 192(1–3), 315-322.

[48]. Hall, E.R., Onysko, K.A. and Parker, W.J. (1995) Enhancement of bleached kraft organochlorine removal by coupling membrane filtration and anaerobic treatment. Environmental Technology 16(2), 115-126.

[49]. Helton, J.C. and Davis, F.J. (2002) Illustration of sampling-based methods for uncertainty and sensitivity analysis. Risk Analysis 22(3), 591-622.

[50]. Helton, J.C. and Davis, F.J. (2003) Latin hypercube sampling and the propagation of uncertainty in analyses of complex systems. Reliability Engineering & System Safety 81(1), 23-69.

[51]. Helton, J.C., Johnson, J.D., Sallaberry, C.J. and Storlie, C.B. (2006) Survey of sampling-based methods for uncertainty and sensitivity analysis. Reliability Engineering & System Safety 91(10-11), 1175-1209.

[52]. Henze, M., Grady, C.P.L., Gujer, W., Marais, G.V.R. and Matsuo, T. (1987) A general model for single-sludge wastewater treatment systems. Water Research 21(5), 505-515.

[53]. Henze, M., Gujer, W., Mino, T. and van Loosdrecht, M. (2000) Activated sludge models: ASM1, ASM2, ASM2d and ASM3, IWA Publishing,London, UK.

[54]. Hogetsu, A., Ishikawa, T., Yoshikawa, M., Tanabe, T., Yudate, S. and Sawada, J. (1992) High rate anaerobic digestion of wool scouring wastewater in a digester combined with membrane filter. Water Science and Technology 25(7), 341-350.

[55]. Huang, R.-R., Hoinkis, J., Hu, Q. and Koch, F. (2009) Treatment of dyeing wastewater by hollow fiber membrane biological reactor. Desalination and Water Treatment 11(1-3), 288-293.

[56]. Hung, L.-Y., Lue, S.J. and You, J.-H. (2011) Mass-transfer modeling of reverse-osmosis performance on 0.5-2% salty water. Desalination 265(1-3), 67-73.

[57]. Hung, P.V.X., Cho, S.-H. and Moon, S.-H. (2009) Prediction of boron transport through seawater reverse osmosis membranes using solution-diffusion model. Desalination 247(1-3), 33-44.

[58]. Jiao, W. (2014) Advanced Treatment of Coking Wastewater by Sequencing Batch MBR-RO. Advanced Materials Research 838-841, 2791-2796.

[59]. Judd, S. and Claire, J. (2010) The MBR Book - Second Edition: Principles and Applications of Membrane Bioreactors in Water and Wastewater Treatment, Elsevier, London, UK.

[60]. Förster, J. (2014) Water use in industry. http://ec.europa.eu /eurostat/ statistics explained/index.php/Water_use_in_industry

[61]. Kamali, M. and Khodaparast, Z. (2015) Review on recent developments on pulp and paper mill wastewater treatment. Ecotoxicology and Environmental Safety 114, 326-342.

[62]. Karrasch, B., Parra, O., Cid, H., Mehrens, M., Pacheco, P., Urrutia, R., Valdovinos, C. and Zaror, C. (2006) Effects of pulp and paper mill effluents on the microplankton and microbial self-purification capabilities of the Biobío River, Chile. Science of The Total Environment 359(1–3), 194-208.

[63]. Kataoka, N., Tokiwa, Y., Tanaka, Y., Fujiki, K., Taroda, H. and Takeda, K. (1992) Examination of bacterial characteristics of anaerobic membrane bioreactors in three pilot-scale plants for treating low-strength wastewater by application of the colony-forming-curve analysis method. Applied and Environmental Microbiology 58(9), 2751-2757.

[64]. Kataoka, T., Tsuru, T., Nakao, S. and Kimura, S. (1991) Permeation equations developed for prediction of membrane performance in pervaporation, vapor permeation and reverse-osmosis based on the solution-diffusion model. Journal of Chemical Engineering of Japan 24(3), 326-333.

[65]. Kim, Y.M., Kim, S.J., Kim, Y.S., Lee, S., Kim, I.S. and Kim, J.H. (2009) Overview of systems engineering approaches for a large-scale seawater desalination plant with a reverse osmosis network. Desalination 238(1-3), 312-332.

[66]. Kong, F.-x., Yang, H.-w., Wu, Y.-q., Wang, X.-m. and Xie, Y.F. (2015) Rejection of pharmaceuticals during forward osmosis and prediction by using the solution-diffusion model. Journal of Membrane Science 476, 410-420.

[67]. Konsowa, A.H., Eloffy, M.G. and El-Taweel, Y.A. (2013) Treatment of dyeing wastewater using submerged membrane bioreactor. Desalination and Water Treatment 51(4-6), 1079-1090.

[68]. Lai, J.-Y., Tung, K.-L., Lee, D.-J., Wang, D.-M., You, S.-J., Tseng, D.-H. and Deng, J.-Y. (2008) Using combined membrane processes for textile dyeing wastewater reclamation. Desalination 234(1), 426-432.

[69]. Le-Clech, P., Chen, V. and Fane, T.A.G. (2006) Fouling in membrane bioreactors used in wastewater treatment. Journal of Membrane Science 284(1–2), 17-53.

[70]. Lee, Y.G., Lee, Y.S., Jeon, J.J., Lee, S., Yang, D.R., Kim, I.S. and Kim, J.H. (2009) Artificial neural network model for optimizing operation of a seawater reverse osmosis desalination plant. Desalination 247(1-3), 180-189.

[71]. Leiviska, T., Ramo, J., Nurmesniemi, H., Poykio, R. and Kuokkanen, T. (2009) Size fractionation of wood extractives, lignin and trace elements in pulp and paper mill wastewater before and after biological treatment. Water Research 43(13), 3199-3206.

[72]. Lerner, M., Stahl, N. and Galil, N.I. (2007) Comparative study of MBR and activated sludge in the treatment of paper mill wastewater. Water Science and

Technology 55(6), 23-29.

[73]. Lin, C.-J., Zhang, P., Pongprueksa, P., Liu, J., Evers, S.A. and Hart, P. (2014) Pilot-Scale Sequential Anaerobic-Aerobic Biological Treatment of Waste Streams from a Paper Mill. Environmental Progress & Sustainable Energy 33(2), 359-368.

[74]. Lin, H.J., Xie, K., Mahendran, B., Bagley, D.M., Leung, K.T., Liss, S.N. and Liao, B.Q. (2009) Sludge properties and their effects on membrane fouling in submerged anaerobic membrane bioreactors (SAnMBRs). Water Research 43(15), 3827-3837.

[75]. Liu, C., Rainwater, K. and Song, L. (2011) Energy analysis and efficiency assessment of reverse osmosis desalination process. Desalination 276(1–3), 352-358.

[76]. Lonsdale, H.K., Merten, U. and Riley, R.L. (1965) Transport properties of cellulose acetate osmotic membranes Journal of Applied Polymer Science 9(4), 1341-&.

[77]. Lopes, G.H., Ibaseta, N., Guichardon, P. and Haldenwang, P. (2015) Predicting Permeate Fluxes and Rejection Rates in Reverse Osmosis and Tight-Nanofiltration Processes. Chemical Engineering & Technology 38(4), 585-594.

[78]. Lu, S.G., Imai, T., Ukita, M., Sekine, M., Fukagawa, M. and Nakanishi, H. (2000) The performance of fermentation wastewater treatment in ultrafiltration membrane bioreactor by continuous and intermittent aeration processes. Water Science and Technology 42(3-4), 323-329.

[79]. Lubello, C., Caffaz, S., Mangini, L., Santianni, D. and Caretti, C. (2007) MBR pilot plant for textile wastewater treatment and reuse. Water Science and Technology 55(10), 115-124.

[80]. Lubello, C. and Gori, R. (2005) Membrane bio-reactor for textile wastewater treatment plant upgrading. Water Science and Technology 52(4), 91-98.

[81]. Lucas, M., Martinez, P.J. and Viedma, A. (2012) Experimental determination of drift loss from a cooling tower with different drift eliminators using the chemical balance method. International Journal of Refrigeration-Revue Internationale Du Froid 35(6), 1779-1788.

[82]. Madaeni, S.S. and Mansourpanah, Y. (2006) Screening membranes for COD removal from dilute wastewater. Desalination 197(1-3), 23-32.

[83]. Maere, T., Verrecht, B., Moerenhout, S., Judd, S. and Nopens, I. (2011) BSM-

MBR: A benchmark simulation model to compare control and operational strategies for membrane bioreactors. Water Research 45(6), 2181-2190.

[84]. Malek, A., Hawlader, M.N.A. and Ho, J.C. (1994) A lumped transport parameter approach in predicting B10 RO permeator performance. Desalination 99(1), 19-38.

[85]. Manser, R., Gujer, W. and Siegrist, H. (2006) Decay processes of nitrifying bacteria in biological wastewater treatment systems. Water Research 40(12), 2416-2426.

[86]. Manttari, M. and Nystrom, M. (2007) Membrane filtration for tertiary treatment of biologically treated effluents from the pulp and paper industry. Water Science and Technology 55(6), 99-107.

[87]. Marchetti, P. and Livingston, A.G. (2015) Predictive membrane transport models for Organic Solvent Nanofiltration: How complex do we need to be? Journal of Membrane Science 476, 530-553.

[88]. McKay, M.D., Beckman, R.J. and Conover, W.J. (1979) A comparison of three methods for selecting values of input variables in the analysis of output from a compute code. Technometrics 21(2), 239-245.

[89]. Meng, F., Chae, S.-R., Drews, A., Kraume, M., Shin, H.-S. and Yang, F. (2009) Recent advances in membrane bioreactors (MBRs): Membrane fouling and membrane material. Water Research 43(6), 1489-1512.

[90]. Merayo, N., Hermosilla, D., Blanco, L., Cortijo, L. and Blanco, A. (2013) Assessing the application of advanced oxidation processes, and their combination with biological treatment, to effluents from pulp and paper industry. Journal of Hazardous Materials 262, 420-427.

[91]. Miguel Ochando-Pulido, J. and Martinez-Ferez, A. (2015) On the Recent Use of Membrane Technology for Olive Mill Wastewater Purification. Membranes 5(4), 513-531.

[92]. Minami, K. (1994) A trial of high performance anaerobic treatment on wastewater from a kraft pulp mill. Desalination 98(1-3), 273-283.

[93]. Mohana, S., Acharya, B.K. and Madamwar, D. (2009) Distillery spent wash: Treatment technologies and potential applications. Journal of Hazardous Materials 163(1), 12-25.

[94]. Moonkhum, M., Lee, Y.G., Lee, Y.S. and Kim, J.H. (2010) Review of seawater natural organic matter fouling and reverse osmosis transport modeling for

seawater reverse osmosis desalination. Desalination and Water Treatment 15(1-3), 92-107.

[95]. Munz, G., Gualtiero, M., Salvadori, L., Claudia, B. and Claudio, L. (2008) Process efficiency and microbial monitoring in MBR (membrane bioreactor) and CASP (conventional activated sludge process) treatment of tannery wastewater. Bioresource Technology 99(18), 8559-8564.

[96]. Murthy, Z.V.P. and Chaudhari, L.B. (2009a) Rejection behavior of nickel ions from synthetic wastewater containing Na(2)SO(4), NiSO(4), MgCl(2) and CaCl(2) salts by nanofiltration and characterization of the membrane. Desalination 247(1-3), 610-622.

[97]. Murthy, Z.V.P. and Chaudhari, L.B. (2009b) Treatment of distillery spent wash by combined UF and RO processes. Global Nest Journal 11(2), 235-240.

[98]. Murthy, Z.V.P. and Choudhary, A. (2012) Separation and estimation of nanofiltration membrane transport parameters for cerium and neodymium. Rare Metals 31(5), 500-506.

[99]. Mutamim, N.S.A., Noor, Z.Z., Abu Hassan, M.A., Yuniarto, A. and Olsson, G. (2013) Membrane bioreactor: Applications and limitations in treating high strength industrial wastewater. Chemical Engineering Journal 225, 109-119.

[100]. Na, L., Fenglin, Y., Meihong, N., Qingwei, P., Jian, Z. and Haiqiang, S. (2013) Characteristics and Treatment of Reed Pulping Medium Wastewater by Membrane Bioreactor. Advanced Materials Research 610-613, 1605-1609.

[101]. Naidoo, D., Ramdhani, N. and Bux, F. (2008) Microbial community analysis of a full-scale membrane bioreactor treating industrial wastewater. Water Science and Technology 58(8), 1589-1594.

[102]. Nataraj, S.K., Hosamani, K.M. and Aminabhavi, T.M. (2006) Distillery wastewater treatment by the membrane-based nanofiltration and reverse osmosis processes. Water Research 40(12), 2349-2356.

[103]. Nir, O. and Lahav, O. (2013) Coupling mass transport and chemical equilibrium models for improving the prediction of SWRO permeate boron concentrations. Desalination 310, 87-92.

[104]. Ochando Pulido, J.M. (2016) A review on the use of membrane technology and fouling control for olive mill wastewater treatment. Science of the Total Environment 563, 664-675.

[105]. Ogawa, N., Kimura, K. and Watanabe, Y. (2010) Membrane fouling in

nanofiltration/reverse osmosis membranes coupled with a membrane bioreactor used for municipal wastewater treatment. Desalination and Water Treatment 18(1-3), 292-296.

[106]. Oh, H.-J., Hwang, T.-M. and Lee, S. (2009) A simplified simulation model of RO systems for seawater desalination. Desalination 238(1-3), 128-139.

[107]. Oi, B., Wang, Y., Xu, S., Wang, Z. and Wang, S. (2012) Operating Energy Consumption Analysis of RO Desalting System: Effect of Membrane Process and Energy Recovery Device (ERD) Performance Variables. Industrial & Engineering Chemistry Research 51(43), 14135-14144.

[108]. Pages, N., Yaroshchuk, A., Gibert, O. and Luis Cortina, J. (2013) Rejection of trace ionic solutes in nanofiltration: Influence of aqueous phase composition. Chemical Engineering Science 104, 1107-1115.

[109]. Pandey, S.R., Jegatheesan, V., Baskaran, K. and Shu, L. (2012) Fouling in reverse osmosis (RO) membrane in water recovery from secondary effluent: a review. Reviews in Environmental Science and Bio-Technology 11(2), 125-145.

[110]. Pandey, S.R., Jegatheesan, V., Baskaran, K., Shu, L. and Muthukumaran, S. (2014) Performance of reverse osmosis (RO) for water recovery from permeates of membrane bio- reactor (MBR). Desalination and Water Treatment 52(4-6), 600-611.

[111]. Paul, D.R. (2004) Reformulation of the solution-diffusion theory of reverse osmosis. Journal of Membrane Science 241(2), 371-386.

[112]. Pearce, C.I., Lloyd, J.R. and Guthrie, J.T. (2003) The removal of colour from textile wastewater using whole bacterial cells: a review. Dyes and Pigments 58(3), 179-196.

[113]. Peñate, B. and García-Rodríguez, L. (2012) Current trends and future prospects in the design of seawater reverse osmosis desalination technology. Desalination 284, 1-8.

[114]. Pimple, S., Karikkat, S., Devanna, M., Yanamadni, V., Sah, R. and Prasad, S.M.R. (2016) Comparison of MBR/RO and UF/RO hybrid systems for the treatment of coke-oven effluents. Desalination and Water Treatment 57(7), 3002-3010.

[115]. Prodanovic, J.M. and Vasic, V.M. (2013) Application of membrane processes for distillery wastewater purification-a review. Desalination and Water Treatment 51(16-18), 3325-3334.

[116]. Qin, L., Zhang, G., Meng, Q., Xu, L. and Lv, B. (2012) Enhanced MBR by internal micro-electrolysis for degradation of anthraquinone dye wastewater. Chemical Engineering Journal 210, 575-584.

[117]. Quevedo, N., Sanz, J., Lobo, A., Temprano, J. and Tejero, I. (2012) Filtration demonstration plant as reverse osmosis pretreatment in an industrial water treatment plant. Desalination 286, 49-55.

[118]. Ragona, C.S.F. and Hall, E.R. (1998) Parallel operation of ultrafiltration and aerobic membrane bioreactor treatment systems for mechanical newsprint mill whitewater at 55 degrees C. Water Science and Technology 38(4-5), 307-314.

[119]. Rath, R.L., Bhattacharjee, C., Jain, S. and Bhattacharya, P.K. (2005) Treatment of prehydrolysis liquor from a pulp mill using a biological route followed by reverse osmosis. Chemical Engineering & Technology 28(10), 1201-1211.

[120]. Ravanchi, M.T., Kaghazchi, T. and Kargari, A. (2009) Application of membrane separation processes in petrochemical industry: a review. Desalination 235(1-3), 199-244.

[121]. Ross, W.R., Barnard, J.P., Strohwald, N.K.H., Grobler, C.J. and Sanetra, J. (1992) Practical application of the ADUF process to the full-scale treatment of a maize-processing effluent. Water Science and Technology 25(10), 27-39.

[122]. Ryan, D., Gadd, A., Kavanagh, J. and Barton, G.W. (2009) Integrated biorefinery wastewater design. Chemical Engineering Research & Design 87(9A), 1261-1268.

[123]. Saddoud, A., Hassairi, I. and Sayadi, S. (2007) Anaerobic membrane reactor with phase separation for the treatment of cheese whey. Bioresource Technology 98(11), 2102-2108.

[124]. Sanchez Perez, J.A., Carra, I., Sirtori, C., Agueera, A. and Esteban, B. (2014) Fate of thiabendazole through the treatment of a simulated agro-food industrial effluent by combined MBR/Fenton processes at mu g/L scale. Water Research 51, 55-63.

[125]. Santos, A., Ma, W. and Judd, S.J. (2011) Membrane bioreactors: Two decades of research and implementation. Desalination 273(1), 148-154.

[126]. Sarioglu, M., Insel, G., Artan, N. and Orhon, D. (2009) Model evaluation of simultaneous nitrification and denitrification in a membrane bioreactor operated without an anoxic reactor. Journal of Membrane Science 337(1-2), 17-27.

[127]. Satyawali, Y. and Balakrishnan, M. (2009) Performance enhancement with

powdered activated carbon (PAC) addition in a membrane bioreactor (MBR) treating distillery effluent. Journal of Hazardous Materials 170(1), 457-465.

[128]. Satyawali, Y. and Balakrishnan, M. (2008) Wastewater treatment in molasses-based alcohol distilleries for COD and color removal: A review. Journal of Environmental Management 86(3), 481-497.

[129]. Schoeberl, P., Brik, M., Braun, R. and Fuchs, W. (2005) Treatment and recycling of textile wastewater —case study and development of a recycling concept. Desalination 171(2), 173-183.

[130]. Scott, J.A. and Smith, K.L. (1997) A bioreactor coupled to a membrane to provide aeration and filtration in ice-cream factory wastewater remediation. Water Research 31(1), 69-74.

[131]. Sekino, M. (1993) Precise analytical model of hollow fiber reverse osmosis modules. Journal of Membrane Science 85(3), 241-252.

[132]. Sheldon, M.S., Zeelie, P.J. and Edwards, W. (2012) Treatment of paper mill effluent using an anaerobic/aerobic hybrid side-stream Membrane Bioreactor. Water Science and Technology 65(7), 1265-1272.

[133]. Sher, F., Malik, A. and Liu, H. (2013) Industrial polymer effluent treatment by chemical coagulation and flocculation. Journal of Environmental Chemical Engineering 1(4), 684-689.

[134]. Simstich, B., Beimfohr, C. and Horn, H. (2012) Lab scale experiments using a submerged MBR under thermophilic aerobic conditions for the treatment of paper mill deinking wastewater. Bioresource Technology 122, 11-16.

[135]. Simstich, B. and Oeller, H.J. (2010) Membrane technology for the future treatment of paper mill effluents: chances and challenges of further system closure. Water Science and Technology 62(9), 2190-2197.

[136]. Sin, G., Gernaey, K.V., Neumann, M.B., van Loosdrecht, M.C.M. and Gujer, W. (2011) Global sensitivity analysis in wastewater treatment plant model applications: Prioritizing sources of uncertainty. Water Research 45(2), 639-651.

[137]. Sin, G., Gernaey, K.V., Neumann, M.B., van Loosdrecht, M.C.M. and Gujer, W. (2009) Uncertainty analysis in WWTP model applications: A critical discussion using an example from design. Water Research 43(11), 2894-2906.

[138]. Sin, G., Van Hulle, S.W.H., De Pauw, D.J.W., van Griensven, A. and Vanrolleghem, P.A. (2005) A critical comparison of systematic calibration protocols for activated sludge models: A SWOT analysis. Water Research

39(12), 2459-2474.

[139]. Song, L.F., Hu, J.Y., Ong, S.L., Ng, W.J., Elimelech, M. and Wilf, M. (2003) Emergence of thermodynamic restriction and its implications for full-scale reverse osmosis processes. Desalination 155(3), 213-228.

[140]. Spérandio, M. and Espinosa, M.C. (2008) Modelling an aerobic submerged membrane bioreactor with ASM models on a large range of sludge retention time. Desalination 231(1-3), 82-90.

[141]. Sridang, P.C., Pottier, A., Wisniewski, C. and Grasmick, A. (2008) Performance and microbial surveying in submerged membrane bioreactor for seafood processing wastewater treatment. Journal of Membrane Science 317(1-2), 43-49.

[142]. Srinivasan, G., Sundaramoorthy, S. and Murthy, D.V.R. (2009) Separation of dimethyl phenol using a spiral-wound RO membrane - Experimental and parameter estimation studies. Desalination 243(1-3), 170-181.

[143]. Stamatelatou, K., Kopsahelis, A., Blika, P.S., Paraskeva, C.A. and Lyberatos, G. (2009) Anaerobic digestion of olive mill wastewater in a periodic anaerobic baffled reactor (PABR) followed by further effluent purification via membrane separation technologies. Journal of Chemical Technology and Biotechnology 84(6), 909-917.

[144]. Suchanek, G. (2006) Mechanistic equations for membrane transport of multicomponent solutions. General Physiology and Biophysics 25(1), 53-63.

[145]. Sun, X. and Zuo, J. (2009) Influence factor and membrane fouling in SMBR for food wastewater treatment.

[146]. Sun, Y., Hua, X., Ge, R., Guo, A., Guo, Z., Dong, D. and Sun, W. (2013) Investigation on pretreatment of centrifugal mother liquid produced in the production of polyvinyl chloride by air-Fenton technique. Environmental Science and Pollution Research 20(8), 5797-5805.

[147]. Tacidelli, A.R., Alves, J.J.N., Vasconcelos, L.G.S. and Brito, R.P. (2009) Increasing PVC suspension polymerization productivity—An industrial application. Chemical Engineering and Processing: Process Intensification 48(1), 485-492.

[148]. Tan, T.W. and Ng, H.Y. (2008) Influence of mixed liquor recycle ratio and dissolved oxygen on performance of pre-denitrification submerged membrane bioreactors. Water Research 42(4-5), 1122-1132.

[149]. Toffoletto, M., Merdaw, A.A., Sharif, A.O. and Bertucco, A. (2010) Experimental approaches to feed solution permeability in pressure-driven membrane separation processes. Journal of Membrane Science 364(1-2), 27-33.

[150]. Tu, K.L., Nghiem, L.D. and Chivas, A.R. (2010) Boron removal by reverse osmosis membranes in seawater desalination applications. Separation and Purification Technology 75(2), 87-101.

[151]. Ugurlu, M. and Karaoglu, M.H. (2009) Removal of AOX, total nitrogen and chlorinated lignin from bleached Kraft mill effluents by UV oxidation in the presence of hydrogen peroxide utilizing TiO2 as photocatalyst. Environmental Science and Pollution Research 16(3), 265-273.

[152]. Vandevivere, P.C., Bianchi, R. and Verstraete, W. (1998) Treatment and reuse of wastewater from the textile wet-processing industry: Review of emerging technologies. Journal of Chemical Technology and Biotechnology 72(4), 289-302.

[153]. Verrecht, B., Judd, S., Guglielmi, G., Brepols, C. and Mulder, J.W. (2008) An aeration energy model for an immersed membrane bioreactor. Water Research 42(19), 4761-4770.

[154]. Verrecht, B., Maere, T., Benedetti, L., Nopens, I. and Judd, S. (2010a) Model-based energy optimisation of a small-scale decentralised membrane bioreactor for urban reuse. Water Research 44(14), 4047-4056.

[155]. Verrecht, B., Maere, T., Nopens, I., Brepols, C. and Judd, S. (2010b) The cost of a large-scale hollow fibre MBR. Water Research 44(18), 5274-5283.

[156]. Wang, J., Dlamini, D.S., Mishra, A.K., Pendergast, M.T.M., Wong, M.C.Y., Mamba, B.B., Freger, V., Verliefde, A.R.D. and Hoek, E.M.V. (2014) A critical review of transport through osmotic membranes. Journal of Membrane Science 454, 516-537.

[157]. Wang, Y., Huang, X. and Yuan, Q. (2005) Nitrogen and carbon removals from food processing wastewater by an anoxic/aerobic membrane bioreactor. Process Biochemistry 40(5), 1733-1739.

[158]. Wenten, I.G. and Khoiruddin (2016) Reverse osmosis applications: Prospect and challenges. Desalination 391, 112-125.

[159]. Wilf, M. (1997) Design consequences of recent improvements in membrane performance. Desalination 113(2), 157-163.

[160]. Wintgens, T., Rosen, J., Melin, T., Brepols, C., Drensla, K. and Engelhardt, N.

(2003) Modelling of a membrane bioreactor system for municipal wastewater treatment. Journal of Membrane Science 216(1–2), 55-65.

[161]. Xie, K., Lin, H.J., Mahendran, B., Bagley, D.M., Leung, K.T., Liss, S.N. and Liao, B.Q. (2010) Performance and fouling characteristics of a submerged anaerobic membrane bioreactor for kraft evaporator condensate treatment. Environmental Technology 31(5), 511-521.

[162]. Yanagi, C., Sato, M. and Takahara, Y. (1994) Treatment of wheat starch waste water by a membrane combined two phase methane fermentation system. Desalination 98(1-3), 161-170.

[163]. Yang, W., Cicek, N. and Ilg, J. (2006) State-of-the-art of membrane bioreactors: Worldwide research and commercial applications in North America. Journal of Membrane Science 270(1–2), 201-211.

[164]. Yaroshchuk, A., Martinez-Llado, X., Llenas, L., Rovira, M. and de Pablo, J. (2011) Solution-diffusion-film model for the description of pressure-driven trans-membrane transfer of electrolyte mixtures: One dominant salt and trace ions. Journal of Membrane Science 368(1-2), 192-201.

[165]. Yaroshchuk, A.E. (1995) Solution-diffusion-imperfection model revised. Journal of Membrane Science 101(1), 83-87.

[166]. Yigit, N.O., Uzal, N., Koseoglu, H., Harman, I., Yukseler, H., Yetis, U., Civelekoglu, G. and Kitis, M. (2009) Treatment of a denim producing textile industry wastewater using pilot-scale membrane bioreactor. Desalination 240(1-3), 143-150.

[167]. You, S.-J. and Teng, J.-Y. (2009) Anaerobic decolorization bacteria for the treatment of azo dye in a sequential anaerobic and aerobic membrane bioreactor. Journal of the Taiwan Institute of Chemical Engineers 40(5), 500-504.

[168]. Yun, L., Harder, E., Faibish, R.S. and Roux, B. (2011) Computer simulations of water flux and salt permeability of the reverse osmosis FT-30 aromatic polyamide membrane. Journal of Membrane Science 384(1-2), 1-9.

[169]. Yun, M.-A., Yeon, K.-M., Park, J.-S., Lee, C.-H., Chun, J. and Lim, D.J. (2006) Characterization of biofilm structure and its effect on membrane permeability in MBR for dye wastewater treatment. Water Research 40(1), 45-52.

[170]. Yurtsever, A., Sahinkaya, E., Aktas, O., Ucar, D., Cinar, O. and Wang, Z. (2015) Performances of anaerobic and aerobic membrane bioreactors for the treatment of synthetic textile wastewater. Bioresource Technology 192, 564-573.

[171]. Zhang, Y., Ma, C., Ye, F., Kong, Y. and Li, H. (2009) The treatment of wastewater of paper mill with integrated membrane process. Desalination 236(1-3), 349-356.

[172]. Zhu, A.H., Christofides, P.D. and Cohen, Y. (2010) Effect of Stream Mixing on RO Energy Cost Minimization. Desalination 261(3), 232-239.

7. Appendixes

7.1 Structure and Sankey diagram of IWEMM

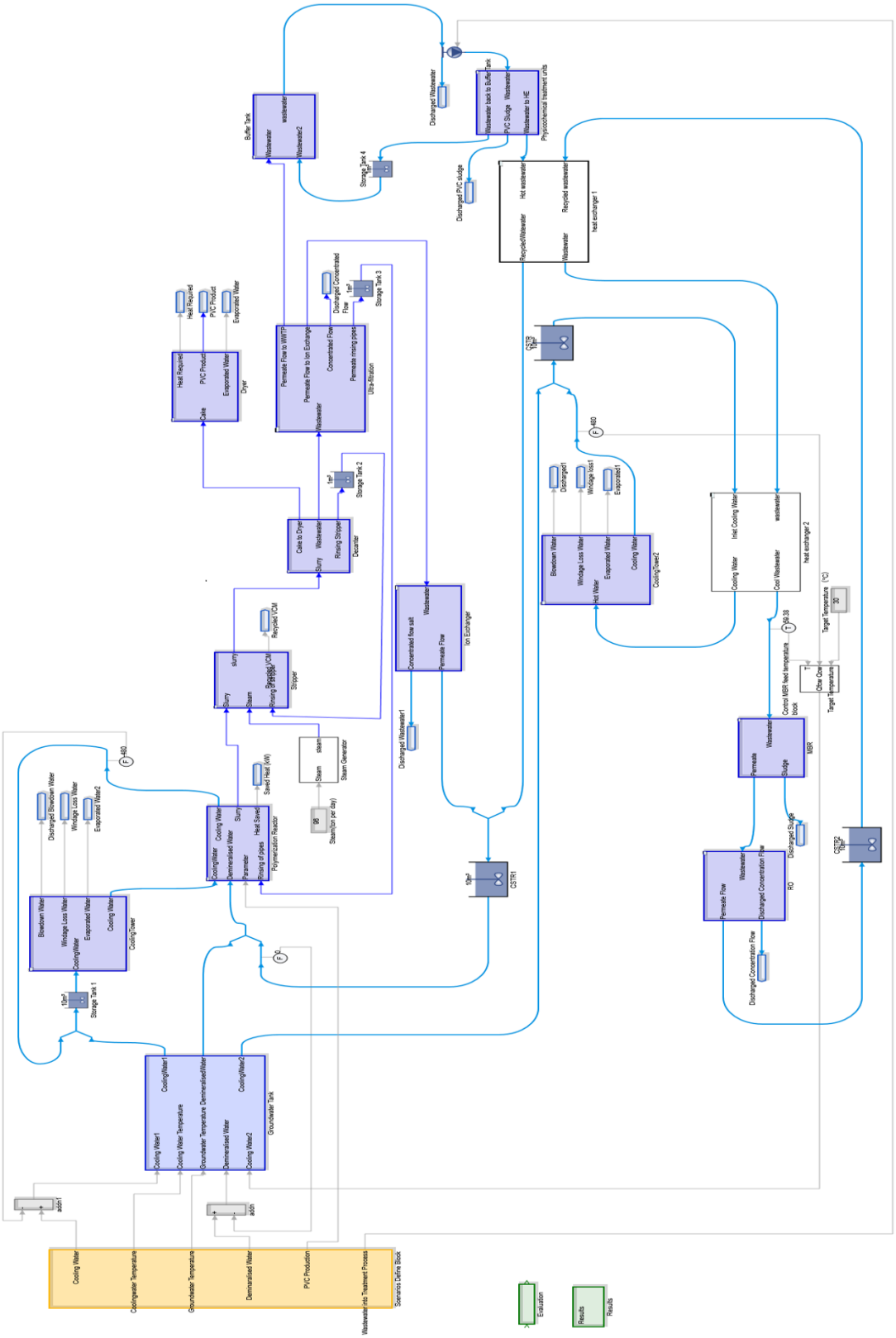

Figure 7-1 Structure of IWEMM

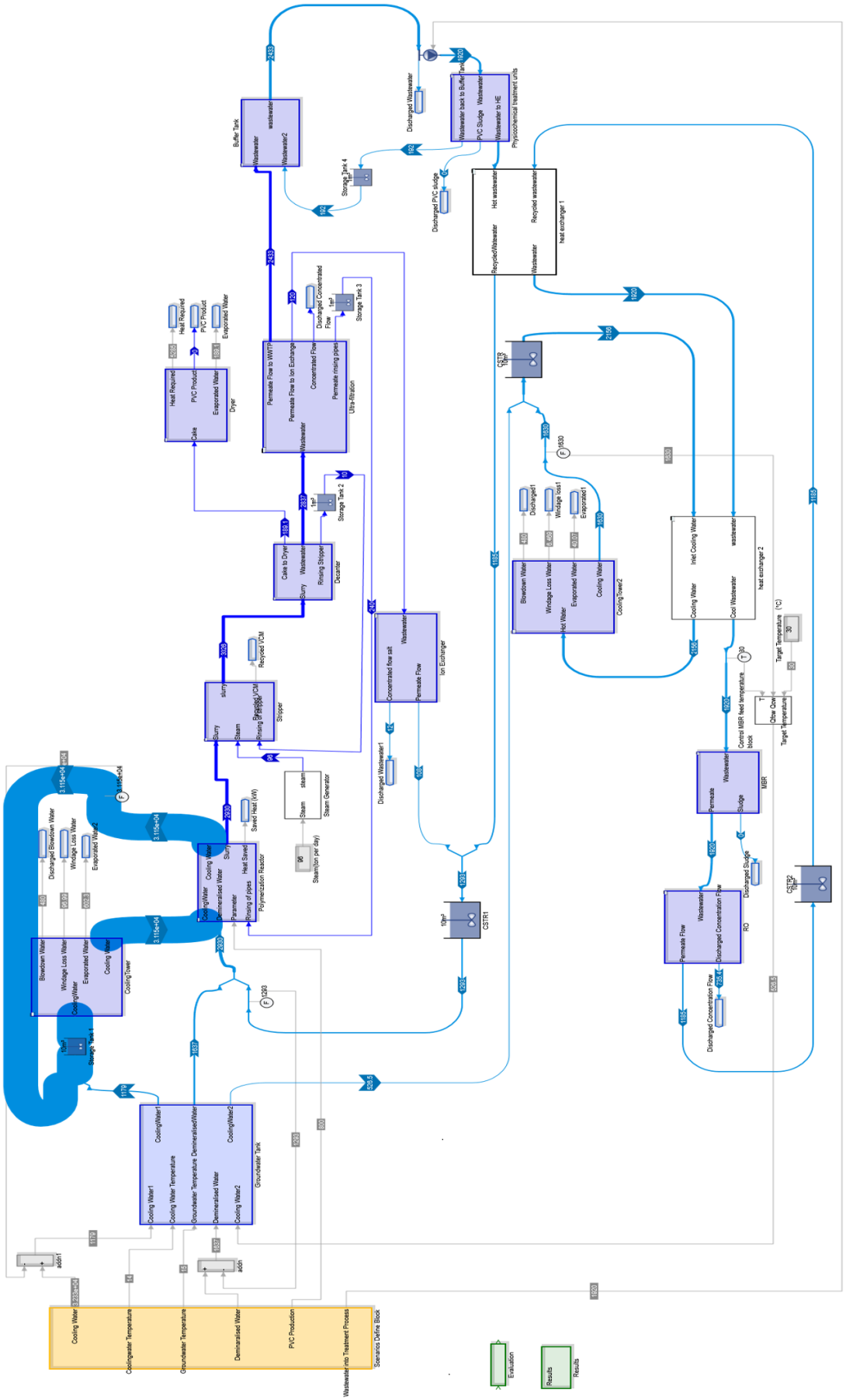

Figure 7-2 Sankey diagram of water mass flow

7.2 Definition and description of the parameters

7.2.1 Parameters from the PVC production site

These parameters are extracted and collected from production experience as well as the production equipment monitoring. They determine the intermediate and final output results. The model gets the following inputs from the PVC production site:

(1) VCM monomer polymerization efficiency (R_{VCM})

The VCM monomer polymerization efficiency is the fraction of VCM present in the raw material converted into PVC in polymerization tank.

$$R_{VCM} = 100\times (\text{VCM in} - \text{VCM out})/\text{VCM out}$$

With the progress of polymerization reaction, the reaction rate gradually slows down. In order to improve production efficiency, the terminating agent is added to stop the polymerization when VCM conversion rate reaches a certain value during the industrial production. Most of the studies report VCM monomer polymerization efficiency to be about 85 % or a little lower. In IWEMM, it has been assumed to be 84% as the nominal value, but the model user can specify it based on manufacturing equipment and technological raw material formula.

(2) Raw materials and proportion of each component in raw materials (η)

The raw materials of the polymerization reaction are mainly demineralised water, VCM monomer, initiator agent and disperse agent (the other additives are ignored due to minor influence/quantity). Generally, the proportion of each component can be represented by its mass ratio to mass of VCM.

Proportion of VCM monomer= 1 kg $(kg\cdot VCM)^{-1}$

Proportion of demineralization water= η_{dw} kg $(kg\cdot VCM)^{-1}$

Proportion of initiator agent= η_{ia} kg $(kg\cdot VCM)^{-1}$

Proportion of disperse agent= η_{da} kg $(kg\cdot VCM)^{-1}$

(3) Nominal PVC loss rate in production process (R)

Ideally, the PVC produced in polymerization tank is the yield of the plant. Actually, there is the inevitable loss in the production process. The level of PVC loss rate

mainly depends on the production process, especially the production equipment and operations.

PVC loss rate in polymerization tank= R_{tank} (%)

PVC loss rate in stripper= $R_{stripper}$ (%)

PVC loss rate in decanter= $R_{decanter}$ (%)

PVC loss rate in dryer= R_{dryer} (%)

(4) Steam pressure= P_{steam} (kPa) steam temperature= T_{steam} (°C)

(5) Pressure in the bottom of stripper= $P_{str,bot}$ (kPa)

Temperature in the bottom of stripper= $T_{str,bot}$ (°C)

(6) Pressure in the top of stripper = $P_{str,top}$ (kPa)

Temperature in the top of stripper= $T_{str,top}$ (°C)

(7) Heat-transfer area size of polymerization tank= S (m^2)

(8) Temperature to start polymerization reaction= $T_{poly,start}$ (°C)

(9) Initial temperature of polymerization tank and raw materials= $T_{initial}$ (°C)

(10) Water content in slurry entering dryer= $R_{dryer,dw}$ (%)

(11) Temperature of PVC entering dryer= $T_{dryer,PVC}$ (°C)

(12) Temperature of PVC after drying= T_{PVC} (°C)

7.2.2 Physical parameters

(1) The specific heat capacity of the composition of slurry :

This is the approximate specific heat capacity of each substance in the slurry produced during polymerization. It can be calculated by means of interpolation based on the standard table of specific heat capacity which is a function of temperature.

Specific heat capacity of VCM= $C_{p,VCM}$ (T) (kJ kg^{-1} K^{-1})

Specific heat capacity of PVC= $C_{p,PVC}$ (T) (kJ kg^{-1} K^{-1})

Specific heat capacity of water= $C_{p,dw}$ (T) (kJ kg^{-1} K^{-1})

(2) VCM heat of vaporization= L_{VCM} (P,T) (kJ kg^{-1})

(3) The polymerization reaction is strongly exothermic (approximately 1,600 kJ kg^{-1}):

Heat of polymerization reaction= H_{poly} (kJ kg^{-1})

(4) Thermal conductivity of polymerization tank= K (kJ $m^{-2} \cdot h^{-1} K^{-1}$)

(5) Enthalpy of steam [H_{steam} (P,T) (kJ kg^{-1})]

H_{steam} (P,T) is the enthalpy or heat content of the steam at a pressure of P and a temperature of T. In the PVC production site, the heat for recycling VCM in stripper is provided as overheated steam, and it is around 180 °C and 900 kPa. From the steam-tables, the enthalpy H_{steam} (900,180) is found to be about 2.785 kJ kg^{-1}.

(6) Enthalpy of demineralization water [H_{dw} (P,T) (kJ kg^{-1})]

H_{dw} (P,T) is the enthalpy or heat content of the demineralised water at a pressure of P and a temperature of T.

7.2.3 Parameters controlling water flow and heat

These are the key input parameters below:

(1) Yield of PVC= Y_{pvc} (kg h^{-1})

(2) Water content in PVC= $R_{PVC,dw}$ (%)

(3) The amount of wastewater entering treatment process= M_{ww} (kg h^{-1})

(4) The amount of treated wastewater entering natural water bodies from R-207= M_{tw} (kg h^{-1})

(5) Temperature of cooling water inlet cooling tower= T_i (°C)

In order to prevent natural water bodies from heat pollution, the maximum temperature of discharged water into natural water bodies is limited. As efficiency of the cooling tower is limited, the temperature of cooling water entering should not exceed a maximum temperature.